NASA Conference Publication 2452

Joint University Program for Air Transportation Research—1984

Proceedings of a conference held at
Langley Research Center
Hampton, Virginia
January 18, 1985

NASA

NASA Conference Publication 2452

Joint University Program for Air Transportation Research—1984

Compiled by
Frederick R. Morrell
Langley Research Center
Hampton, Virginia

Proceedings of a conference sponsored by
the National Aeronautics and Space Administration
and the Federal Aviation Administration and held at
Langley Research Center
Hampton, Virginia
January 18, 1985

NASA
National Aeronautics
and Space Administration

**Scientific and Technical
Information Branch**

1987

PREFACE

The Joint University Program for Air Transportation Research is a coordinated set of three grants jointly sponsored by NASA Langley Research Center, and the Federal Aviation Administration, one each with Massachusetts Institute of Technology (NGL-22-009-640), Ohio University (NGR-36-009-017), and Princeton University (NGL-31-001-252), to support the training of students for the air transportation system. These grants, initiated in 1971, encourage the development of innovative curriculums and support the establishment of graduate and undergraduate research assistantships and internships.

An important feature of this program is the quarterly review, one held at each of the schools and a fourth at a NASA or FAA facility. This latter review for 1984 was held at the NASA Langley Research Center, Hampton, Virginia, January 18, 1985. At these reviews the program participants, both graduate and undergraduate, have an opportunity to present their research activities to their peers, professors, and invited guests from government and industry.

This conference publication represents the fifth in a series of yearly summaries of the activities of the program (the 1983 summary appears in NASA CP-2451). The majority of the material is the effort of the students supported by the grants.

Three types of contributions are included. Completed works are represented by full technical papers. Research reported in the open literature (for example, theses or journal articles) is presented in an annotated bibliography. Status reports of ongoing research are represented by copies of viewgraphs augmented with a brief descriptive text.

Use of trade names or manufacturers in this report does not constitute an official endorsement of such products or manufacturers, either expressed or implied, by the National Aeronautics and Space Administration or the Federal Aviation Administration.

Frederick R. Morrell
NASA Langley Research Center

CONTENTS

PRINCETON UNIVERSITY

MASSACHUSETTS INSTITUTE OF TECHNOLOGY

INVESTIGATION OF AIR TRANSPORTATION TECHNOLOGY AT MASSACHUSETTS INSTITUTE OF TECHNOLOGY, 1984

Robert W. Simpson
Flight Transportation Laboratory
Massachusetts Institute of Technology
Cambridge, Massachusetts

SUMMARY OF RESEARCH

There have been three projects sponsored by the Joint University Program at MIT during 1984. Two projects are focussed on the potential application of Loran-C in flying nonprecision approaches to general-aviation runways, and the third project involves basic research on aircraft icing. Four faculty members were responsible for supervising student research in the program: Robert Simpson, Antonio Elias, R. J. Hansman and Walter Hollister.

Aircraft Approach Guidance Using Relative Loran-C Navigation

This project was aimed at a flight test demonstration of an approach guidance system based on the relative navigation concept of Professor Antonio Elias. It uses the difference in TD's from those of the touchdown point to simplify and speed navigation computer processing, and to take advantage of the short-term accuracy of less than 100 feet for Loran-C. The project led to three sub-project areas concerning methods of displaying guidance information to the pilot, investigation of dynamic response of the Loran-C receiver, and possible smoothing with rate gyro data, and the need to study the micro-distortion of the Loran-C field discovered in surface measurements over open terrain.

The system being constructed for flight testing by Norry Dogan is based on a Micrologic M3000 Loran-C receiver especially modified to output TD's, and TD's in digital form every 12 GRI, and whose tracking filter constants can be set by the experimenter. A flight test pallet has been constructed to carry the receiver, the memory storage system, power supply, auxiliary display, etc. Three different display devices have been constructed. The original display was an LED bar-graph display of cross track distance and velocity, and an LED numeric digital display of range and desired altitude. This system will now display these data to the experimenter from the flight test rack. For the pilot, a CRT cross-pointer display has been constructed, driven by software resident in an Apple II computer. This has the advantage of flexible formats and ease in programming software changes for the pilot's display. The third display was developed by another student, Lee Marzke, using a Sharp LM-24003G Graphics Display. This is an 128×240 pixel display, which uses liquid crystal technology, and is roughly 4×8 inches in size. A special, programmable controller using the MCG-8085 processor was built to accept data over an RS-232 line and convert it to a cross-pointer display, with TO-FROM, altitude, and airspeed. It was decided to use the CRT display for flight test and to retain this display for other applications in future research. Flight testing of the system was planned for early in 1985, at a few selected sites in the 9960 Loran-C chain.

In the course of constructing the system, ground surveys were conducted using the Loran-C receiver and Apple Computer. These discovered that there were unexplainable micro-distortions of the Loran-C signals over a grid of roughly 50 meters. The averaged position deviation from the grid was repeatable and of the order of 10 meters. This would appear as noise to the receiver if it exists above the Earth's surface in the approach path to the runway. This has triggered investigations of methods to survey the approach airspace using the flight test pallet mounted on a tethered balloon or kitoon. The size of these micro-distortions will affect the performance of the Loran-C guidance system in estimating cross track velocities and thus its dynamic response in displaying cross track deviations to the pilot. Further research is planned by Professor Antonio Elias to gather more data on these microdistortions.

Probabilistic Modelling of Loran-C Errors for Nonprecision Approaches

The goals of this project are to develop a mathematical model which will predict the probability that an approach flown to a runway with a particular Loran-C receiver will fall within a given standard (such as FAA AC90-45A). Flight tests will be used to validate the model performance. During 1984, the model was developed and programmed to handle both short-term update (5 minutes) and long-term update (6 weeks) cases. It accounts for runway heading, the chain and slaves used and their geometry and distance relative to the airport, the current SNR (signal-to-noise ratio), and the seasonal history of Loran-C deviations at nearby monitoring stations. Several models for predicting long-term drift have been examined. The model produces a bivariate normal error ellipse for the position of the aircraft on approach to the runway. The percentage of this ellipse which falls within any other geometric standard can be computed.

This research is being performed by John Einhorn, with supervision by Walter Hollister.

Aircraft Icing Research

This research is a continuation of work done originally by R. J. Hansman as a graduate student in the Joint University Program. Experimental work in 1984 has focussed on two main areas:

1) Measurement of droplet trajectories and droplet impingement/runback characteristics

2) Measurement of real-time ice accretion using ultrasonic pulse-echo techniques

DROPLET RESEARCH

In order to experimentally measure the trajectories of droplets, a controlled method for producing droplets of the known, repeatable initial conditions to be "injected" into the free-stream flow at any desired location has been successfully developed. The system utilizes a syringe reservoir connected to an extremely fine bore length of tubing, described in the next section.

The syringe reservoir supplies water to a 0.005 in. (ID) tube approximately 2 in. long. The tube is extended into the free-stream flow at a 30 degree angle. Droplets bead at the end of the tube until they are drawn off by the free-stream drag. In order to minimize the droplet size at which this occurs, the tube tip is coated with wax to increase the droplet/tube contact angle. Droplets can be produced at a rate of several per second using this technique, although the current trajectory measurement scheme does not require such a "stream" of droplets. The approach being taken to measure the droplet trajectories is to use a double strobe light pulse to illuminate the droplet at two points along its trajectory. Since the time between these points is fixed by the strobe pulse interval, the velocity of the droplet between the points can be obtained by measuring the distance travelled in this interval from a 35-mm photograph. By moving the injection point across the entire injection plane upstream of the body, the velocity field around the body can be completely mapped. One of the distinct advantages of the developed injection technique is that the initial droplet conditions can be accurately measured and thus used as inputs to existing trajectory codes to aid verification and/or development of trajectory codes

for complex bodies such as glaze ice shapes. Since the droplet is pulled off the injector tip, the initial velocity of the droplet is zero; furthermore the initial co-ordinates of the droplet are also those of the injector tip. The initial size of the droplet is obtained from a triggered photograph taken immediately after the droplet release occurs.

REAL-TIME ICE ACCRETION MEASUREMENT

Experiments to measure ice growth on a cylinder have been conducted in the Icing Research Tunnel (IRT) at the NASA Lewis facility in Cleveland, Ohio. A 4 in. (OD) cylinder approximately 12 in. long was suspended vertically from the roof of the IRT and exposed to a variety of icing conditions[1] at the velocities from 110 mph to 230 mph. The cylinder was instrumented with 4 ultrasonic transducers to measure the real-time ice accretion using the pulse-echo technique. The transducers were all of the longitudinal wave type, three being 0.5 in. diameter transducers and a 0.25 in. diameter delay-line transducer. The transducers are mounted flush with the cylinder surface and are thus "non-intrusive." For the series of tests performed at NASA Lewis three of the transducers were mounted on the cylinder stagnation line and the remaining (0.5 in.) transducer was mounted 25 degrees off-axis to allow simultaneous measurement of horn growth rates and the growth rate on the stagnation line. Data were collected by video-taping the oscilloscope output from the transducers and pulser/receivers. Although data reduction from the entire series of tests is still under way (over three hours of real-time ice accretion data were recorded in 38 tests in the IRT), initial results have shown the following:

1) The ultrasonic pulse-echo system is capable of measuring ice thickness in real time over a wide range of icing conditions. Ice thickness data were successfully recorded for all the tests conducted, although ice formations at warmer temperatures (+27°F) sometimes resulted in a cavity forming over the transducer at some point in the ice growth, after which the transducer can no longer measure further ice accretion (due to the reflection of the pulse signal from the air cavity). At the colder temperatures (+10°F to -10°F) the pulse-echo system performed extremely well, producing a discrete, large amplitude echo at the moving ice/air interface.

2) The optimum transducer frequency appears to be 5 MHz, although even higher frequencies have yet to be evaluated. The optimum transducer size for ice accretion measurement is driven by two conflicting requirements. A small diameter transducer is relatively insensitive to the irregular ice/air surfaces that are characteristic of ice accretion at warm temperature, and hence produces a "narrower" interface echo than a larger diameter transducer would under similar condition.[2] However under the same warm (glaze) icing conditions, air cavities and inclusions were observed which

---

[1] A temperature range of 37 degrees Fahrenheit was covered, with runs from -10 degrees Fahrenheit to +27 degrees Fahrenheit. Liquid water contents were varied from 0.6 g/m^3 to 2.4 g/m^3. Droplet diameter was also varied from 12 micrometers to 20 micrometers.

[2] The ice thickness resolution achievable is fundamentally limited by the ice thickness variation across the ultrasonic field produced by the transducer, and hence by the diameter of the transducer (since the ultrasonic field is a collimated beam of the same diameter as the transducer).

threaten to "blind" a small diameter transducer to further ice accretion and thus dictate either a transducer large enough to see around these cavities or else several smaller transducers operating in parallel.

3) In addition to providing information on the thickness and surface variation of the accreted ice formation, the ultrasonic system also clearly shows the presence of liquid water on top of the ice layer, and it is hoped that further measurements on the data recorded will allow the thickness of this layer to be determined. At the colder temperatures no such water layer was observed, from which it can be concluded that the droplets are indeed freezing "on impact," as in the classical rime ice model.

FURTHER WORK

Droplet Studies

Having developed and tested the droplet injection technique, work is now under way on the development of a laser triggered multiple strobe setup. By breaking a laser beam aimed across its path, the droplet triggers a multiple strobe arrangement that allows the desired point velocity measurement to be photographically recorded as described earlier. In addition the laser trigger will also be used to study droplet impingement on bodies and runback characteristics. This can be accomplished by aiming the laser beam on the desired impingement point to be studied, and triggering from the droplet's occlusion of the reflected beam signal.

Ultrasonic Pulse-Echo Developments

Following the successful series of tests at NASA Lewis, work was conducted to allow flight testing of the ultrasonic system aboard the NASA Lewis icing research Twin Otter aircraft. Signal processing algorithms to track the ice/air interface echo under all icing conditions are being studied with a view to building a real-time data acquisition system providing ice thickness and ice accretion rate output. Existing, commercially available pulse-echo thickness readers will also be investigated for this prupose. Data reduction from the IRT tests will continue and were presented at the 23rd Aerospace Conference (Hansman R. J., and Kirby M. S., "Measurement of Ice Accretion Using Ultrasonic Pulse-Echo Techniques," AIAA 85-0471). The real-time ice accretion data taken will also be compared with existing computer model predictions for "identical" icing conditions on a cylinder. Additional theoretical modelling of the ultrasonic wave propagation in different ice types will also be undertaken and analytic models developed for wave propagation and reflection characteristics. Further refinement of the speed of sound in ice will be made from the results of the Lewis tests. It is hoped that fundamental information on the elastic properties of different ice types may be obtained from this velocity data.

Bibliography

1. Lee Howard Marzke, A Microprocessor Driven Liquid Crystal Graphics Display for Aircraft Use, S.B. Thesis, MIT, 1984 (also FTL Report 84-2, Flight Transportation Lab, MIT).

2. R. J. Hansman, and M. S. Kirby, Investigation of Air Transportation Technology at Massachusetts Institute of Technology - 1984, AIAA Paper 85-0471, January 1985.

3. Antonio L. Elias, Aircraft Approach Guidance Using Relative Loran-C Navigation, NAVIGATION: Journal of the Institute of Navigation, vol. 32, no. 1, Spring 1985.

AIRCRAFT APPROACH GUIDANCE USING RELATIVE LORAN-C NAVIGATION

Antonio L. Elias
Flight Transportation Laboratory
Massachusetts Institute of Technology
Cambridge, Massachusetts

The experiments carried out during 1984 at MIT focused on two aspects of LORAN-C relative navigation that will impact system performance at the sub-microsecond level of accuracy: tracking loop bandwidth and localized field deformations. Figures 1 to 3 show the result of a basic experiment illustrating both these effects. A Micrologic Model 3000 receiver mounted on a vehicle is accelerated to a constant speed and then decelerated to a full stop between points A and B. After a 2-minute pause, the vehicle is reversed and the maneuver repeated in the opposite direction from points C to D. The first measured set of TD's in the sample was taken as the definition of point "A", and all subsequent positions plotted relative to this datum. Features of interest in Figure 1 include: a) the random noise in the plotted position is sufficiently low to discern the 10-m width of the road over which the test was performed; b) the navigated position overshoots the actual position during braking (and lags it during acceleration); and c) a reduction in signal-to-noise ratio (SNR), as occurred at the end of the run while the vehicle was standing at point D, substantially increases the navigated position random noise.

The effect of vehicle acceleration and deceleration is better seen in the plot of Figure 2; here, measured and position-derived TD's are plotted against time. As can be seen, the tracking loops can be very well approximated by second-order linear systems, in spite of the discrete digital implementation used in this receiver. The trade-off between random noise and lag/overshoot in the navigated position implied by selection of the tracking loop bandwidth is illustrated in Figure 3, where the test of Figure 1 is repeated with a tracking loop filter bandwidth four times larger than that used in Figure 1.

If the tracking loops can be modeled as simple second-order linear systems with constant damping ratio (0 to 5 was assumed after Figure 2), then it is possible to determine analytically what the root mean square of the random component of time difference will be as a function of filter bandwidth. Figure 4 shows this relationship, where the filter is characterized by its time constant and acceleration gain $\left(\text{-3dB bandwidth} = \omega = \frac{1}{\pi}\sqrt{K_A},\ \tau = \frac{1}{\sqrt{K_A}} = \frac{1}{\pi\omega}\right)$. Also plotted in Figure 4 are some experimental points obtained with the Micrologic 3000 receiver in a single, stationary location with various levels of SNR and two tracking loop bandwidths. As it can be seen, there is general agreement between experimental results and the simple linear model.

Such simple linear models, if assumed valid, can then be used to optimize the tradeoff between acceleration-induced errors, which increase with reduced tracking loop bandwidth, and the random component of TD, which increases with increased tracking loop bandwidth. Figure 5 shows the 2-σ TD error versus SNR, resulting from choosing a bandwidth such that the acceleration-induced bias (at the level of acceleration indicated by the curve label) equals the 2-σ TD random noise at each SNR value. Marked along the curves are the optimal loop gains in each case. As can be seen, the resulting system performance is significantly lower than that which would be expected from a cursory look at Figure 4 (0.1 μsec is approximately 60 feet or 20 meters).

Performance at the sub-microsecond level of accuracy, as seems to be feasible in view of the results of Figure 5, requires that the Loran-C signal field itself be consistent to that accuracy in the area around the datum point in which operations will be carried out. A survey of measured TD's in the vicinity of Hanscom AFB, MA, indicates that there may be local distortions in the stationary Loran-C electromagnetic field much larger than 1 microsecond. Figure 6 shows vector differences between TD-derived and map-derived antenna positions around the base; the reference

TD's were selected so as to zero the sum of these vector differences, and thus can be interpreted as an "area average" ASF correction. Figure 7 summarizes those vector differences in a single plot; of interest is that the dispersion seems largest in the direction of the gradient of the second pair of stations, which happen to have the largest SNR in the area. As it can be seen, the 2-σ error is about 1 microsecond.

It was postulated that these large stationary differences might have been caused by large terrain features, metallic structures (e.g. hangars) and CW interference (e.g. power lines) in the area. Thus a second set of experiments, depicted in Figure 8, was carried out over a flat, obstacle-free area. Two hundred and eighty data points were taken at each location in a grid 300 ft by 200 ft in side, at 100 feet intervals. The resulting sampling error of estimate of the mean of each sample is less than 1 m. As can be seen, the differences between actual and (averaged) measured position are of the order of 10 to 20 meters (the point with zero difference was taken as the "anchor point" and the average TD's used as the reference TD's). We have labeled this repeatable distortion field "microdeformation" and intend to further explore this effect, both at ground level and at altitude, using NASA-supplied kitoons (kite-balloons).

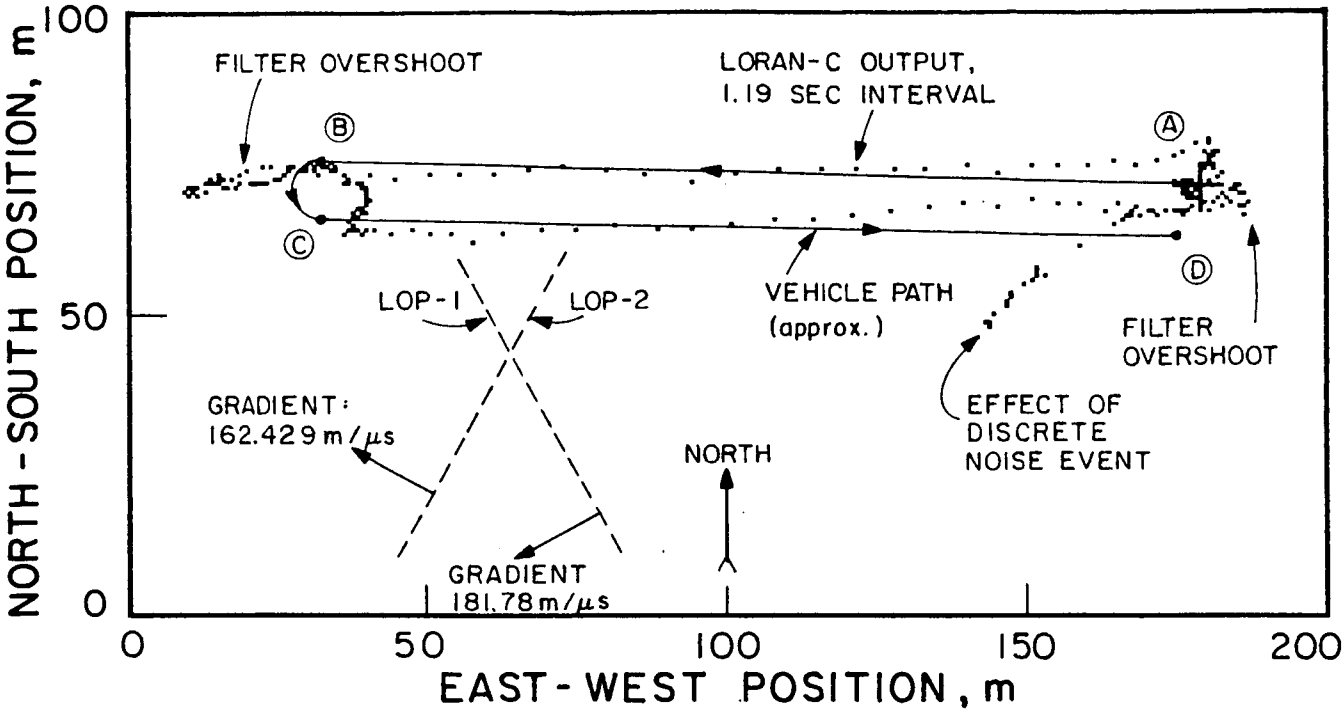

Figure 1. Vehicle-mounted relative Loran-C test (loop time constant was 18 seconds).

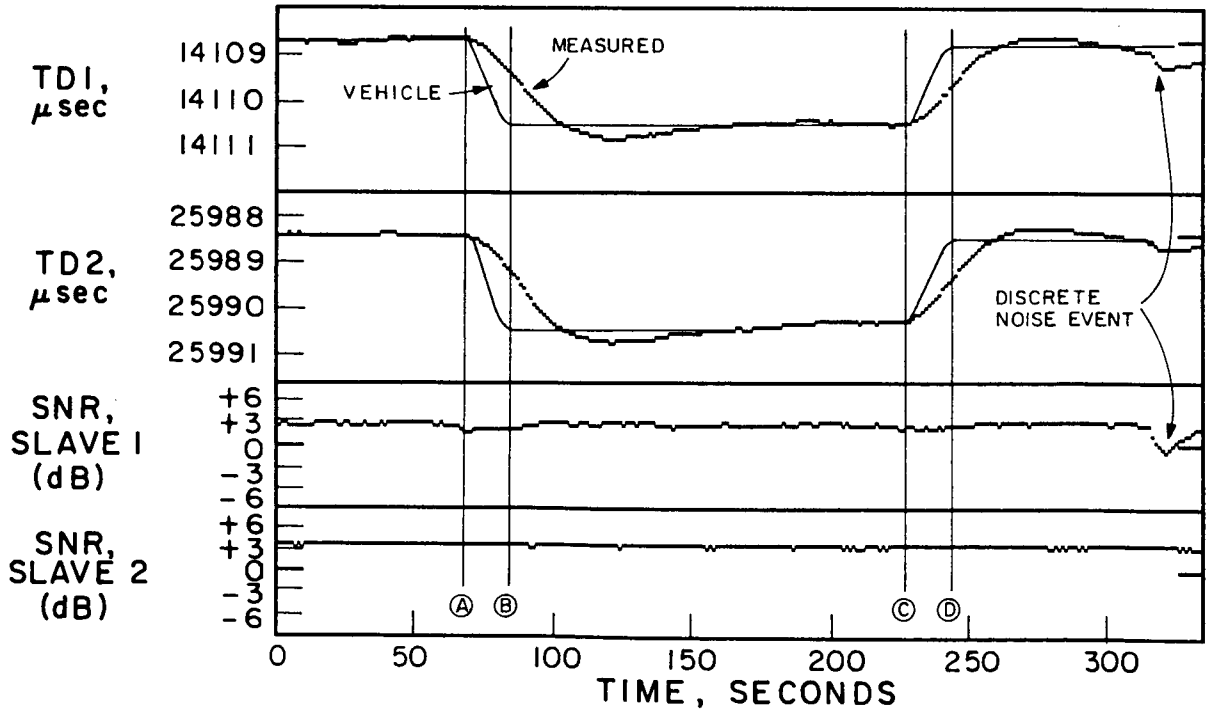

Figure 2. Measured and theoretical time differences and measured SNR's for the test of Figure 1.

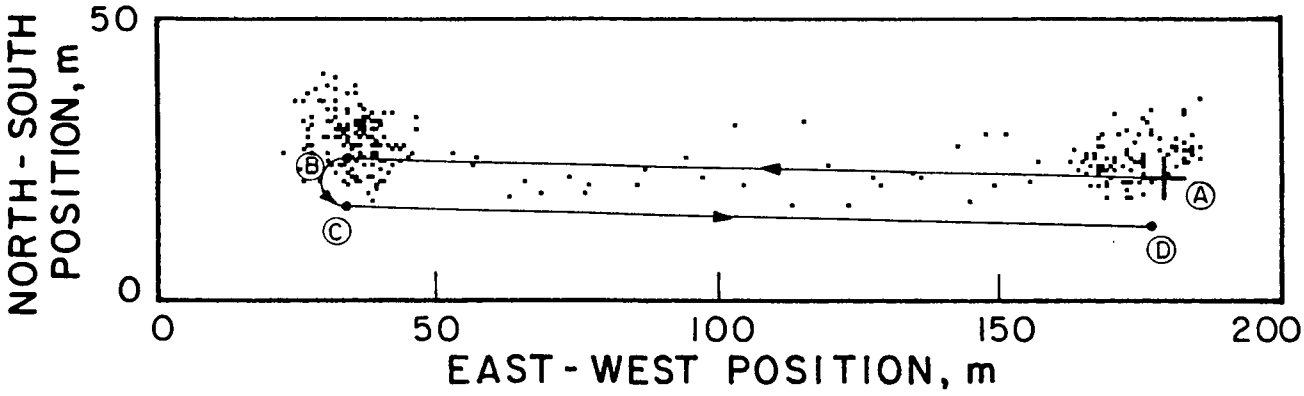

Figure 3. Vehicle-mounted test (loop time constant was 4 seconds).

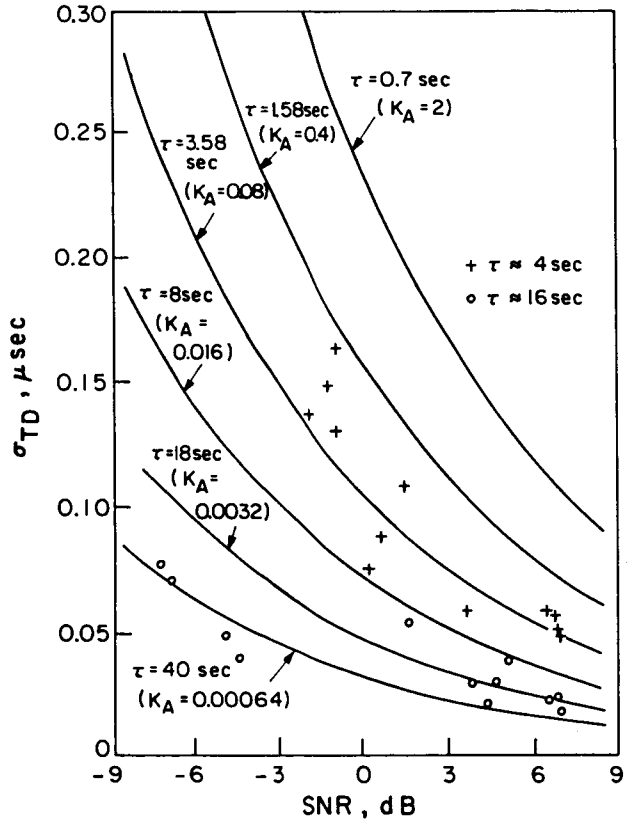

Figure 4. Theoretical and measured time difference variances as a function of SNR for various loop time constants.

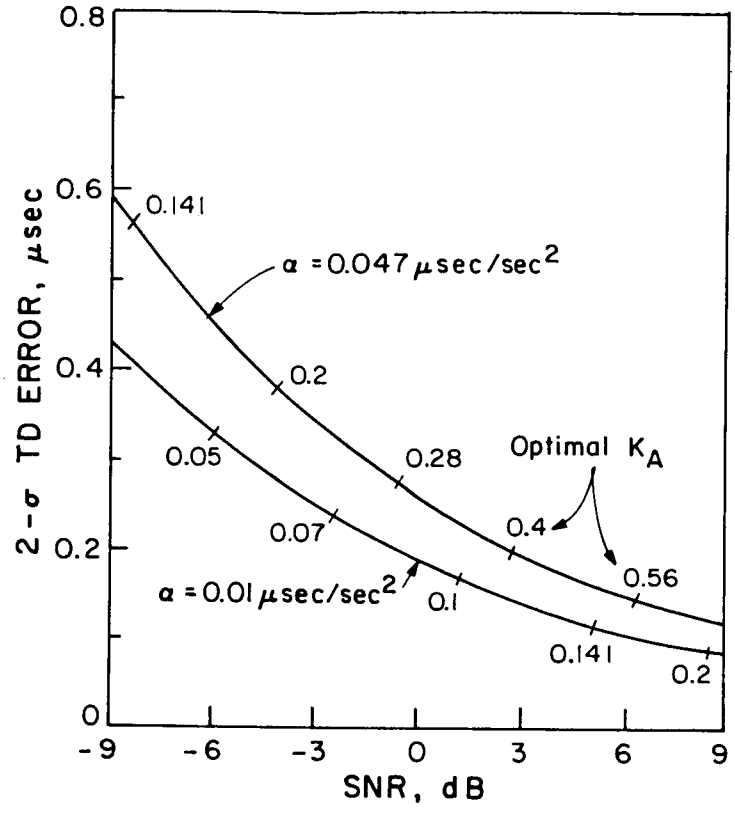

Figure 5. The 2-σ error as a function of SNR for balanced-design loop time constants.

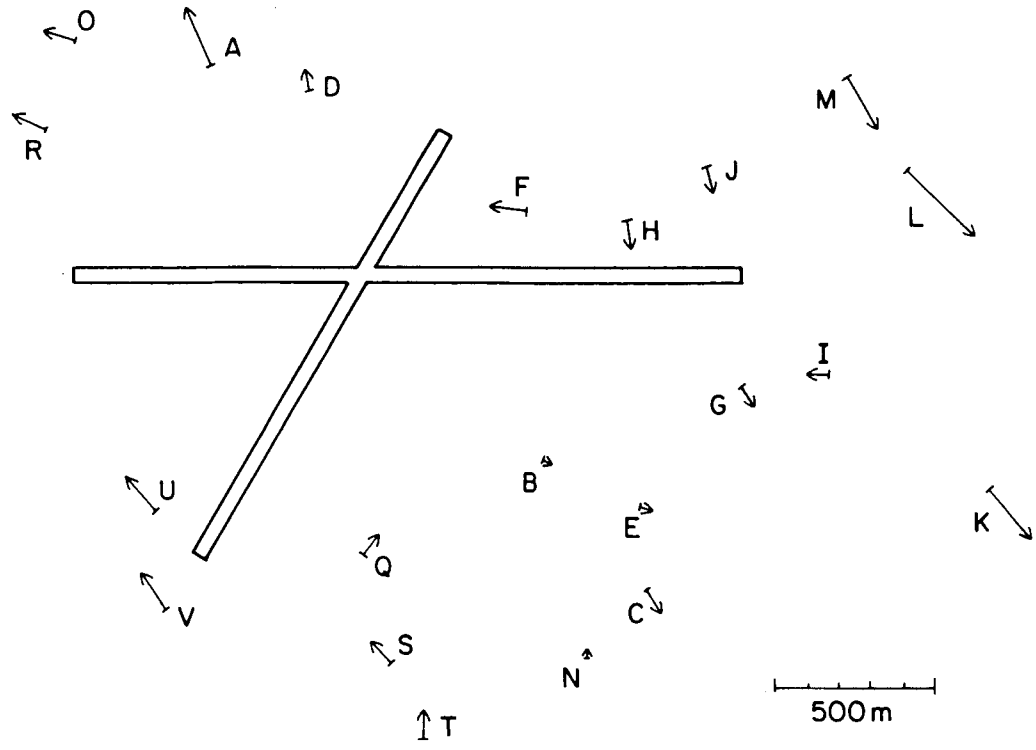

Figure 6. Differences between actual and relative Loran-C derived positions around Hanscom AFB, MA.

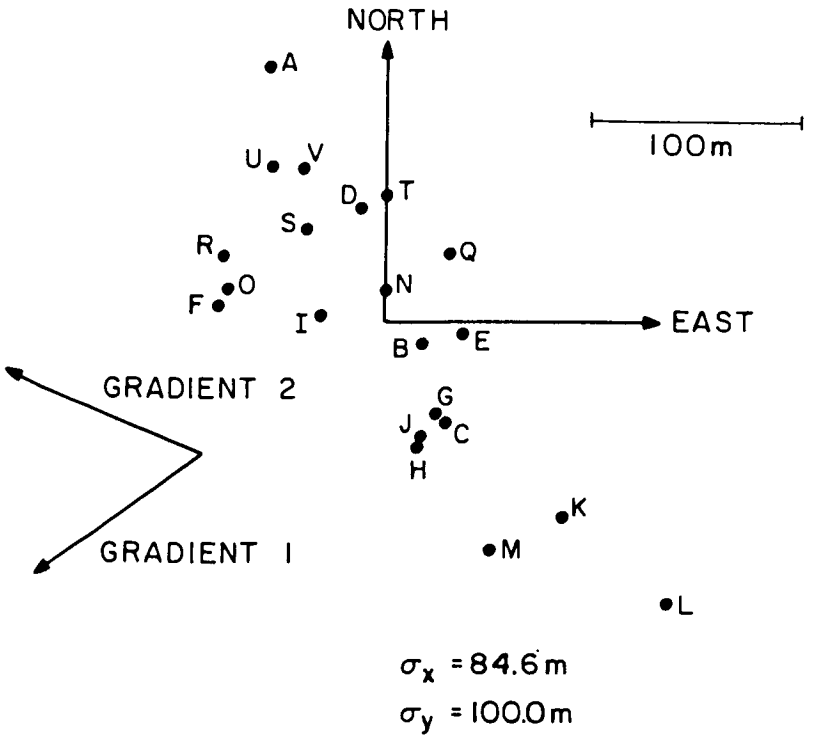

Figure 7. Distribution of the position errors of Figure 6.

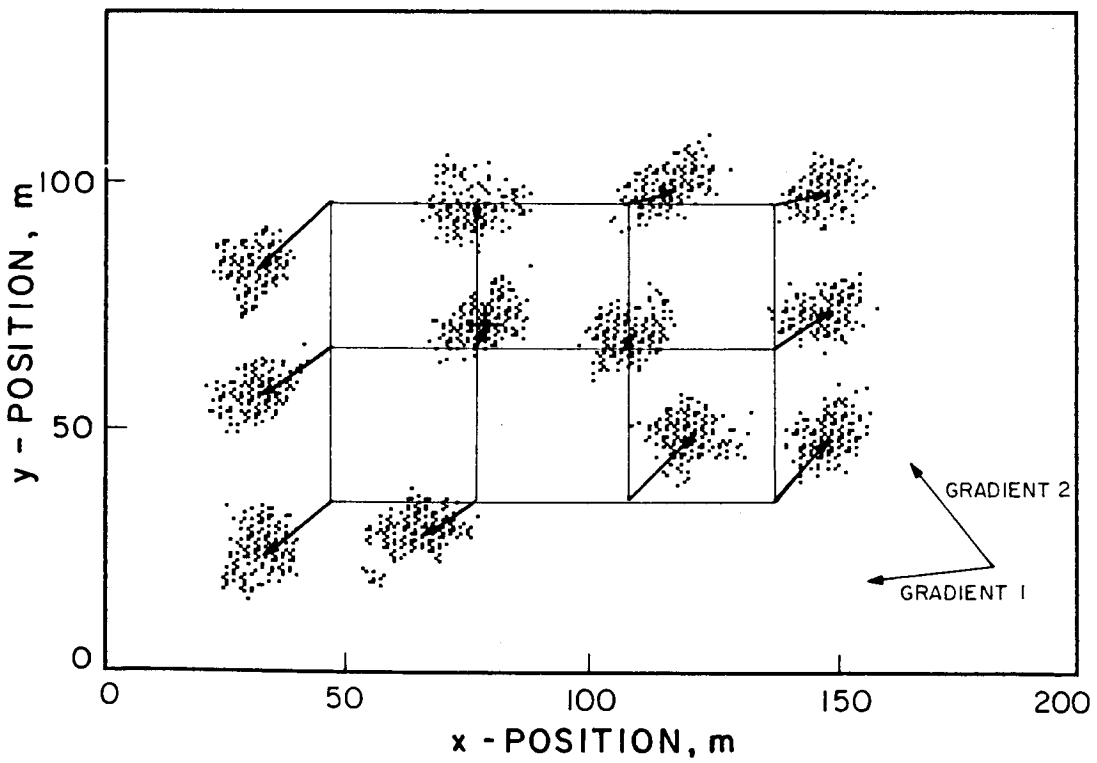

Figure 8. Actual and relative Loran-C derived position over open terrain.

PROBABILISTIC MODELING OF LORAN-C FOR NONPRECISION APPROACHES

N87-22607

John K. Einhorn
Massachusetts Institute of Technology
Cambridge, Massachusetts

Abstract

The overall idea of this work is to predict the errors to be encountered during an approach using available data from the U.S. Coast Guard and standard normal distribution probability analysis for a number of airports in the North East CONUS.

The work consists of two parts: an analytical model that will predict the probability of an approach falling within a given standard (AGS, a given standard), not necessarily AC90-45A), and a series of flight tests designed to test the validity of the model.

GOALS

- Develop a mathematical model that will predict the probability that an approach using LORAN-C will fall within a given standard (AGS).

- Conduct flight tests to determine the validity of the model.

This figure outlines the mathematical model. A computer program takes as input geometrical considerations such as receiver and transmitter location, and propagation factors such as update frequency (these factors to be explained in the next figure). From these, a position error ellipse is created. The probability of falling within the ellipse is known and can be adjusted by varying its size. Once along- and cross-track error standards are chosen, such as those in AC90-45A, these will be compared with the error ellipse, and a probability of falling within the standard will be computed.

MATHEMATICAL MODEL

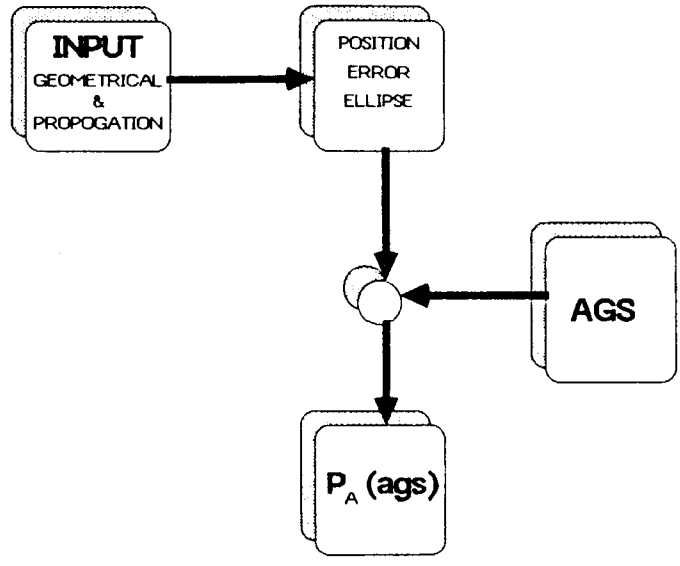

This figure shows the completed work. The program that creates the position error ellipse has been completed and is in FORTRAN. It takes into account runway heading, touchdown point, and chain and slaves, all of which are self-explanatory. The program also needs expected standard deviations of the TD coordinates. These are broken down into long-term and short-term σ's. The short-term σ is on the order of 1 to 5 minutes, and the long-term σ is on the order of weeks and months. The long-term σ is a function of what is called "update frequency." This assumes that the TD's of the touchdown point are updated on certain intervals, such as every 8 weeks, with the publication of approach plates. Using two slaves and their respective σ's, a position error ellipse is generated.

COMPLETED WORK

Program that computes ellipse semi-diameters.

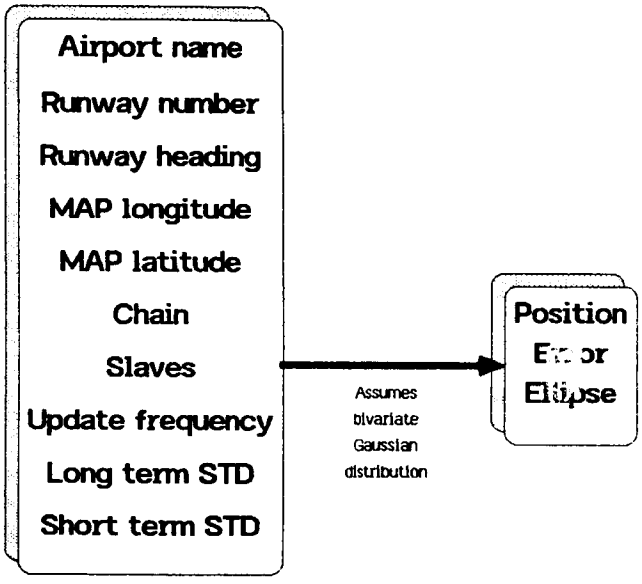

A way must be found in the future to accurately predict the long term σ. Two routes to be investigated are 1) looking at seasonal variations in the Loran signal, and 2) looking at the U.S. Coast Guard "Double-Range difference (DRD)" model. In addition, the short-term must be predicted. Possibilities are:

1) Picking a σ needed to achieve AGS and calculating necessary SNR to achieve that σ. In order to make the approach, the SNR must be at least that high.

2) Examine models for σ as a function of distance from transmitters.

3) Use the "DRD" model to predict σ.

Finally, the probability that an approach will be inside AGS by looking at how much probability inside the ellipse is within the overlayed standard (most likely through numerical integration) must be completed.

FUTURE WORK

- Long term STD modeling
  - Seasonal changes
    - USCG "DRD" model
- Short term STD modeling
  - Pick a short term STD, minimum SNR to achieve that accuracy
  - Models for STD as a function of distance from transmitters
  - "DRD" model to predict STD
- Compute what % of ellipse is inside AGS

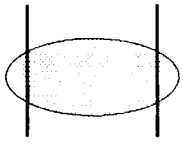

This is a simple "definition" of the Coast Guard "Double-Range difference" model, the key to which is the so-called "Double Range difference" (DRD).

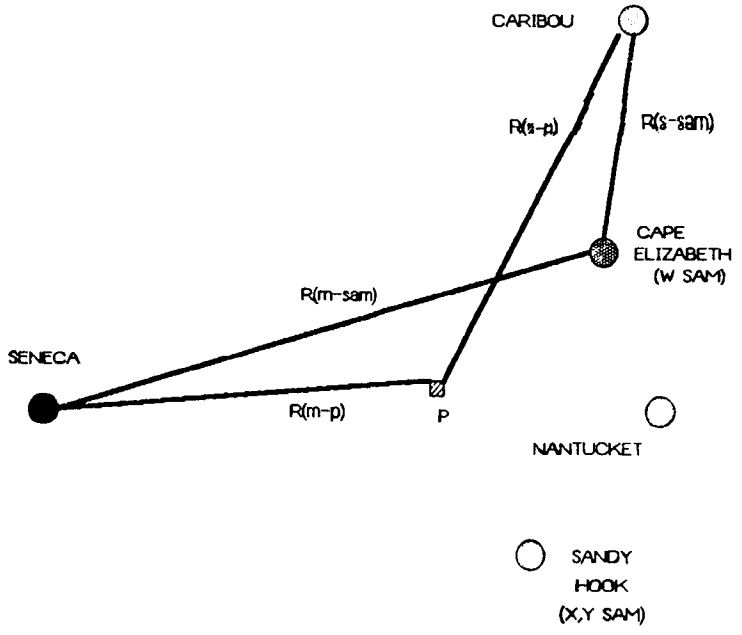

DRD={ R(s-p) - R(m-p) - [R(s-sam) - R(m-sam)] }

This figure outlines the basic idea for the flight tests.

1) Choose airports that have both good and poor probabilities of falling within AGS

2) Fly approaches to those airports using recorded data from the ILS localizer as a "control" reference

3) Eliminate error due to pilotage, using ILS data

4) Plot path that Loran says was flown.

The equipment needed to go up in the tests (for which a pallet is being constructed) includes:

1) Apple II Plus with disc drive and monitor

2) Loran-C (Micrologic ML-3000)

3) Power inverter

4) Gel-cell batteries to power equipment

FLIGHT TESTS

- Pick several airports with both "good" and "bad" probabilities

- Compare LORAN to ILS localizer error for X-track and use visual references for along track error.

Work in progress

- Building a pallet to carry equipment

N87-22608

MEASUREMENT OF ICE ACCRETION USING ULTRASONIC PULSE ECHO TECHNIQUES

R. John Hansman, Jr. and Mark S. Kirby
Dept. of Aeronautics and Astronautics
Massachusetts Institute of Technology
Cambridge, Massachusetts

This figure shows the need for ice accretion measurement.*

- Operational (rotary and fixed wing)
  - Avoidance & Escape (requires icing rate)
  - C & W
  - Management of Ice Protection Systems
    - Boots
    - Electrothermal
- Research
  - Support Ice Modeling Efforts
    - Time Dependence
  - Document Meterological Conditions
  - Certification

*Original figures in this paper not available at time of publication.

This figure depicts the basic concept of ultrasonic pulse-echo measurement. The thickness of the ice is related to the pulse-echo time T_{P-E} by the speed of sound C.

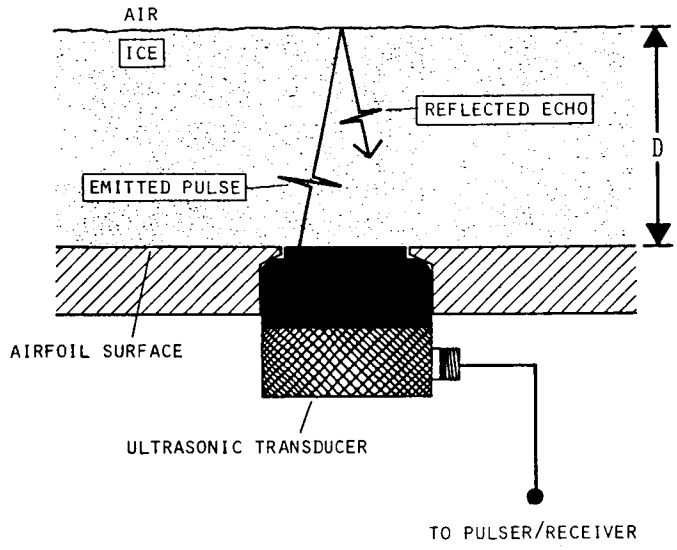

$$D = \frac{C_{ICE} T_{P-E}}{2}$$

This figure shows a typical pulse-echo signal, showing multiple echoes from the ice-air interface.

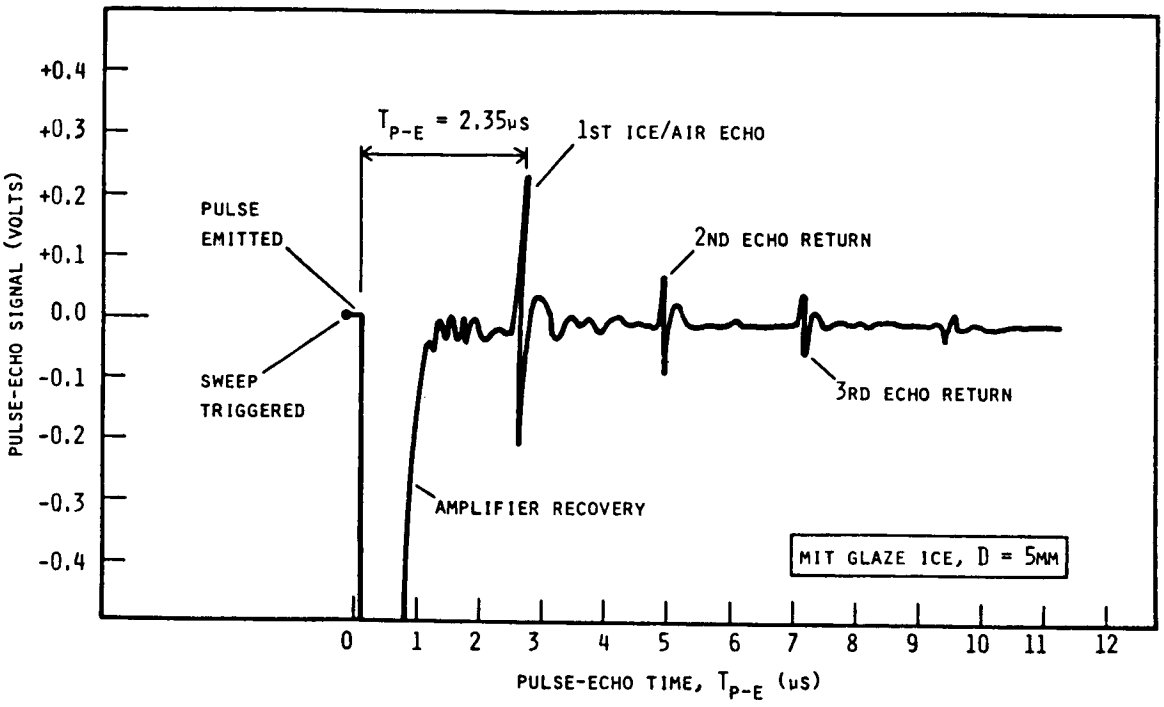

The results of static calibration tests on a variety of NASA and MIT ice samples are shown in this figure. The speed of sound appears to be insensitive to ice type, with a value of approximately 3.8 mm/sec.

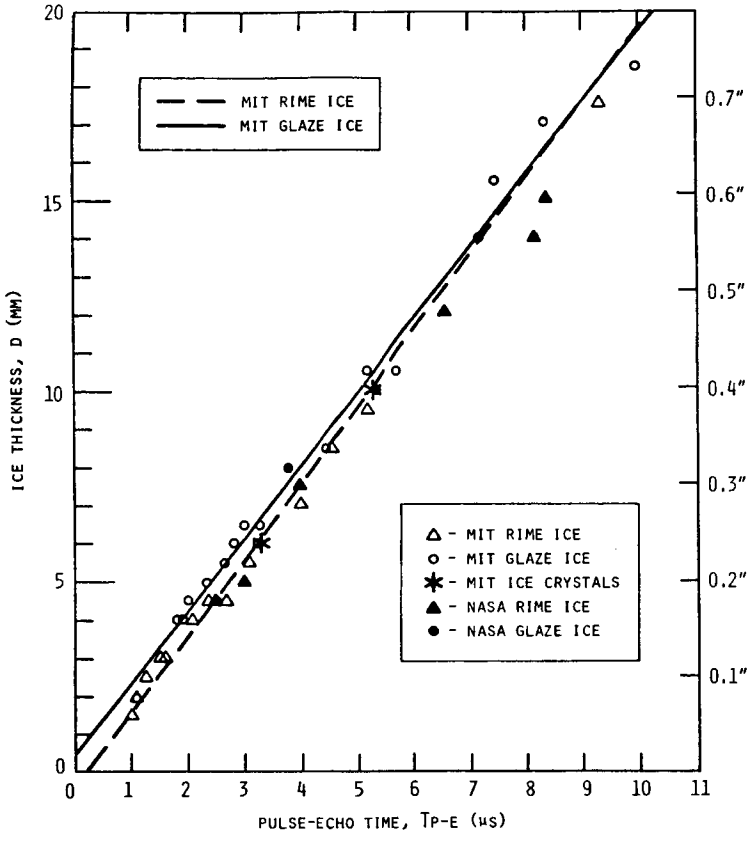

This figure is a schematic of the setup for ice accretion tests in the Icing Research Tunnel (IRT). Several transducers were mounted on a 4-in. diameter cylinder in the IRT. Echo patterns were videotaped during icing exposures under a variety of conditions.

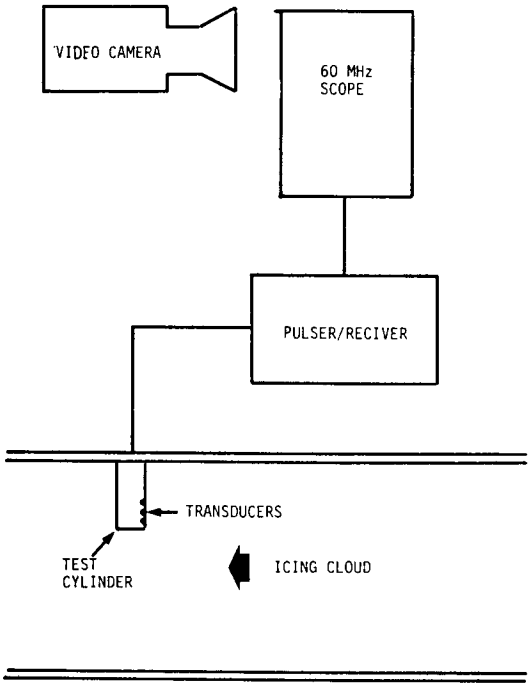

The location of the test cylinder in the IRT is shown in this figure. It should be noted that the cylinder is not in the calibrated region of the tunnel.

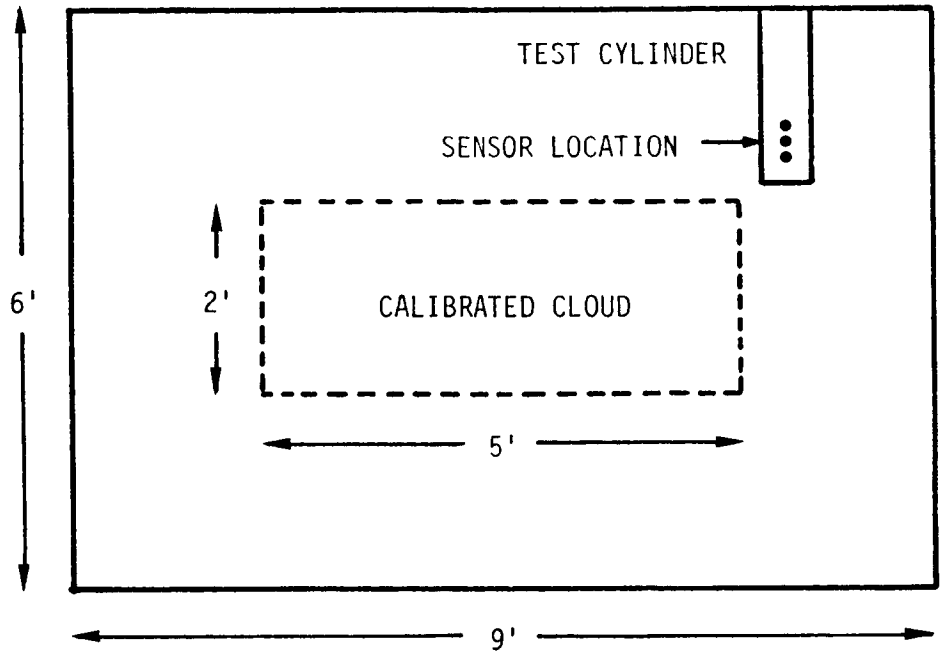

This figure shows typical echo patterns for rime and glaze ice. The echo is broadened in the glaze case due to the irregularity of the air-ice interface.

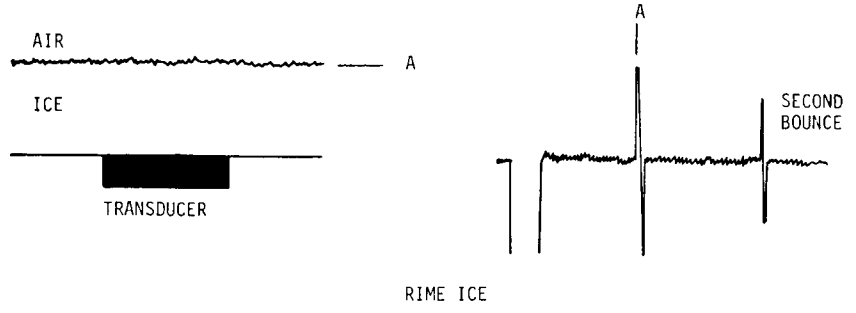

RIME ICE

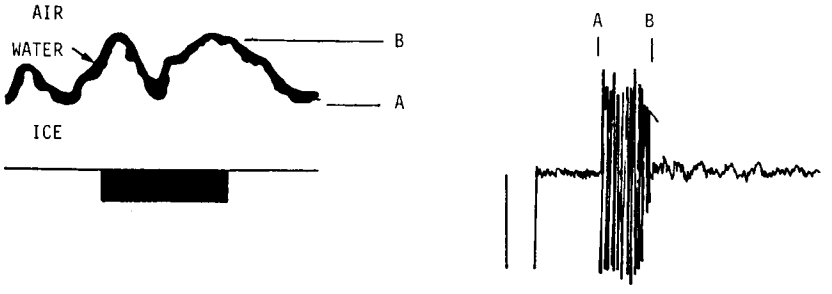

This figure shows typical echo patterns for thin ice samples in which the pulse-echo time is shorter than the recovery time of the amplifier. The echo signal can be delayed by use of a delay line. For normal transducers, the pulse-echo time can be inferred from the time between multiple echoes.

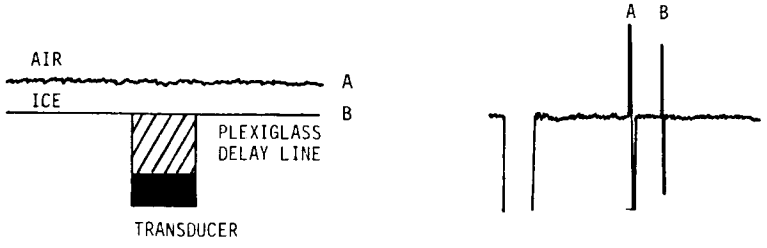

DELAY LINE TRANSDUCER

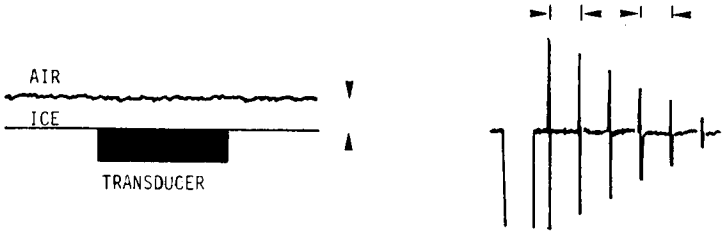

A typical echo pattern for glaze ice with surface water present is shown in this figure. Surface waves in the water cause fluctuations in the echo pattern. This technique should allow accurate determination of the conditions under which runback occurs.

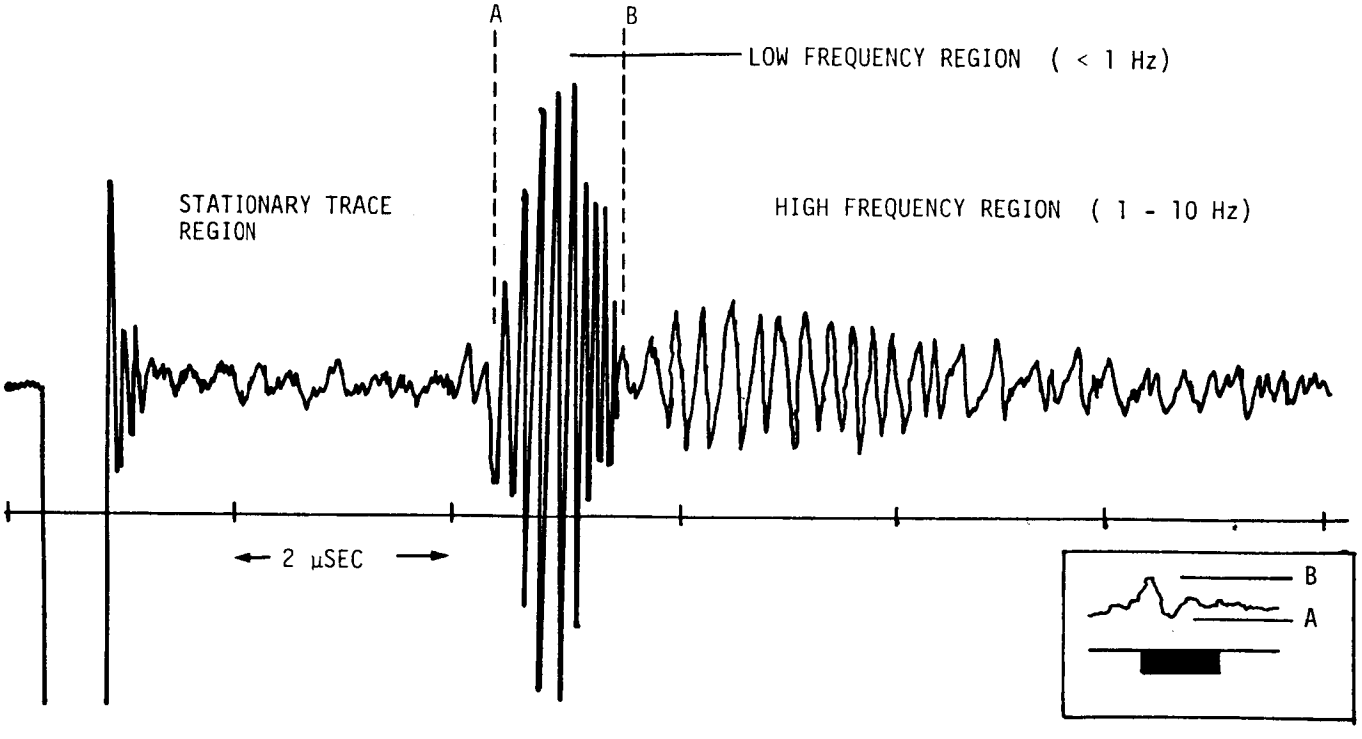

This figure shows ice thickness measured by the ultrasonic technique versus icing time for heavy icing conditions.

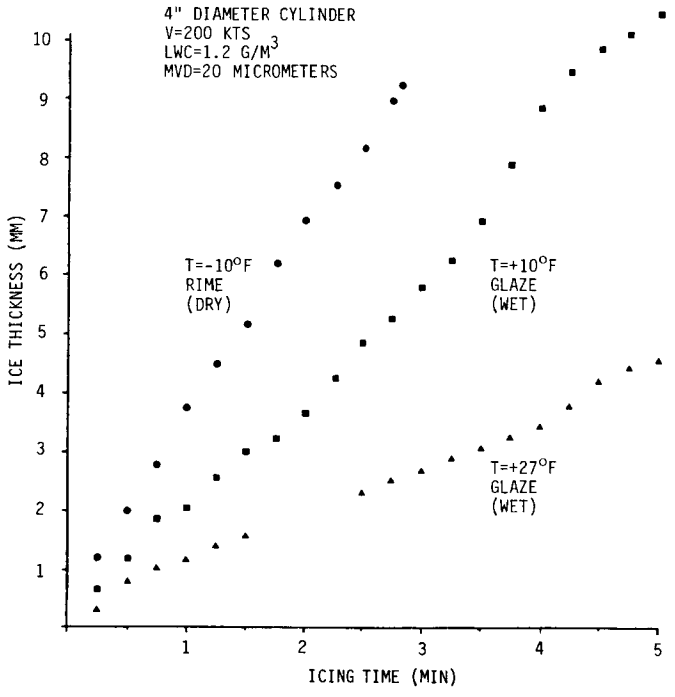

Shown below is the ice thickness measured by the ultrasonic technique versus icing time for light icing conditions.

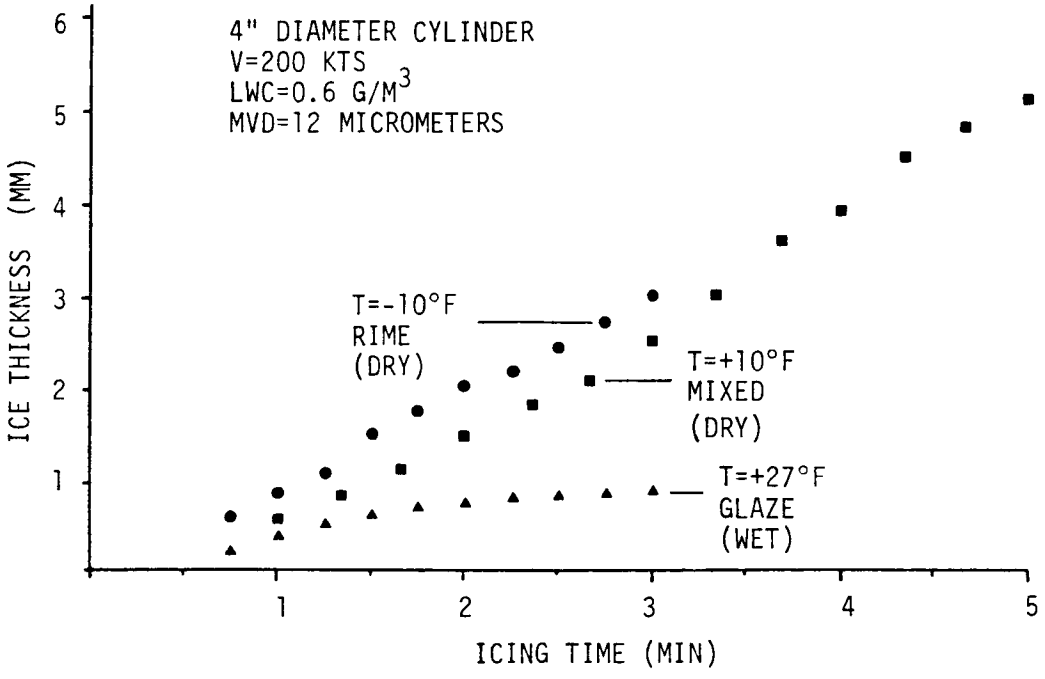

This table summarizes the icing rates measured in the IRT, as well as the presence or absence of surface water.

ICING RATES FOR A 4" CYLINDER IN THE IRT

V=200 KTS (CYLINDER WAS NOT IN CALIBRATED REGION)

TEMPERATURE	+27°F	+10°F	-10°F
HEAVY ICING CONDITIONS	0.75 MM/MIN	2.10 MM/MIN	3.15 MM/MIN
LWC=1.2 G/M^3	GLAZE	GLAZE	RIME
MVD=20 µM	WET	WET	DRY
LIGHT ICING CONDITIONS	0.55 MM/MIN	1.05 MM/MIN	1.05 MM/MIN
LWC=0.6 G/M^3	GLAZE	MIXED	RIME
MVD=12 µM	WET	DRY	DRY

This figure shows the ice growth and echo patterns for a glaze ice run. The top trace is the delay line echo. The bottom trace is the normal transducer echo.

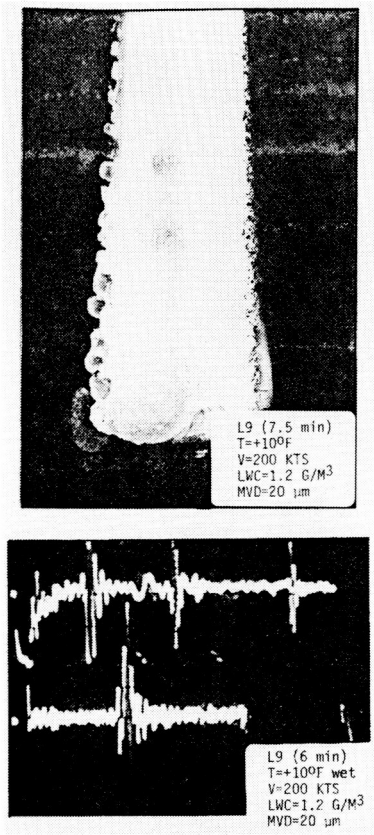

This figure shows the ice growth and echo patterns for a rime ice run. The top trace is the delay line echo. The bottom trace is the normal transducer echo.

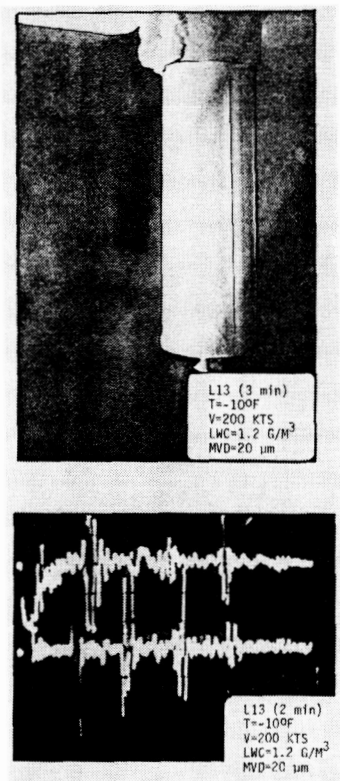

This figure is an example of ice thickness versus time for a horn ice growth.

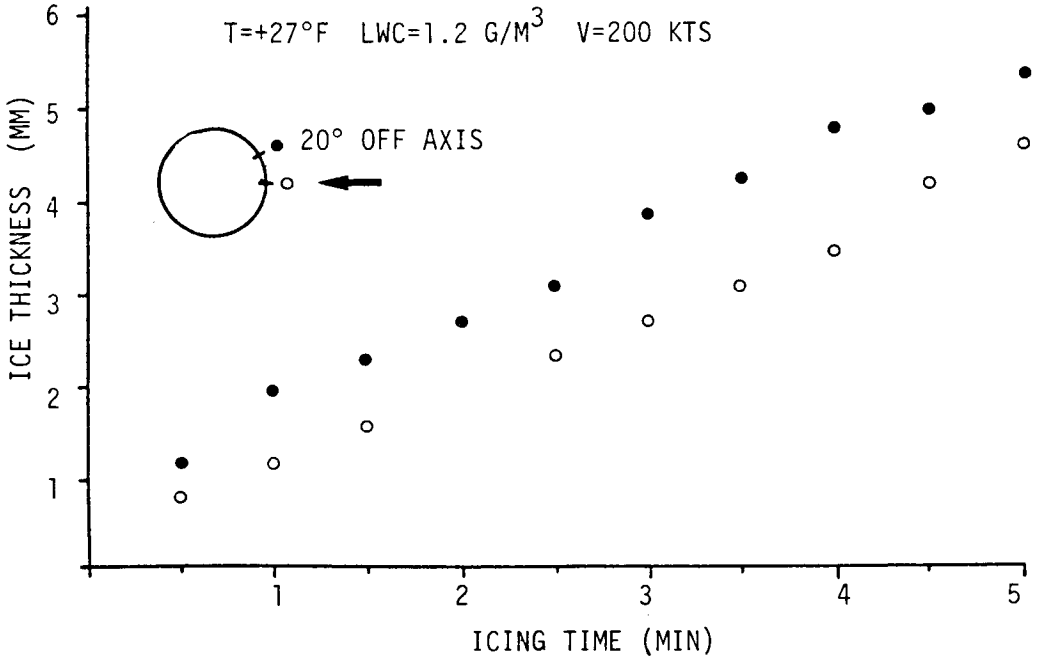

This figure shows ice thickness versus icing time for the multiple-echo resulting from an ice ridge growing over the transducer in glaze conditions.

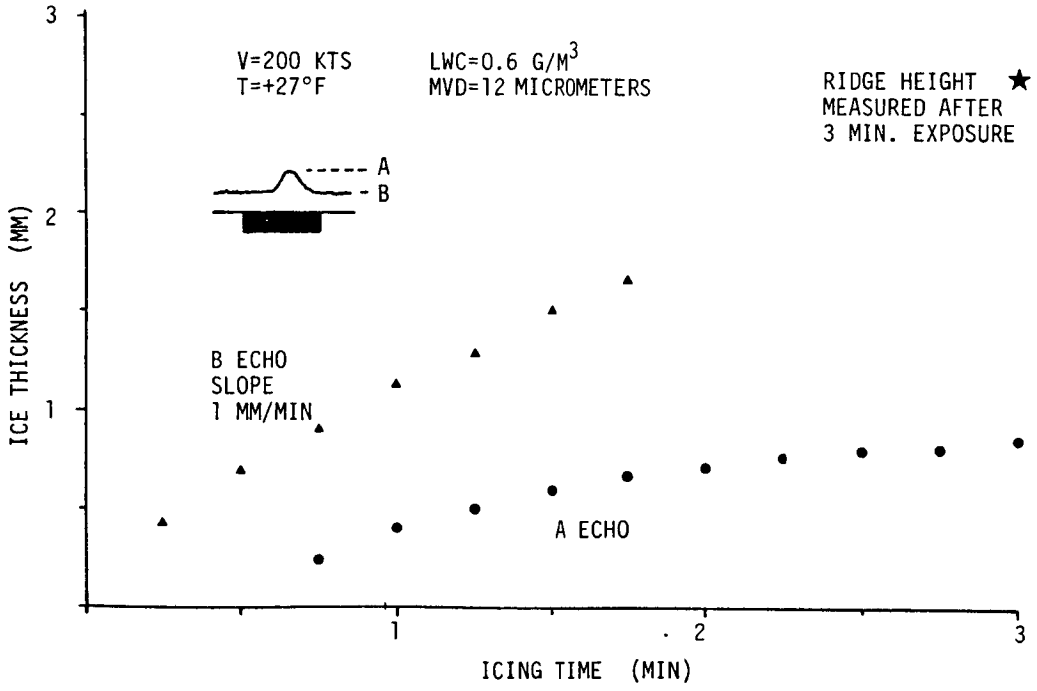

INVESTIGATION OF AIR TRANSPORTATION TECHNOLOGY AT OHIO UNIVERSITY, 1984

Richard H. McFarland
Ohio University
Athens, Ohio

INTRODUCTORY REMARKS

The year 1984 was one of transition, change, and growth for the Joint University Program for Air Transportation at Ohio University. The Loran-C work changed direction from that of receiver hardware development to the operational development of Loran-C for enroute navigation and non-precision approaches. Mr. Stanley M. Novacki III returned from his intern residency at NASA Langley Research Center and continued his work on the DATAC data bus monitor. During the summer, participation in a promotional effort resulted in the Federal Aviation Administration joining NASA Langley Research Center in supporting this program. This partnership allowed for increased funding to the JUP universities and, at Ohio University, allowed for the formation of three new research areas: global positioning system test-bed receiver development; fiber optic data bus applications in general-aviation aircraft; and advanced remote monitoring techniques.

One of the last hardware upgrades to the Ohio University Loran-C receiver was performed under the direction of Dr. Robert W. Lilley. The Memory Aided Phase Locked-Loop (MAPLL) developed for the O.U. Loran-C receiver was modified to reduce the number of devices required to control the MAPLL and to improve the efficiency and speed of the 6502 MAPLL device driver software. These modifications have been documented by Lilley in Ohio University NASA TM 90 (ref. 1).

One of the operational problems with using the O.U. Loran-C receiver for enroute navigation studies was due to the calculation of heading and distance to waypoints with respect to true north as opposed to magnetic north. Rajan Kaul, a JUP graduate intern, implemented a magnetic variation model for the continental United States, in FORTRAN IV, on Ohio University's IBM 370 mainframe computer and then in the 6502 machine language for use in the O.U. Loran-C receiver. This work is discussed in further detail by Kaul in Ohio University NASA TM 91 (ref. 2).

Rajan Kaul made a second contribution to the study of the operational enroute capabilities of Loran-C in his master's thesis, "Comparison of Great Circle and Rhumb Line Flight Paths in the Continental United States Using Simulation and Test Flights," also published in Ohio University NASA TM 93 (ref. 3). This paper discusses the discrepancies encountered between the two route structures, particularly over large distances, and the possible conflicts which may arise with their simultaneous use in the national airspace.

The work on the DATAC data bus monitor was initiated by the second NASA Langley Research Center/Ohio University Internship and continued through the work of that intern appointee, Mr. Stanley M. Novacki, III.

Novacki developed a program downloader, plus other utility software, for the DATAC bus monitor unit (documented by Novacki in Ohio University NASA TM 92, ref. 4). His later work involved the development of necessary tools, which with the aforementioned utility programs, provided the working base to complete the DATAC data bus monitor unit.

One of the new areas of research involved the siting of the Ohio University Gordon K. Bush Airport for Loran-C non-precision (NP) approaches. Dr. Robert W. Lilley, Associate Project Director, and Mr. Daryl L. McCall, JUP Project Engineer, have performed most of the required surveying tasks. The results of the survey data will be used in the calculation of the final approach fix (FAF) and approach path for a Loran-C NP approach. It was planned that Lilley, McCall, and an intern would perform flight tests for the purpose of evaluating the defined NP approach path.

Another new area of work involved the development of a reconfigurable GPS receiver test-bed. Work had already begun through the efforts of JUP graduate intern Mr. Samuel J. P. Laube who implemented and tested some antenna designs for use at GPS frequencies. Also, Ohio University planned to receive, as an equipment grant from the FAA Technical Center, Atlantic City, NJ, the dual channel GPS receiver hardware developed by Stanford Telecommunications, Inc. Upon receipt of this hardware, work was to begin to make the unit airworthy as soon as possible. Flight tests of the dual channel receiver were planned to examine the enroute capabilities of GPS.

The new effort to develop a fiber optic data bus was begun through work by JUP undergraduate intern Mr. Steve Shreve. This work was enhanced by corporate gifts from Aero Mechanisms, Chatsworth, CA and Electrosonics, Columbus, OH. The supporting gift items consisted of two blind encoding altimeters, two digital altitude displays, and an encoding transponder. This equipment, which normally requires a twelve conductor data bus, was to be serially interconnected by a fiber optic cable. Once the fiber optic hardware was developed and laboratory tested, several flight tests/experiments were to be considered.

The third area of new work involved the application of image processing techniques to monitor facilities remotely, such as antenna arrays, whose operation may be sensitive to various unexpected obstructions (e.g. fallen trees, ground slippage, vehicles, etc.). This work was to involve the use of Ohio University's COMTAL Vision One image processor with either the University's IBM/370 or the Department of Electrical and Computer Engineering's VAX 11/750. Digitized photographs, and later, actual data from navaids sites, were to be used to develop and demonstrate processing and data transmission techniques for successful monitoring.

REFERENCES

1. PROCESSOR-CONTROLLED TIMING MODULE FOR LORAN-C RECEIVER, Robert W. Lilley, February 1984, OU NASA TM-90.

   Hardware documentation is provided for the modified Loran-C timing module, which uses direct software control in determining loop sample times. Computer loading is reduced by eliminating polled operation of the timing loop.

2. A MICROCOMPUTER-BASED SYSTEM TO COMPUTE MAGNETIC VARIATION, Rajan Kaul, March 1984, OU NASA TM-91.

   A microcomputer-based implementation of a magnetic variation model for the continental United States is presented. The implementation computes magnetic variation as a function of latitude and longitude for general aviation receivers such as Loran-C.

3. COMPARISON OF GREAT CIRCLE AND RHUMB LINE FLIGHT PATHS IN THE CONTINENTAL UNITED STATES USING SIMULATION AND FLIGHT TESTS, Rajan Kaul, November 1984 (M.S. Thesis), OU NASA TM-93.

4. A PROGRAM DOWNLOADER AND OTHER UTILITY SOFTWARE FOR THE DATAC BUS MONITOR UNIT,
   Stanley M. Novacki, III, July 1984, OU NASA TM-92.

   A set of programs designed to facilitate software testing on the DATAC Bus Monitor is described.

N87-22610

DIGITAL AUTONOMOUS TERMINAL ACCESS COMMUNICATION SYSTEM (DATAC)

Stanley M. Novacki, III
Ohio University
Athens, Ohio

In order to accommodate the increasing number of computerized subsystems aboard today's more fuel-efficient aircraft, the Boeing Company has developed the DATAC (Digital Autonomous Terminal Access Control) bus to minimize the need for point-to-point wiring to interconnect these various systems, thereby reducing total aircraft weight and maintaining an economical flight configuration. The DATAC bus is essentially a local area network providing interconnections for any of the flight management and control systems aboard the aircraft. The bus itself is passive: a twisted-pair, coax, or fiber-optic line with stub connectors for each DATAC terminal, the device which interfaces the various subsystems with the bus. DATAC uses a line-topology and CSMA (Carrier Sense, Multiple Access) protocol, much like the commercial Ethernet local-area network proposed by Intel and Xerox, which is in use in many large offices today. The main purpose of the Bus Monitor Unit is to receive all data which appear on the bus, reconstitute it into "real-word" parameters (e.g., altitude, heading, etc.), and display it in an easily interpreted form. This provides an indication of the overall operation of the bus without the liability of a total system failure caused by a central controller-type device, which could be disastrous at 35,000 feet.

The task of developing a Bus Monitor Unit can be broken down into four subtasks: 1) Providing a hardware interface between the DATAC bus and the Z8000-based microcomputer system to be used as the Bus Monitor; 2) Establishing a communications link between the Z8000 system and a CP/M-based computer system, which will be used as the Bus Monitor Unit console; 3) Generation of data reduction and display software to output data to the console device; and 4) Development of a DATAC Terminal Simulator to facilitate testing of the hardware and software which transfer data between the DATAC bus and the operator's console in a near real-time environment.

A. DATAC Terminal Interface Card:

The subsystem interface used on the DATAC bus terminals used the ZILOG Zbus system interconnect specification. However, the Bus Monitor test system uses the IEEE-696 bus. An interface card has been developed that will translate the two sets of signals, interchangeably, to allow each system to transfer data to or from the other in the same manner that a DATAC terminal will communicate with a conventional bus subsystem.

B. Software Communications Driver for Z8000 to VT-180:

A program will be written in Z8000 assembly language to detect new data placed in the Bus Monitor memory by the DATAC terminal, reduce it to a format which allows for some kind of error detection (for example, hex-to-ASCII conversion with parity) and transmit it via an RS-232C line to the Digital Equipment Corporation VT-180 microcomputer serving as the BusMon system console.

C. DATAC Bus Data Analysis and Display:

The actual reduction of data from the DATAC bus initially will be performed by a VT-180 using the "C" language. There are several reasons for

this approach: the Z8000 microcomputer will eventually perform most of the operations planned for the Bus Monitor Unit. At this time, however, few development tools can be used on this configuration of a Z8000 system. Further, the Bus Monitor processor system does not currently support any type of mass storage devices, printers, or other peripherals useful for prototype work. The intent is, then, to develop the Bus Monitor software using the standard "C" language under the CP/M operating system for which there are a variety of software development tools. Once the software is completed and tested, any functions that can be supported by the Z8000 system hardware can be transported to that system via a "C" cross-assembler targeted for that system. Also, the ease of writing involved algorithms in a higher-level language facilitates the programming of data analysis tasks, ordinarily cumbersome to write in assembly language. Additionally, a higher level language is portable; the Bus Monitor functions can be transported to a system based on another processor with little additional programmer time should Boeing and NASA decide that a different hardware configuration is needed. Thus, the investment in software is guarded against obsolescence in the event of a system hardware change or eventual upgrade.

D. DATAC Terminal Simulation:

A DATAC terminal simulator is needed because, at present, the only operational model of the DATAC subsystem interface exists on an active DATAC system. A programmable terminal simulator offers the flexibility needed to test and properly debug the Bus Monitor Unit hardware and software under a variety of conditions, something not easily done using an actual DATAC system.

CURRENTLY ENVISIONED BUS MONITOR FUNCTIONS

In order for the BusMon unit to provide a useable picture of the operation of the DATAC bus, it must be able to evaluate the data which appears on the bus and present it in an operator recognizable format. Since bus protocol violations and communications errors (e.g., parity errors, missing words, etc.) are detected by the DATAC terminal hardware and are never seen by any bus subsystem, the Bus Monitor software will address itself to problems determined by the data content of messages from other DATAC terminals:

1. Echo check of Terminal/System Interfaces: BusMon will verify proper operation of other subsystem hardware by means of a transmit block after receive block directive from the BusMon to the system in question. This assures integrity of RAM buffers and other terminal interface devices.

2. Major/Minor Frame Useage: The BusMon will be equipped with the bus system transmission schedule. If a system fails to transmit in its allotted time frame(s), the monitor can signal a device failure.

3. Data Stream Interpretation: The format of the data stream allows the BusMon to identify the source and information content

of the serial message. A useful feature of this function is to provide a check on the reasonability of data being placed on the bus by the various other bus subsystems. Reconstitution of bus data by an independent system provides another check on the accuracy of other devices operating on the bus. For example, if a display unit shows unreasonable data items, the problem could lie in the data source or in the display unit. By monitoring the data intended for the display, BusMon can help locate potential hardware problems.

4. Bus Status: The most passive mode of operation simply displays hexadecimal data extracted from the bus, formats and displays it on the BusMon console to provide transmitter ID, word count, and other raw data items.

WHAT IS DATAC?

- Serial data bus for use aboard aircraft
- Various A/C systems communicate via a single twisted-pair, coaxial, or fiber optic line
- No central controller (As used by MIL STD 1553B, system relatively free from central failures)
- Uses Ethernet-like CSMA/CD access protocol
- Line topology of bus allows for easy addition/deletion of systems for maintenance or expansion

SUMMARY OF DATAC ADVANTAGES

*WEIGHT REDUCTION- a single bus could serve a minimum-configuration system

*REDUCED INSTALLATION COSTS AND COMPLEXITY- 1-5 bus lines as opposed to one bus line per system inter-connect

*IMPROVED DIAGNOSTICS AND MAINTENANCE- subsystems could be programmed to provide status information to the bus monitor

*SIMPLE TO MODIFY- line topology of bus allows for easy addition and removal of subsystems

*POWERFUL LOCAL PROCESSING CAPABILITY- a subsystem could employ a specialized processor especially suited for a particular task

*MINIMUM REPLACEMENT TIMES- line bus configuration means plug-in replacement possible

*IMPROVED FLEXIBILITY- system configuration is independent of the bus itself

*NO BUS INTERFACE SOFTWARE- handled by bus terminal hardware

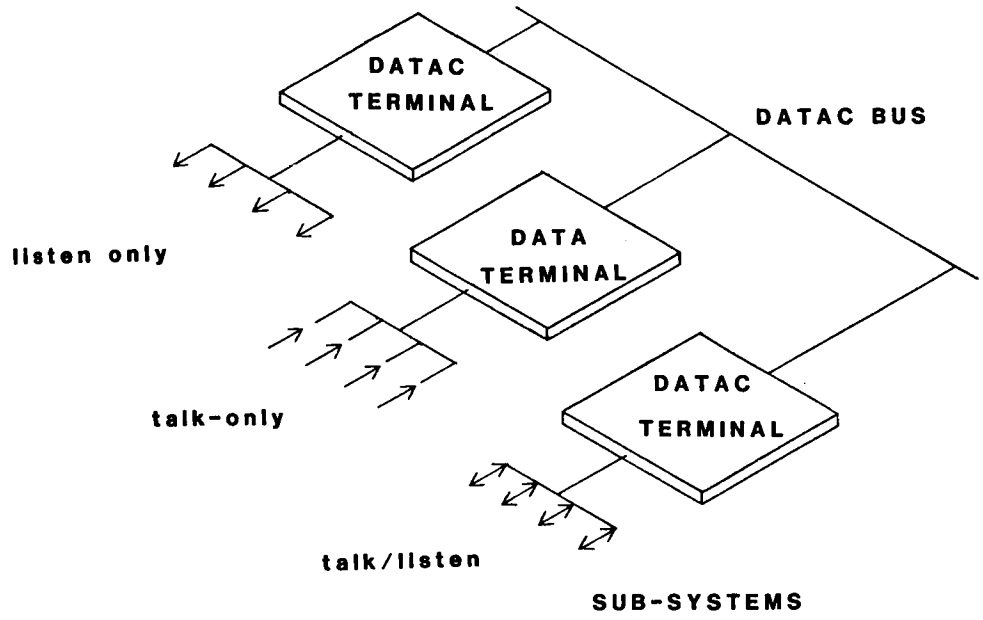

BASIC LAYOUT OF DATAC DATA BUS

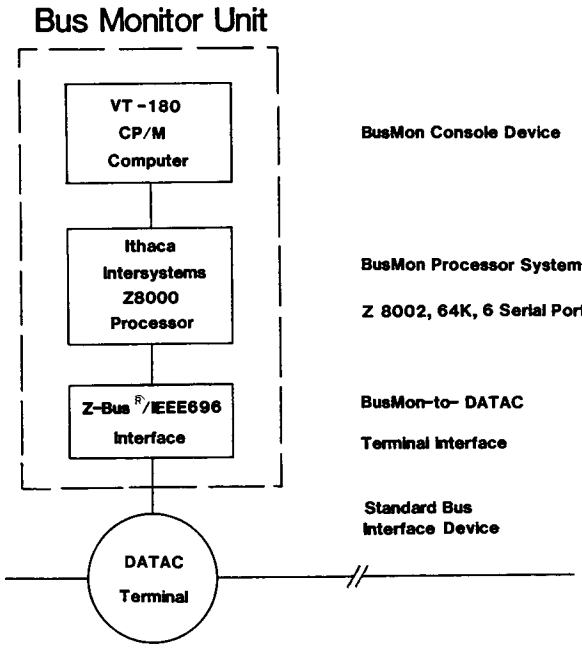

Proposed Bus Monitor Test Configuration

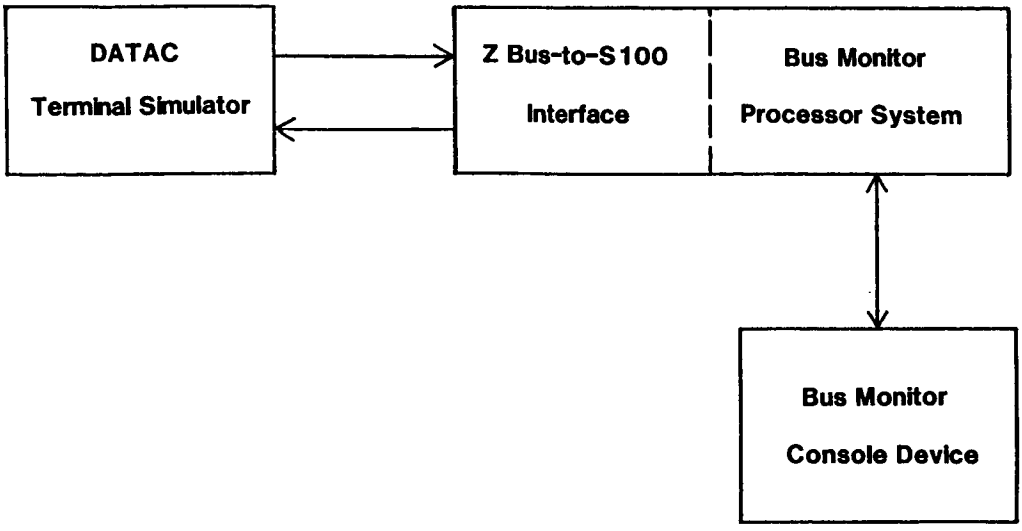

Bus Monitor Software Development System

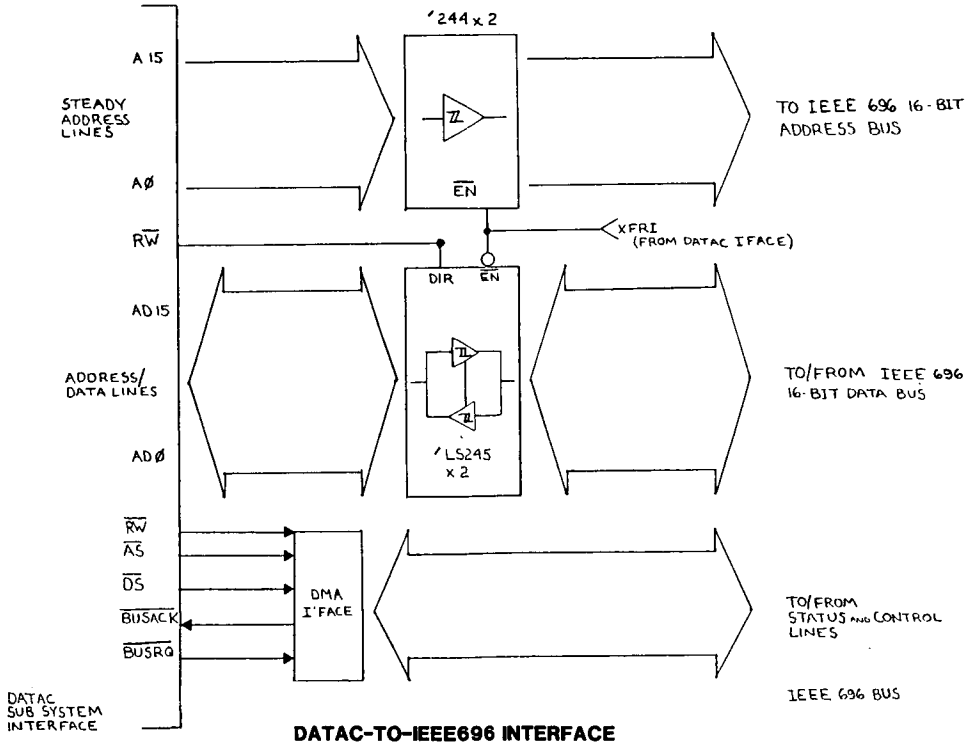

DATAC-TO-IEEE696 INTERFACE

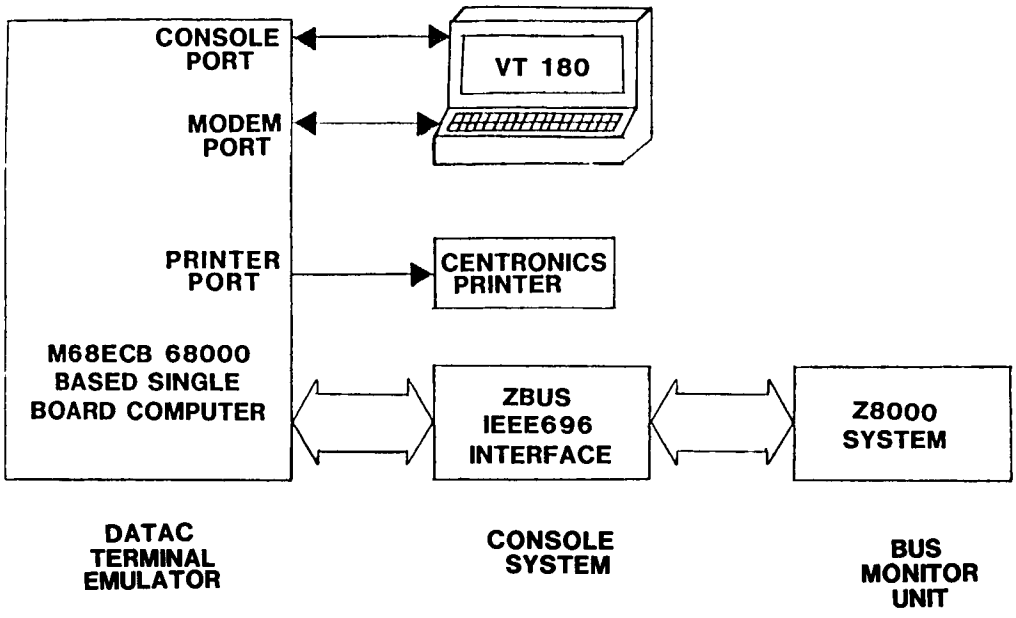

BUS MONITOR SOFTWARE TEST SYSTEM

N87-22611

FIBER OPTIC DATA TRANSMISSION

Steven T. Shreve
Ohio University
Athens, Ohio

Fiber optics (the transmission of light through glass fibers along the inside of plastic tubes) is a relatively new technology in avionics engineering. Present day avionics require sending ever increasing amounts of data through smaller spaces with less interference. Fiber optics appears to be the answer to this demand due to numerous advantages over traditional copper wire communications.

One of the most important advantages of fiber optics to the avionics industry is the weight savings when compared to copper cable. Glass weighs much less than copper, and considering the small size of individual fibers, the weight savings can be significant.

Optical fibers have lower attenuation (the loss of signal intensity as it travels the length of the fiber) than do coaxial cables. The fibers also do not emit energy, thus eliminating the need for shielding.

Greater bandwidth is an important advantage of fiber optic communications. The transmission frequencies of light are several orders of magnitude above those in common cables, allowing greater transfer of information.

With the above facts in mind, the Ohio University Avionics Engineering Center is currently developing a fiber optic data bus transmission and reception system that could eventually replace copper cable connections in airplanes. The original form of the system will transmit information from an encoder to a transponder via a fiber optic cable. An altimeter and an altitude display are connected to a fiber optic transmitter by copper cable (bottom figure). The transmitter converts the altimetry data from nine bit parallel to serial form and sends these data through a fiber optic cable to a receiver. The receiver converts the data using a cable similar to that used between the altimeter and display. The transmitting and receiving ends also include a display readout. After completion and ground testing of the data bus, the system will be tested in an airborne environment.

Thus far, the project has encountered no major problems. The fiber optic link was built from a kit produced by Advanced Fiber Optic Corporation. It has been tested and performed well. Three connectors have been chosen to be used in the circuit. The data modem is near completion and will be tested with the fiber optic link, connectors, and individual components when complete.

EXISTING DATA BUS DESIGN

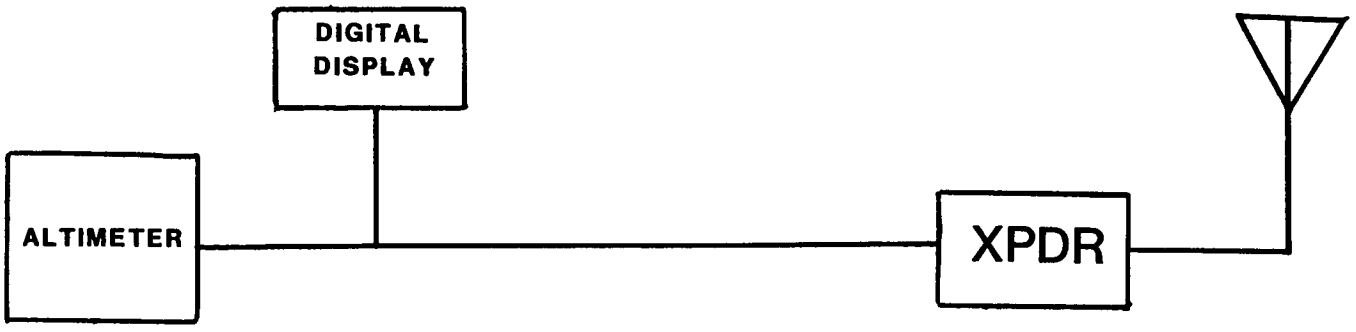

INITIAL FIBER OPTIC DESIGN

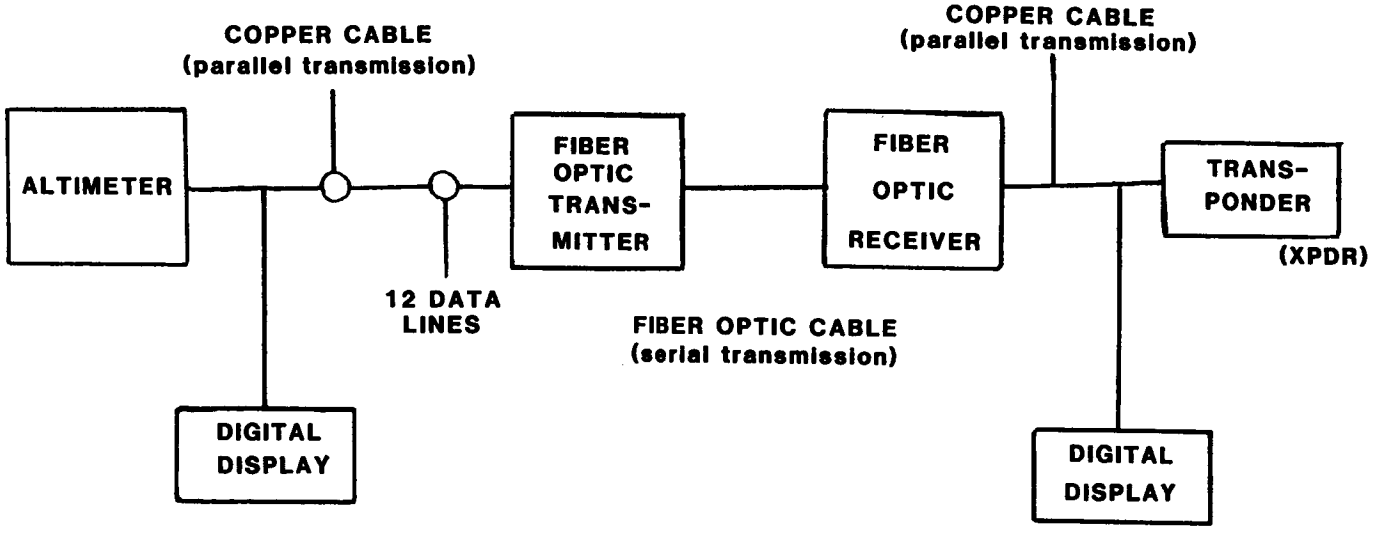

LORAN-C APPROACH CONSIDERATIONS

N87-22612

Robert W. Lilley
Ohio University
Athens, Ohio

Past Joint University Program efforts have resulted in Loran-C receiver design and testing, followed by enhancements for full RNAV operation with CRT pilot display. The use of Loran-C in the airspace and the number of commercial receivers available have exploded in recent years; pressure is mounting for approval of Loran-C use during approaches to landing.

The Avionics Engineering Center, in work for the State of Ohio Department of Development, has evaluated such approach applications at Galion, Ohio Municipal Airport and at Mansfield, Ohio Lahm airport. Loran-C data were referenced to ground-tracker data to determine that the Loran-C approach path was straight, flyable, and parallel to the runway centerline. The 0.2 nm offset, while within FAA requirements for RNAV approaches without correction, can easily be corrected to an on-centerline approach path.

There is little argument that Loran-C signals offer the basic accuracy required to design approaches in the coverage regions of existing chains. Seasonal variation in the Loran-C grid and the permanent grid warp caused by overland propagation can be corrected by publication of offsets, either in Loran-C or geodetic terms, to the WGS-72 coordinates defining FAF and MAP. The remaining concerns, then, center on system integrity. One important integrity factor is the airborne receiver and the means for determining its correct operation prior to initiating an approach.

It is possible that a Loran-C receiver may track a zero-crossing of the 100 kHz signal other than the desired third cycle. The result of a single cycle slip can be a position error of one nautical mile or more, depending upon the receiver's position relative to transmitter pair baselines. A cycle slip on the station being used as the master might cause considerable resultant error, by introducing TD errors in both hyperbolic LOPs being used. Such errors might be tolerable in enroute flight, but are certainly unacceptable in terminal-area operations.

The pilot needs a reliable method for receiver checking before an approach, while still in the enroute phase of flight, when primary (VOR) navigation aids are available. Overflight of a VOR station, comparison of Loran-C with a VOR/DME or VOR-RNAV fix, or perhaps a simple angular comparison when within some established distance from a VOR, all offer candidate cross-checking methods.

Effects of various combinations of cycle slip events upon the approach path flown need to be demonstrated and understood, also.

These Loran-C operational issues will be investigated using the following program steps:

1. A Loran-C approach will be designed for the Ohio University Airport:

a. WGS-72 coordinates will be determined for runway thresholds, using Navy TRANSIT data, ground surveys and compass readings of actual runway bearing.

b. Final approach fixes will be computed, at five miles from each threshold, for straight-in approach paths.

c. TERPS criteria will be consulted to determine compliance with approach obstruction limits.

d. Each approach will be test-flown, using theodolite/ranger ground-truth systems to provide referenced data giving uncorrected Loran-C path position and structure.

e. TD and geodetic correction values will be developed, and the approaches will be re-flown with corrections applied. Video-tape data will be collected to verify the quality of the resulting approaches.

f. The approaches will be re-flown with various combinations of cycle slip, and the resulting path location documented.

g. The offsets observed in item f., above, will give guidance as to available options for receiver integrity checks prior to approach.

Specific test plans are in preparation for each step, and results will be reported as data become available.

SATELLITE SURVEYING FOR A LORAN-C NONPRECISION APPROACH

Daryl L. McCall
Ohio University
Athens, Ohio

Work is continuing to site-in a Loran-C nonprecision approach at the Ohio University Gordon K. Bush Airport located in Albany, Ohio. A point has been surveyed just west of the Avionics Engineering Center's airport laboratory, in WGS-72 coordinates to within approximately 2 meters of latitude and longitude and 1.5 meters in altitude.

This survey was performed using the Motorola Mini-Ranger Satellite Surveying System, which uses the Navy's TRANSIT satellites. This position was obtained using the point-position method only, that is the position was calculated from sequential Doppler measurements as the TRANSIT satellite's passed within view of the receiver's antenna. Another method, called translocation, can use differential techniques which provide better results. However, this method requires two receiver's and a precisely known location. This method was not used earlier for lack of the second receiver.

The accuracies obtained, using the single receiver, are sufficient to site-in a Loran-C nonprecision approach. The end-points of the pavement of runways seven and two-five will be surveyed by extrapolating from the known point adjacent to the airport laboratory. Using a calibrated compass, theodolite, and laser ranger, the necessary angles and ranges were obtained to be used in the calculation of the location of the endpoints and final approach fix points of both runways.

Ohio University may be using the Motorola system again, using two receivers to use the translocation method to site-in the localizer antenna array at the airport to meet FAA certification requirements. This may result in a new benchmark located on the field at the airport, known to submeter accuracy. In this case, this accuracy will be transferred to the runway endpoints and the Loran-C FAF.

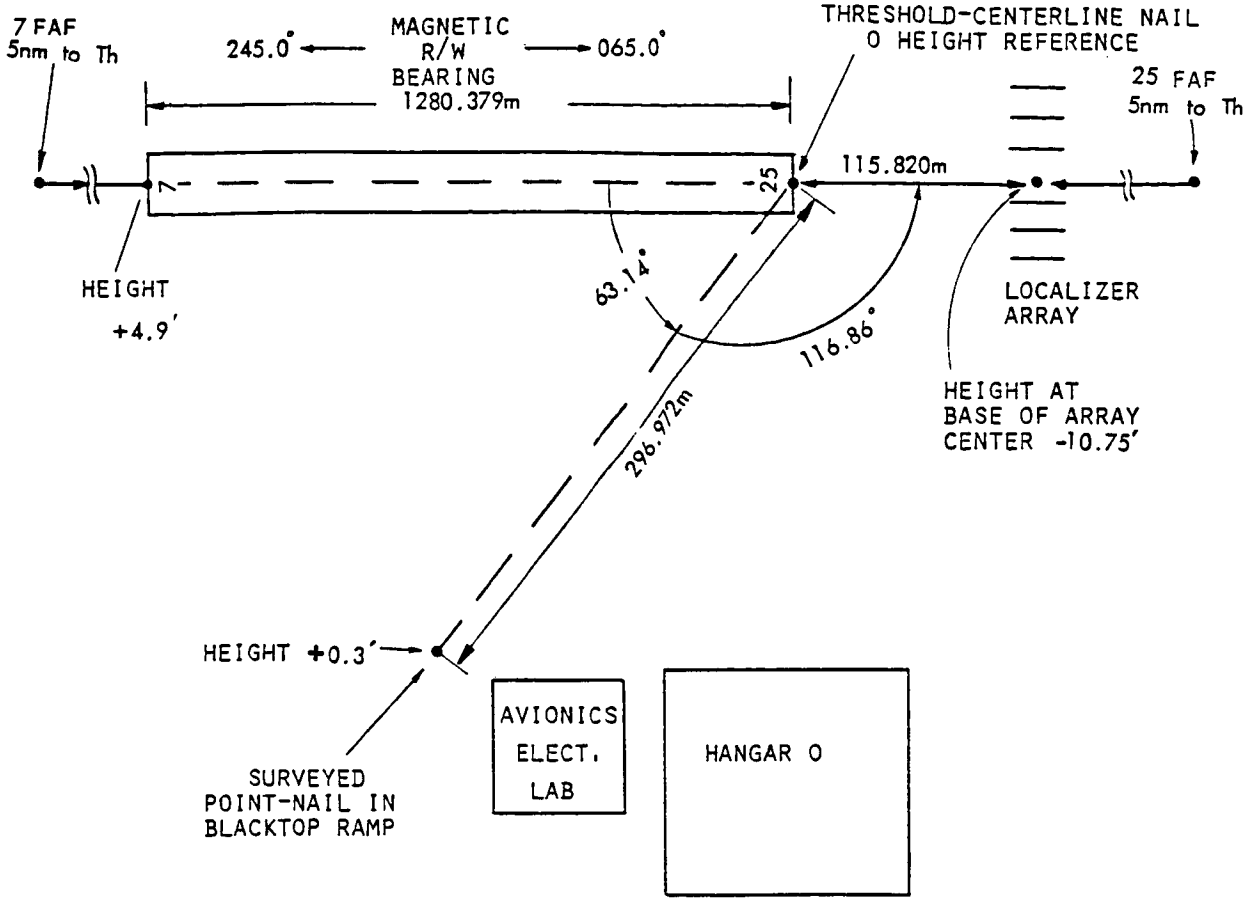

OHIO UNIVERSITY AIRPORT SURVEY POINTS

FOR LORAN-C NONPRECISION APPROACHES

ADVANCED MONITORING CONCEPTS

Robert W. Lilley
Ohio University
Athens, Ohio

The emphasis in initial work will be on application of image processing techniques in the site monitoring of an ILS glide slope transmitting array. The glide slope requires a clear area in front of the antennas for use as a reflecting zone. Reflecting or scattering obstacles in this area can cause incorrect path formation and system outages.

Direct video monitoring is impractical due to the narrow-band nature of communications links from the ILS site to the regional maintenance location. Slow-scan video is possible, but even this technique may require transmission of large amounts of data, tying up remote monitoring lines.

Minimization of data transmitted will be investigated in several steps:

1. Video change detection: subtraction, pixel by pixel, of the current image from a baseline image and transmission of only the changed portion.

2. Edge detection of the changed image, providing a high-contrast outline drawing of the changed portion.

3. Calibration of obstruction shape and size, using known camera tilt angle and ground-plane location; investigation of the need for targets or gnomons in specific locations for image calibration.

4. Investigation of remote or pre-programmed pan/tilt/zoom operations for greater areal coverage or improved characterization of the obstacle.

5. 'Treat analysis' of obstruction versus monitor output versus effect on the glide slope signal in space.

6. Recommendations for interoperation with existing monitor/restart procedures and practices, or for changes in monitor philosophy.

Steps 1 and 2 will be investigated using existing COMTAL Vision One video digitizing and display facilities, with the addition of a data link to the IBM 4341 and 4381 computers, also available. Video digitization at 256x256x8 is implemented; color photographs of actual ILS ground planes, with and without obstructions, will be digitized initially, and used to drive change detection and edge detection algorithms. Required data volume will be measured.

Step 3 will be studied mathematically, using known camera optics and measured ground plane locations.

A prototype installation will be fabricated and tested, providing a test bed for remaining studies. Specific hardware will be selected after the computer studies demonstrate feasibility and necessary sensitivity to potential threats.

ADVANCED MONITORING CONCEPTS

IMAGE PROCESSING

-VIDEO CHANGE DETECTION

-EDGE DETECTION

-OBSTRUCTION CHARACTERIZATION
CALIBRATION GNOMONS?

-REMOTE PAN/TILT/ZOOM

-THREAT ANALYSIS -- VIDEO VS. REAL WORLD

-RECOMMENDATIONS

GPS ANTENNA DESIGNS

N87-22615

Samuel J. P. Laube
Ohio University
Athens, Ohio

PRECEDING PAGE BLANK NOT FILMED

Application of the current GPS NAVSTAR system to civilian service requires that a right-hand, circularly polarized, -160 dBW spread spectrum signal be received from an orbiting satellite, where the antenna environment is also moving. This presents a design challenge when inexpensive antennas are desired. The current trend of the industry is a quadrifilar helix design first perfected by C.C. Kilgus [1], which has become commercially available in a variant form. This is not the only antenna which is usable, however.

A hybrid Archimedian spiral antenna by R. Milne [2] provides signal pattern advantages over the quadrifilar helix, but sacrifices small size and ease of construction. Other types of antennas, such as conical spirals or turnstiles, have not been considered as of yet. The intent of this survey is to provide information on the antennas mentioned above and to construct and test prototypes to determine whether the choice made by industry (of the quadrifilar helix) is the best.

The quadrifilar helix antenna is currently the low cost standard for GPS. It provides cardioid or omnidirectional coverage and right-hand circular polarization. The small size of the antenna at 1575 MHz minimizes wind loading on aircraft. With care in construction, a 20 MHz bandwidth is also achievable at this frequency. A modified version of this antenna provides ruggedness and simplicity.

Prototype versions, based on information from an article by C.C. Kilgus, were constructed using 12-gauge wire and subminiature coaxial hardline. The antenna can be matched using two 90 degree sections of different impedances. The half-turn half-wave helix provides an impedance of 10 to 100 ohms. SMA connectors were used and the copper wire was silverplated after assembly. The equations used to design the antenna and the final working dimensions are shown in figure 1.

The 90 degree balun can be eliminated by increasing one set of element lengths by 45 degrees and decreasing the other set by 45 degrees. This allows feeding the antenna from the top of the helix by using one of the elements as the feeder. Since this is a half-wave configuration, all elements are grounded at the base of the antenna. The helix must have a chosen radius, which determines the pattern of the antenna. The active area of the antenna is limited to the vertical elements. The radial parts of the elements have no radiation. Radial choice provides the cardioid pattern, front-to-back ratio and 3 dB beamwidth. Kilgus provides several graphs and experimental data in his article, and one only has to choose what parameters need to be satisfied for desired GPS antenna characteristics.

The constructed antennas were tested using a signal generator and a reference turnstile. A spectrum analyzer was used to measure the level of the received signal. Measurements were conducted in a large hall at Clippinger labs. The reflections in the hall were found to interfere, so future tests will take place in an open field. The 1575 MHz

signal is of relatively short wavelength, so reflection occurrence was more prominent than expected. Testing was done, as shown in figure 2.

The modified Archimedian spiral was developed by R. Milne. The antenna is basically an Archimedian spiral reflector elements and ground plane radials. The spiral is excited by a cavity which can be mounted inside the aircraft skin. The pattern is a basic cardioid with lobes towards the horizon. The lobes on the horizon are due to the external reflector elements, which provide gain in the direction where it is most needed. The reflector elements are mounted in the radome that covers the spiral. The bandwidth of this antenna is broad enough to cover both the 1575 and the 1227 MHz GPS signal format. Complexity of the antenna makes construction difficult.

Turnstiles and conical spirals offer some usefulness, but lack good cardioid patterns. Using reflectors and directors can provide useful antenna patterns, but sacrifice size.

Industry's choice in using the quadrifilar helix is a valid one when it comes to low cost and ease of construction. The narrow bandwidth limits use of this antenna for C/A GPS work only. The helical spiral offers a better approach when P code reception is desired.

References

[1] Kilgus, C. C., "Resonant Quadrifilar Helix Design," Microwave Journal, pp. 49-54; December, 1970.

[2] Milne, R., "Receiving Antennas for the NAVSTAR Global Positioning System," Government of Canada, Dept. of Communications, Communications Research Center, CRC Report No. 1319, Ottawa; October, 1978.

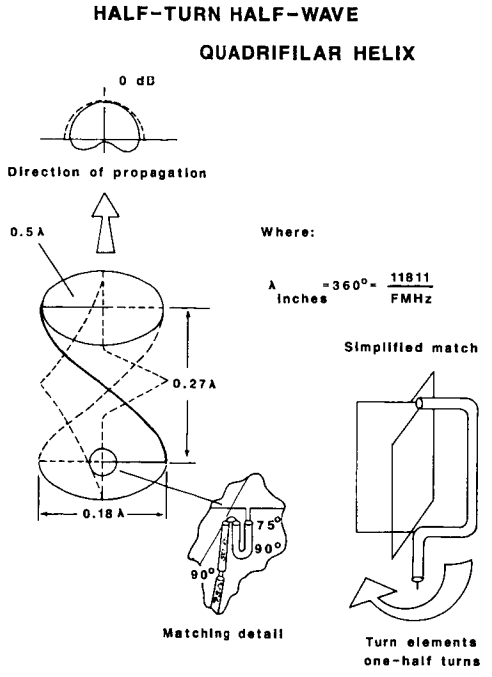

Figure 1.

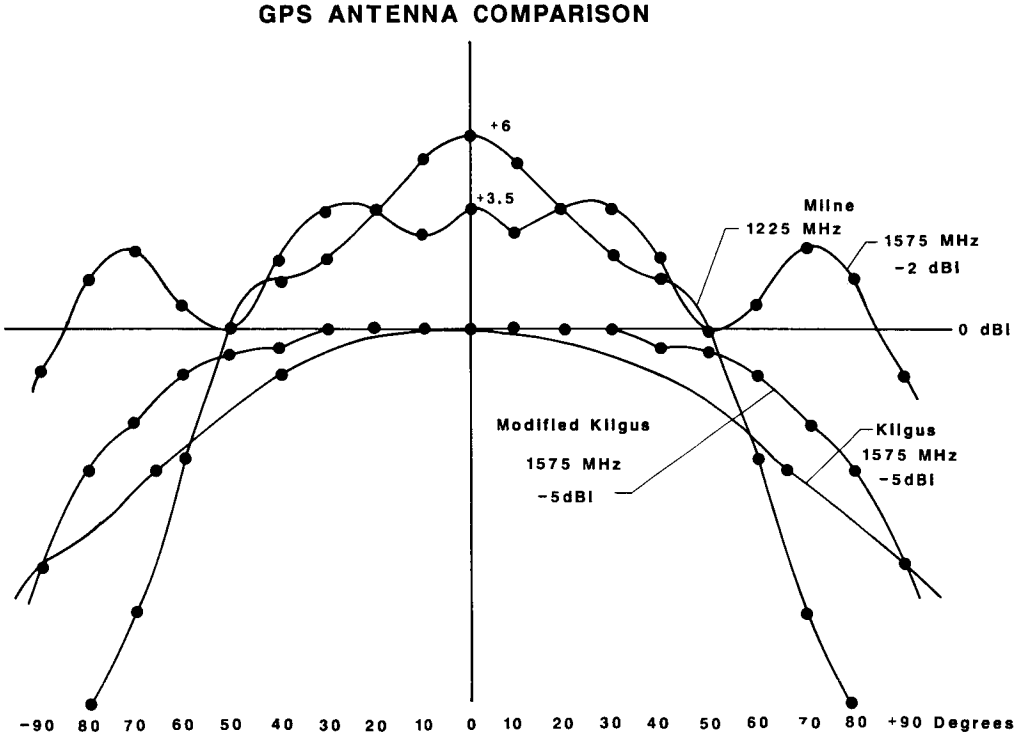

Figure 2.

PROCESSOR-CONTROLLED TIMING MODULE FOR LORAN-C RECEIVER*

Robert W. Lilley
Avionics Engineering Center
Department of Electrical and Computer Engineering
Ohio University
Athens, Ohio

*Published as Ohio University Technical Memorandum 90, February 1984.

Hardware documentation is provided for the modified Loran-C timing module which uses direct software control in determining loop sample times. Computer loading is reduced by eliminating polled operation of the timing loop.

I. SUMMARY

The original design for the Ohio University Loran-C receiver featured a software/hardware locked-loop signal processor, based upon the Mostek 50395 timing integrated circuit (IC) [1,2]. This IC provides a six-digit binary-coded decimal (BCD) counter and a BCD register compared to generate an output pulse when the register and counter contents are equal. Operated at 1 MHz, this timing circuit permits microcomputer-selected sample times to be set precisely within a one-second counter interval, with a resolution of one microsecond.

In order to accomplish the data load for the IC register, the computer must detect that the IC digit scan oscillator has selected the appropriate 4-bit BCD digit, and then strobe the new digit data into the register. The IC design requires a scan oscillator frequency of no higher than 20 kHz, which places a lower limit on the time required to load all six digits. In practice, the complete register load required 500-800 microseconds (μs).

The original receiver design makes all six IC digit strobe signals available to the microcomputer, which then strobes the new digit data into the register after detecting the presence of the appropriate strobe signal. This operation must take place in order to preset the next loop sample time, triggered by the EQUAL pulse from the Mostek IC. Therefore, the register load must be performed between each Loran-C pulse. The technique of polling the digit strobe lines to detect the next digit to be loaded requires full attention from the microcomputer, delaying background processing.

The modified circuit described in this technical memorandum ignores digit strobes, by bringing the SCAN input under control of the processor. Register loading becomes a synchronous process, with no polling loop. When a digit datum is ready for loading, the scan counter is updated immediately by the processor, with no lost time. See figure 1 for a block diagram.

This modification is required to permit the single processor (a MOS Technology 6502) to perform all required computations for the entire Loran-C process. Expansion of the receiver from a three-station tracker to full five-station operation would cause over 20 percent of processor power to be lost to the strobe polling operation, causing a reduction in navigation data output rates, and a reduction in the number of pilot-oriented features which could be added using the single processor. This modified circuit saves some 350 to 650 μs per Loran pulse.

Full hardware documentation is provided in this paper for the circuit card implementing the Loran-C timing loop, and the receiver event-mark and re-track functions. This documentation is to be combined with overall receiver drawings to form the as-built record for this device. Computer software to support this module is integrated with the remainder of the receiver software, in the LORPROM program.

II. CIRCUIT DESCRIPTION

Figure 2 shows the complete logic diagram for the Loran-C timing module. To the far left are signal descriptors for the system computer, an MAI SuperJolt based upon the MOS Technology 6502 with 6520 peripheral interface adapter (PIA). All connections, except for CLOCK and IRQ, are made through the 6520 PIA. Figure 3 gives a summary of PIA pin assignments, useful in software design and coding. The Mostek 50395 chip description is given as figure 4, and pinouts are shown in figure 5.

Referring to figure 2, note that seven lines provide data and control signals to the Mostek IC (U3). All these signals are output by the computer as TTL-compatible signals, and must be changed to the 12-volt MOS specification required by U3. This conversion is performed in open-collector drivers U1 and U2, pulled up to 12v through 1.1 K-ohm resist~ These lines carry the four data bits for register digits Ra, Rb, R the LR (Load Register) strobe and $\overline{SET}$ (Set digit counter to most-significant digit) signals.

The timing chip U3 is wired for free-running counter, counting up is driven by the CLOCK, which is a buffered version of the main microcomputer clock (a temperature-compensated crystal oscillator). The SCAN inp which increments the digit counter to indicate the load window for each register digit is driven by the computer via the SCAN line.

The computer is programmed to select ($\overline{SET}$) the high order digit first, and to set LR to enable the register load digit at a time. Each digit is then placed on RA through RD, and loaded by toggling SCAN.

Once the register is fully loaded, the U5 Loran-C interrupt and data latches are enabled by bringing $\overline{CLRP}$ high. When the free running counter in U3 reaches the register value just loaded, U3 issues an EQUAL pulse for one clock period (one μs) which clocks the U5 latches. The IRQ low since the $\overline{Q}$ output of the U5 interrupt latch always goes low upon clocking. An interrupt is signaled at $\overline{IRQ}$ to the computer. LDAT, latched by the U5 Loran-C latch, assumes the instantaneous value of the Loran-C digital waveform received at $\overline{LRIN}$ from the receiver front-end module. Note that $\overline{LRIN}$ is processed by U4 to set a pulse width of approximately 70 μs before it is sampled. This pulse width is necessary to provide a guard time after the leading pulse edge to permit successful pulse tracking, and to minimize initial search time. Since the various front-end processors designed to date have presented various pulse widths, this U4 mono-stable multivibrator has been provided to equalize the waveform before sampling.

The remainder of the circuit, U12, deals with receiver features included for evaluation. The event latch is driven by a front-panel pushbutton to place on the receiver output tape a unique mark so output data may be correlated with flight events. The retrack latch, also operated by pushbutton, signals the computer that the operator wishes to restart the Loran-C search process. To minimize contact bounce, these latches are configured to operate on the pushbutton release cycle.

Once the computer program has serviced the Loran-C sample interrupt thus generated, the U5 latches are disabled by a low at $\overline{CLRP}$. Another register load sequence begins.

In this manner, successive samples may be taken of the Loran-C input waveform at times which are precisely controlled by the microcomputer. The programmer may now select algorithms for detecting received Loran-C chains and stations by varying the sample time and observing the result at LDAT.

The module pictorial appears in figure 6, giving placement of ICs and other major components.

III. REFERENCES

[1] Lilley, R. W. and D. L. McCall, "A Loran-C Prototype Navigation Receiver for General Aviation," paper (No. 81-2329), presented at the AIAA/IEE Fourth Digital Avionics Systems Conference, November 1981.

[2] Lilley, R. W. and D. L. McCall, "A Loran-C Prototype Navigation Receiver for General Aviation," Technical Memorandum 80, Avionics Engineering Center, Department of Electrical and Computer Engineering, Ohio University, August 1981.

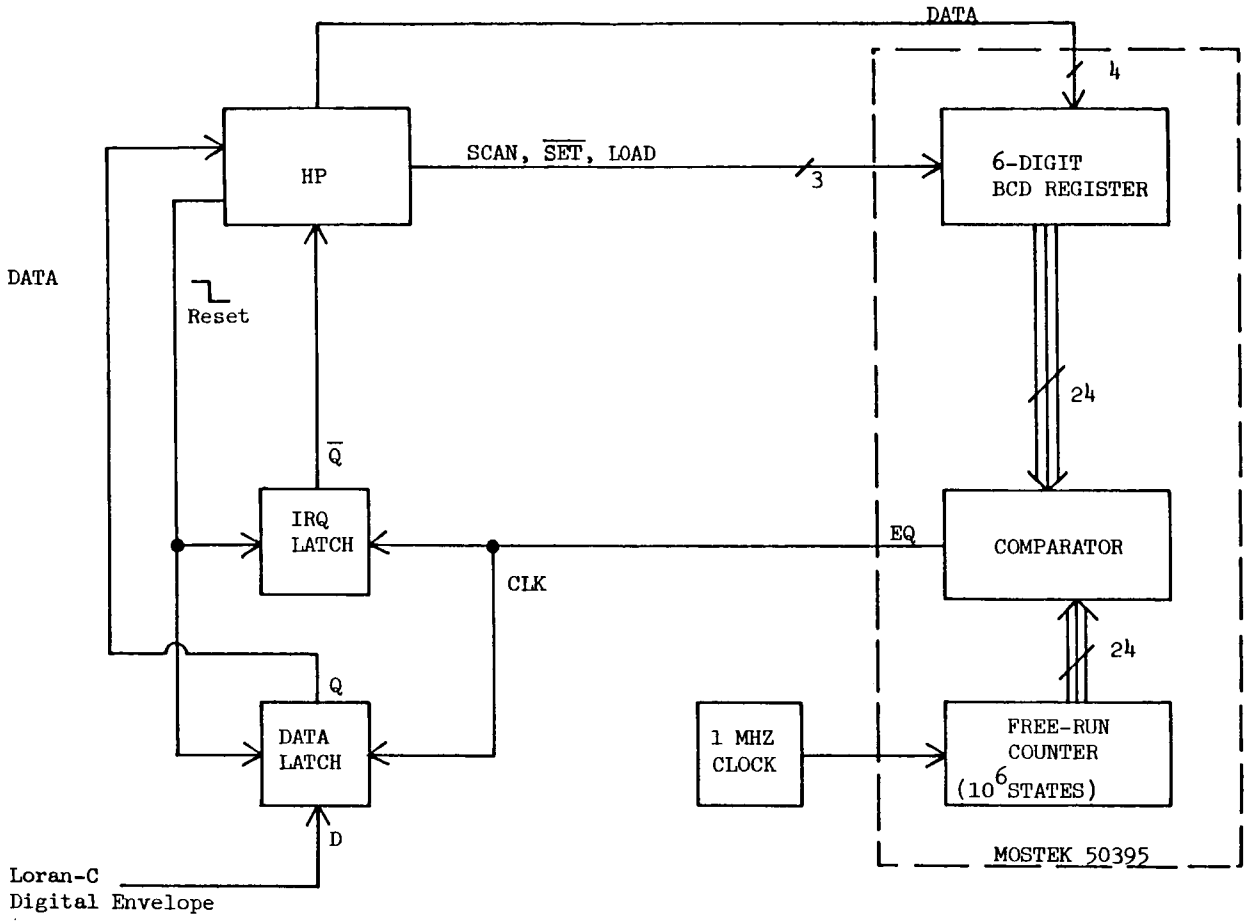

Figure 1. Block diagram, Loran-C timing module.

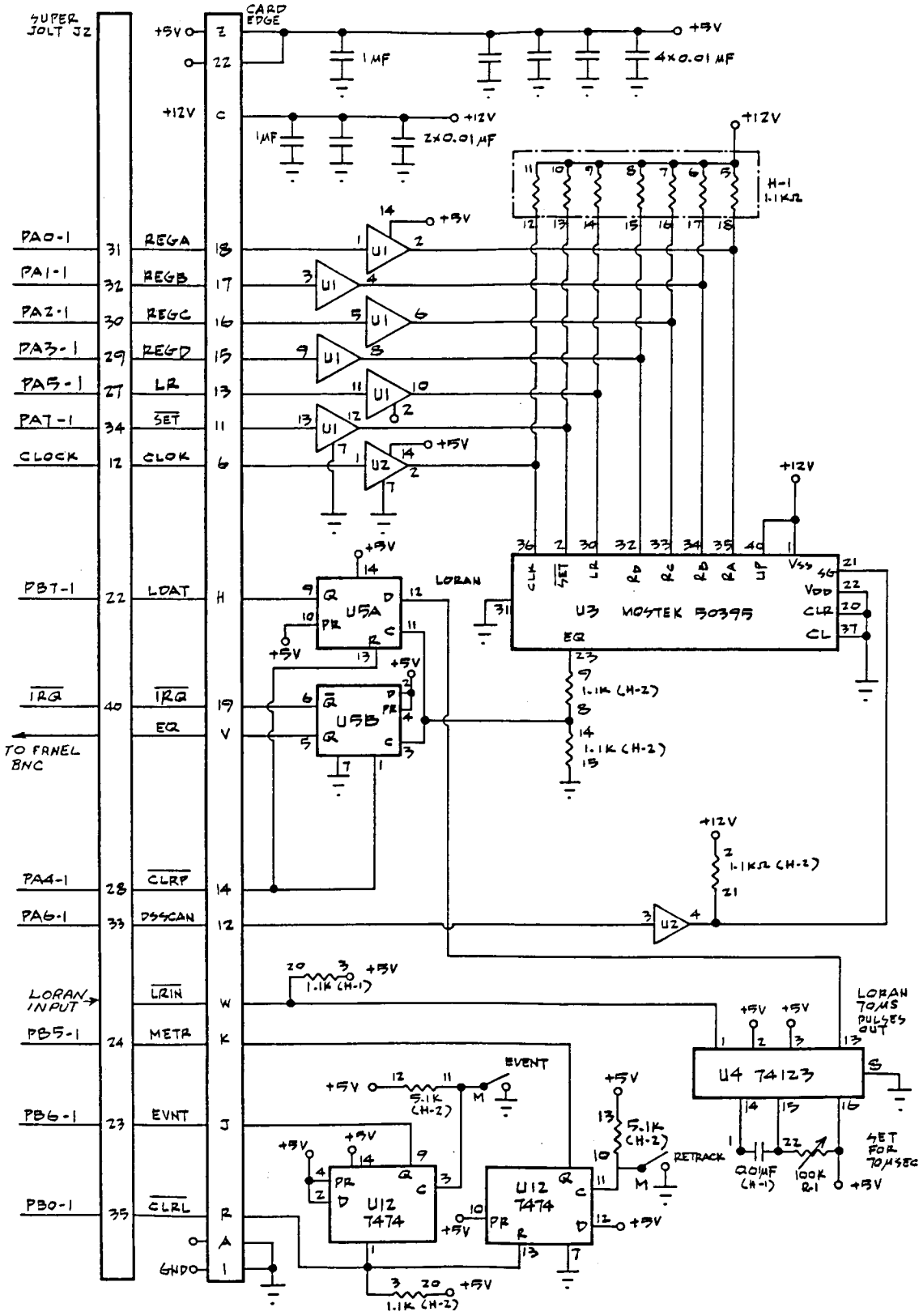

Figure 2. Revised timing board schematic.

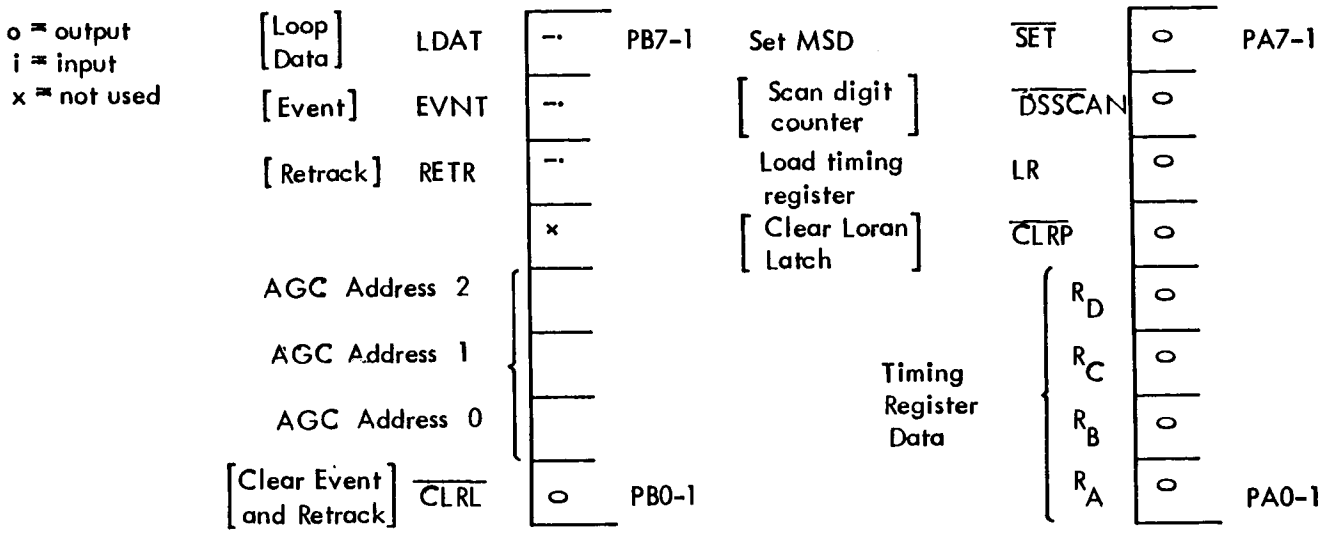

Figure 3. Super Jolt to timing board summary of PIA assignments.

FUNCTIONAL DIAGRAM

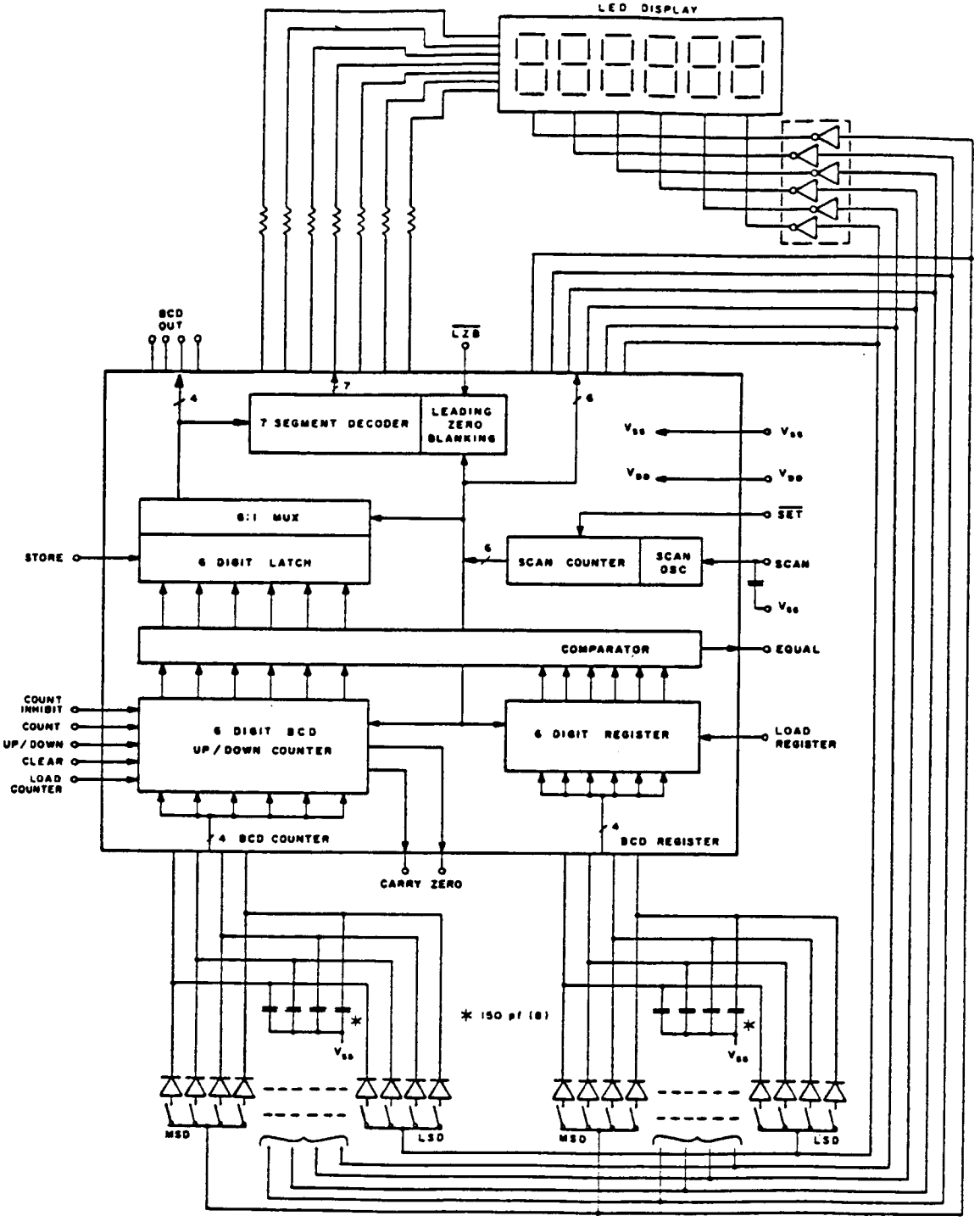

Figure 4. MOSTEK 50395 integrated circuit.

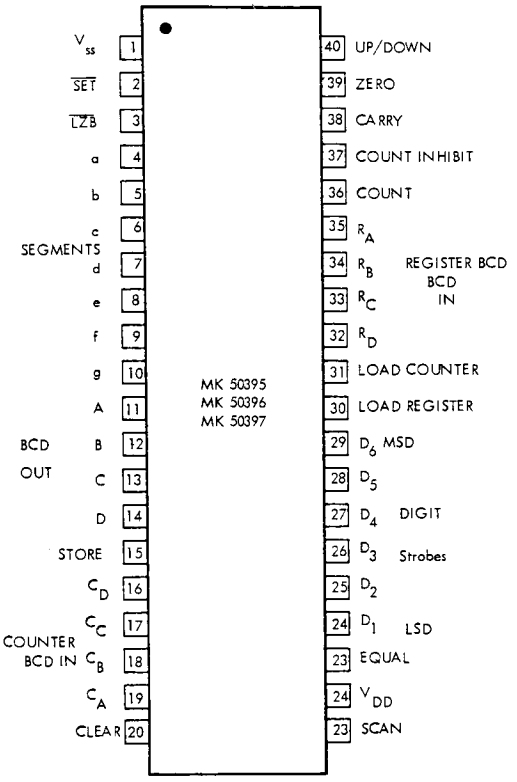

Figure 5. MOSTEK 50395 pinouts.

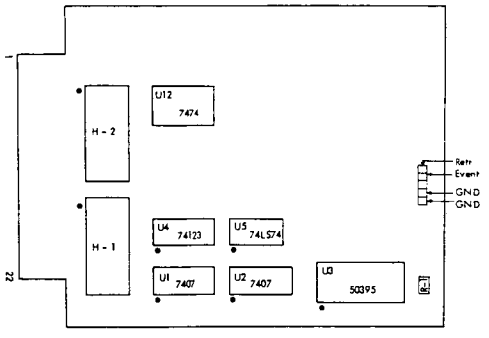

Pin	Signal	Description
R	$\overline{CLRL}$	Low clears retrack & event latches.
J	EVNT	High indicates user event mark, cleared by $\overline{CLRL}$.
K	RETR	High indicates user retrack, cleared by $\overline{CLRL}$.
W	$\overline{LRIN}$	Input Loran-C pulses from front-end. TTL, open-collector, pulled up to 5V on this board
18	REGA	4-bit BCD digit load for U3 register.
17	REGB	
16	REGC	
15	REGD	
13	LR	Load 50395 (U3) Register strobe.
11	$\overline{SET}$	Set U3 to MSD for data load.
6	CLOK	1 MHz clock, from microcomputer.
12	DSSCAN	Scan Input for Digit Counter
14	$\overline{CLRP}$	Low clears Loran data latch.
H	LDAT	Loran data - loop sample output.
19	$\overline{IRQC}$	Combined IRQ from loop and digit strobes.
V	EQ	Equal pulse, for monitoring.

Figure 6. Pictorial and signal glossary.

A MICRO-COMPUTER-BASED SYSTEM TO COMPUTE MAGNETIC VARIATION*

Rajan Kaul
Avionics Engineering Center
Department of Electrical and Computer Engineering
Ohio University
Athens, Ohio

*Published as Ohio University Technical Memorandum 91, March 1984.

A micro-computer-based implementation of a magnetic variation model for the continental United States is presented. The implementation computes magnetic variation as a function of latitude and longitude for general aviation receivers such as Loran-C.

I. INTRODUCTION

A mathematical model of magnetic variation in the continental United States (COT48) has been implemented in the Ohio University Loran-C receiver. The model is based on a least squares fit of a polynomial function. The implementation on the micro-processor based Loran-C receiver is possible with the help of an Am 9511 math chip, manufactured by Advanced Micro Devices, which performs 32 bit floating point mathematical operations. A Peripheral Interface Adapter (M6520) is used to communicate between the 6502 based micro-computer and the 9511 math chip. The implementation provides magnetic variation data to the pilot as a function of latitude and longitude. This report briefly describes the model and the real time implementation in the receiver.

II. THE MATHEMATICAL MODEL

The model was developed at the United States Geological Survey (USGS) by Fabiano et al. [1], by performing least squares analysis on more than 34,000 data measurements taken between 1900 and 1974. The analysis provides an analytical model of the magnetic field which is used to compute the magnetic variation.

For the actual magnetic variation calculation the COT48 region is partitioned into five, 12 degree longitudinal bands from 66 degrees West to 126 degrees West. A set of coefficients for each of the five bands is determined by the analytical model. A seventh order polynomial function of the analytical model is applied to compute the magnetic variation. The secular change is calculated in a similar way, the only difference being that a sixth order polynomial function is used. Also, the secular change case is not partitioned into bands and therefore the same set of coefficients is used for the entire COT48 region.

The polynomial function adapted for the procedure is

$$\sum_{i=0}^{n} \sum_{j=0}^{i} a_{ij} (\theta_c)^{i-j} (\lambda_c)^{j}$$

a_{ij} - co-efficients

θ_c - normalized latitude
$= \theta - 52$

λ_c - normalized longitude
$\lambda - \gamma$

γ - Table 1 - east longitude normalizing factor

θ - co-latitude = 90°-latitude

λ - east longitude = 360°-longitude

The limits on each band and other constants are specified in Table 1 [2].

For the magnetic variation calculation n=7, and thus 36 coefficients are specified for each band in the COT48 region, while in the secular change calculation n=6, therefore only 28 coefficients are required for the whole COT48 region. All the coefficients are given in Appendix A.

The model was simulated in FORTRAN on an IBM 370 computer at Ohio University and a contour plot was made of the magnetic variation in the COT48 region (figure 1). The FORTRAN.program listing is included in Appendix B. A copy of an actual magnetic variation chart published by the Defense Mapping Agency (DMA) is shown in figure 2. Comparisons between actual published values of the magnetic variation and values calculated by the model were made and are described later in this report.

III. MICRO-COMPUTER IMPLEMENTATION

The magnetic variation model was implemented on a 6502 based Super-Jolt micro-computer. The 6502 microprocessor has only an 8-bit data bus, so the processor needs a large amount of memory and rapid access. The calculations in the implementation of the model require complex floating point operations of exponents. It is therefore desirable to use an external hardware device to support the microprocessor in these calculations.

The Am9511 was chosen to be implemented with the Super-Jolt system. It is a peripheral math processor which performs the necessary floating point mathematical operations. The Am9511 is designed to be used in conjunction with microprocessor systems that have an 8-bit data bus. The stack oriented processor can handle 16 and 32-bit floating point operands and performs arithmetic and trigonometric functions. An instruction set of the Am9511 is included in Appendix C [3].

Additional hardware is necessary to allow the microprocessor to communicate with the math processor. An M6520 peripheral Interface Adapter (PIA) is used for handshaking with the microcomputer. The PIA consists of two 8-bit ports and several control registers for interface with external support devices. The overall design of the microcomputer, which is a part of the Ohio University Loran-C project is shown in figure 3.

IV. INTERFACING SOFTWARE

Special software is needed to allow the hardware components to interact with one another. The four subroutines 'PINT', 'PUSH', 'POP' and 'CMND' were written by Fischer [4] with this particular goal in mind. 'PINT' initializes the Am9511 and the PIA and, also, the scratchpad RAM locations. 'PUSH' is used to copy a four byte number from RAM to the stack of the Am9511. 'POP' does exactly the opposite by copying a four byte floating point number from the stack of the Am9511 to scratchpad RAM. 'CMND' sends an instruction byte to the Am9511 to perform the desired operation. It also checks the status register of the math processor to determine the outcome of the operation. Flow charts of the above subroutines are given in figure 4.

The actual magnetic variation program 'MAGVAR', occupies about 800 bytes of memory including scratchpad RAM locations. The coefficients 36

for each of the five bands, occupy 900 bytes of memory. Each of the coefficients is converted into a 32-bit floating point format compatible with the Am9511 representing four bytes. The secular variation calculation is not included in the real time implementation for reasons which shall be addressed later in this report. The complete program listing is given in Appendix D at the end of this report. The 'MAGVAR' program takes about 1.5 seconds in execution time. However, since the magnetic variation does not change rapidly in a small geographic region, it does not need to be computed every time navigation position information is updated, when included in the actual navigation receiver such as the Ohio University Loran-C. For example a small change in the software can allow computation of the magnetic variation every 30 miles, or a one degree change in geographic position or any other interval desired.

V. RESULTS AND CONCLUSIONS

Initially, the values for the magnetic variation were computed by the FORTRAN simulation and compared to values published by National Geophysical Data Center.* The results obtained were accurate to a large degree. Table 2 summarizes two points in each band, of which comparisons were made in the COT48 region. The reason for the discrepancy in the values could arise from the differences between the data and the model. Fabiano and others [1] evaluated the model and compared it to surveyed data for 1,450 points. From these measurements an overall root mean squared deviation of 0.5 degrees was found in the magnetic variation in the COT48 region. Also, a probable cause for the larger discrepancy in the region of bands 2 and 3 could indicate magnetic variation anomalies in the Great Lakes region.

In general, the results were found to be satisfactory and the decision was made to implement the model on the Ohio University Loran-C receiver. The results computed by the microcomputer were within 0.1 degrees of the values computed by the FORTRAN simulation. As indicated earlier, the secular change was not implemented on the receiver. The magnetic variation in the COT48 region changes less than 11 minutes of arc annually at its worst case. This translates to a change of less than one degree over a period of five years at its worst case. Since the Ohio University Loran-C receiver is a research tool, not implementing the secular change function would not have a crucial impact on the outcome of future research. The coefficients for the model are derived every five years by the USGS, and can be updated very easily to keep the model current.

The overall performance of the implementation proves to be satisfactory. The major advantages are that the magnetic variation is available all the time to the pilot to allow accurate determination of the compass heading. It is computed automatically and is one less adjustment or source of error during a flight, thus also reducing the chances of pilot error.

VI. ACKNOWLEDGMENTS

The work presented in this technical memorandum has been supported by the National Aeronautics and Space Administration at Langley Research Center under grant number NGR 36-009-017. It was performed at Ohio University's Avionics Engineering Center.

*National Geophysical Data Center, Boulder, Colorado.

The author would like to acknowledge the help of Dr. Robert Lilley, Associate Director and Mr. James Nickum, project engineer at Avionics Engineering center, whose suggestions proved invaluable in all stages of this research. Special thanks is also due to Dr. Hugh Bloemer, Department of Geography, whose advice was indispensable.

VII. REFERENCES

[1] Fabiano, E. B., W. J. Jones, N. W. Peddie, "The Magnetic Charts of the United States for Epoch, 1975, "United States Geological Survey, Circular No. 810.

[2] Ibid., Fabiano, Jones and Peddie.

[3] "Am9511A Arithmetic Processor Advanced Micro Devices Advanced MOS/LSI," Advanced Micro Devices, Inc., Sunnyvale, California, 1976.

[4] Fischer J.P., "A Microcomputer-based Position Updating System for General Aviation Utilizing Loran-C," M.S. Thesis, Ohio University, Athens, Ohio, March 1982.

VIII. APPENDICES

A. Co-efficients for the 5-band and secular change in COT48.

B. FORTRAN Program Listing of "MAGVAR".

C. Instruction Set for the Am9511.

D. 6502 Assembly Language Program Listing of the Magnetic Variation Implementation on the Ohio University Loran-C Receiver.

Table 1. Limits on Five Bands and the East Longitude Normalizing Factor.

Band	Partition °W longitude	λ(degrees)
1	66-77	289
2	78-89	277
3	90-101	265
4	102-113	253
5	114-125	241

Table 2. Comparisons Between Actual and Computed Values of Magnetic Variation.

Band	Latitude Deg. N	Longitude Deg. W	Magnetic Variation Actual	Computed
1	36	77	7.72°W	7.40°W
66°W - 78°W	40	73	13.05°W	12.71°W
2	32	81	3.98°W	2.78°W
78°W - 90°W	40	87	1.12°W	0.51°W
3	34	93	4.37°E	5.90°E
90°W - 102°W	38	101	9.05°E	10.84°E
4	36	103	9.93°E	10.91°E
102°W - 114°W	40	107	12.62°E	13.54°E
5	38	123	16.18°E	16.59°E
114°W - 126°W	32	113	12.58°E	13.25°E

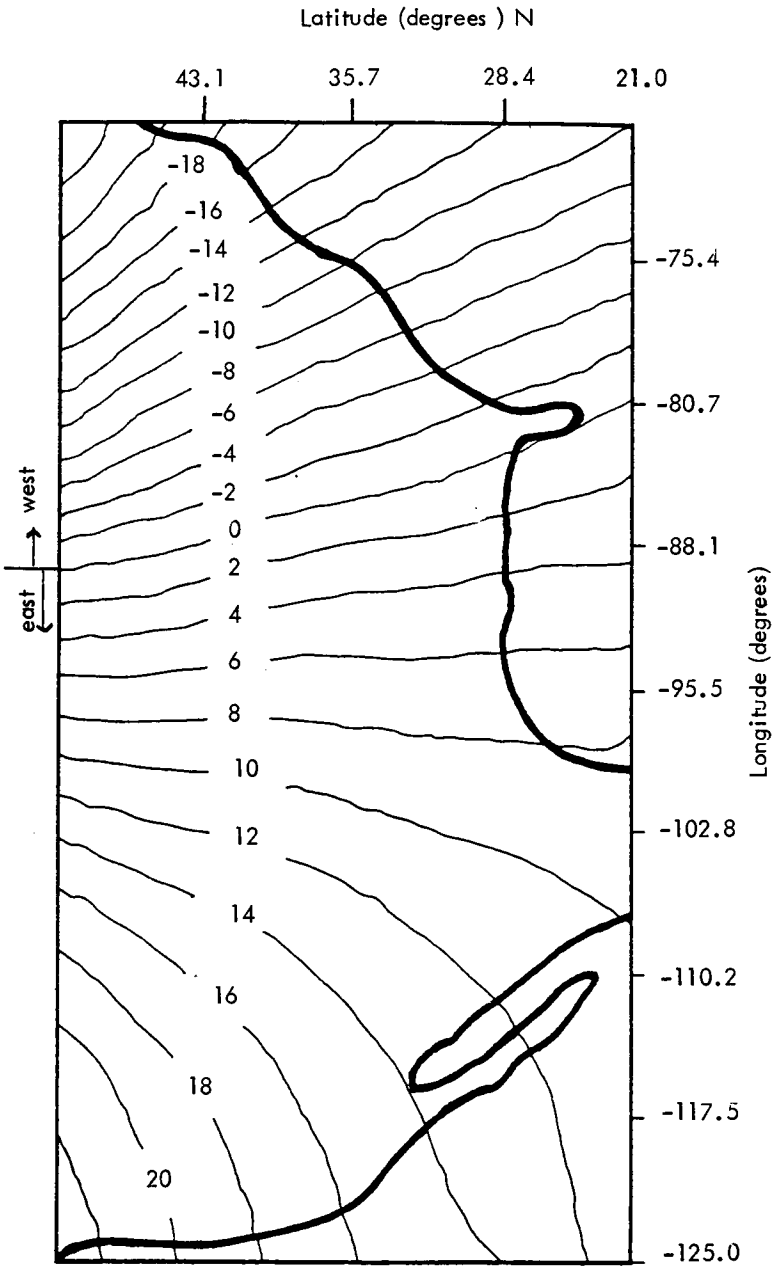

Figure 1. Continental U.S. magnetic variation.

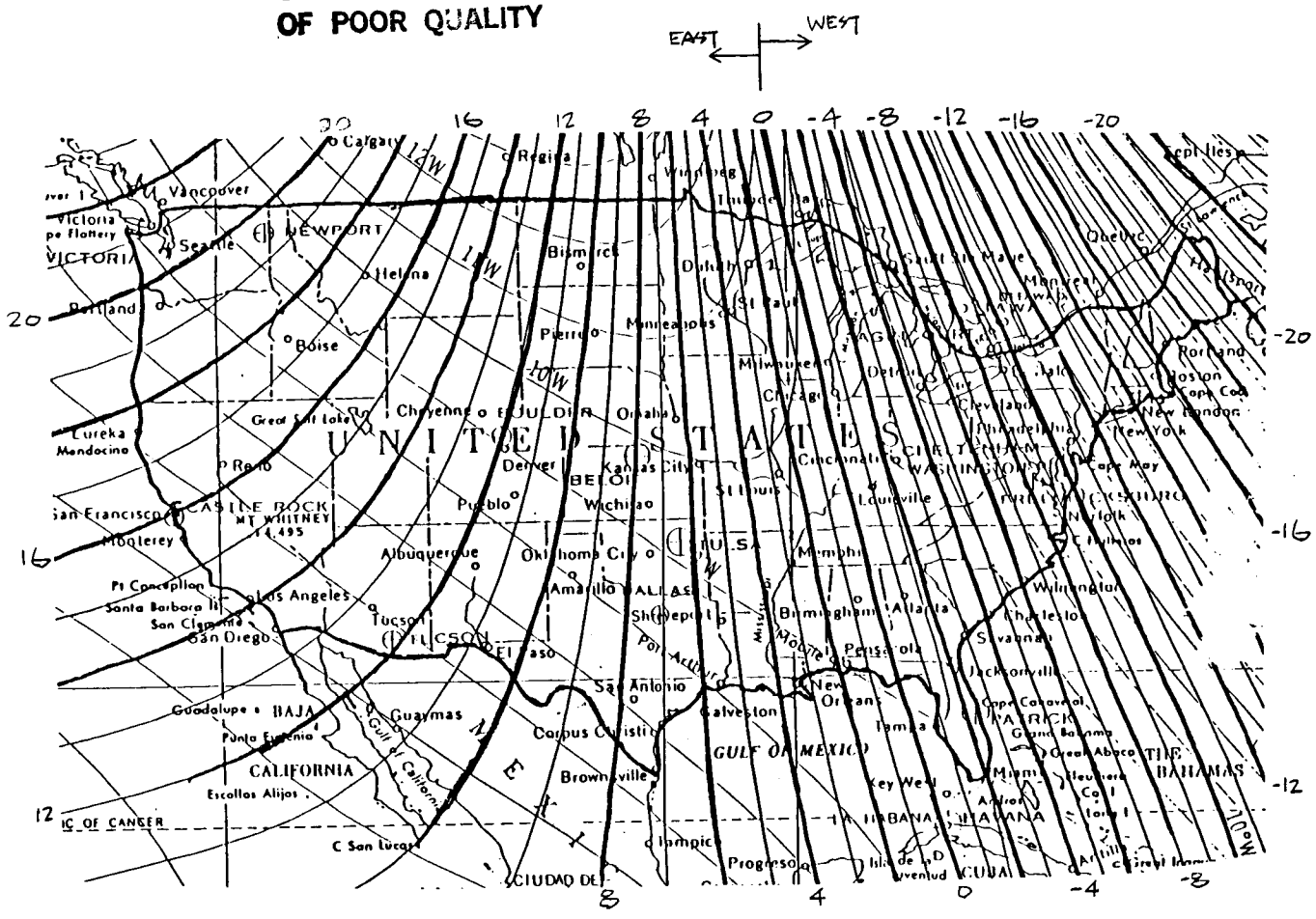

Figure 2. Magnetic variation in the United States from world declination chart (source Defense Mapping Agency).

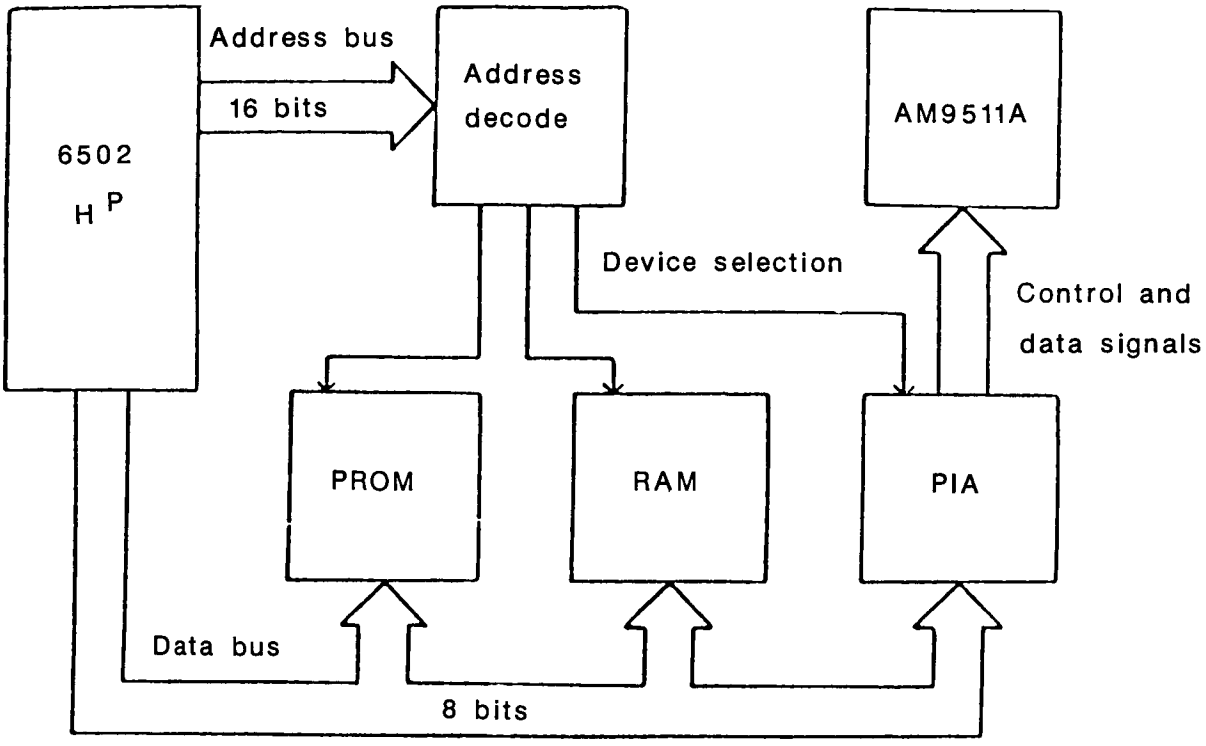

Figure 3. Block diagram for the microcomputer system.

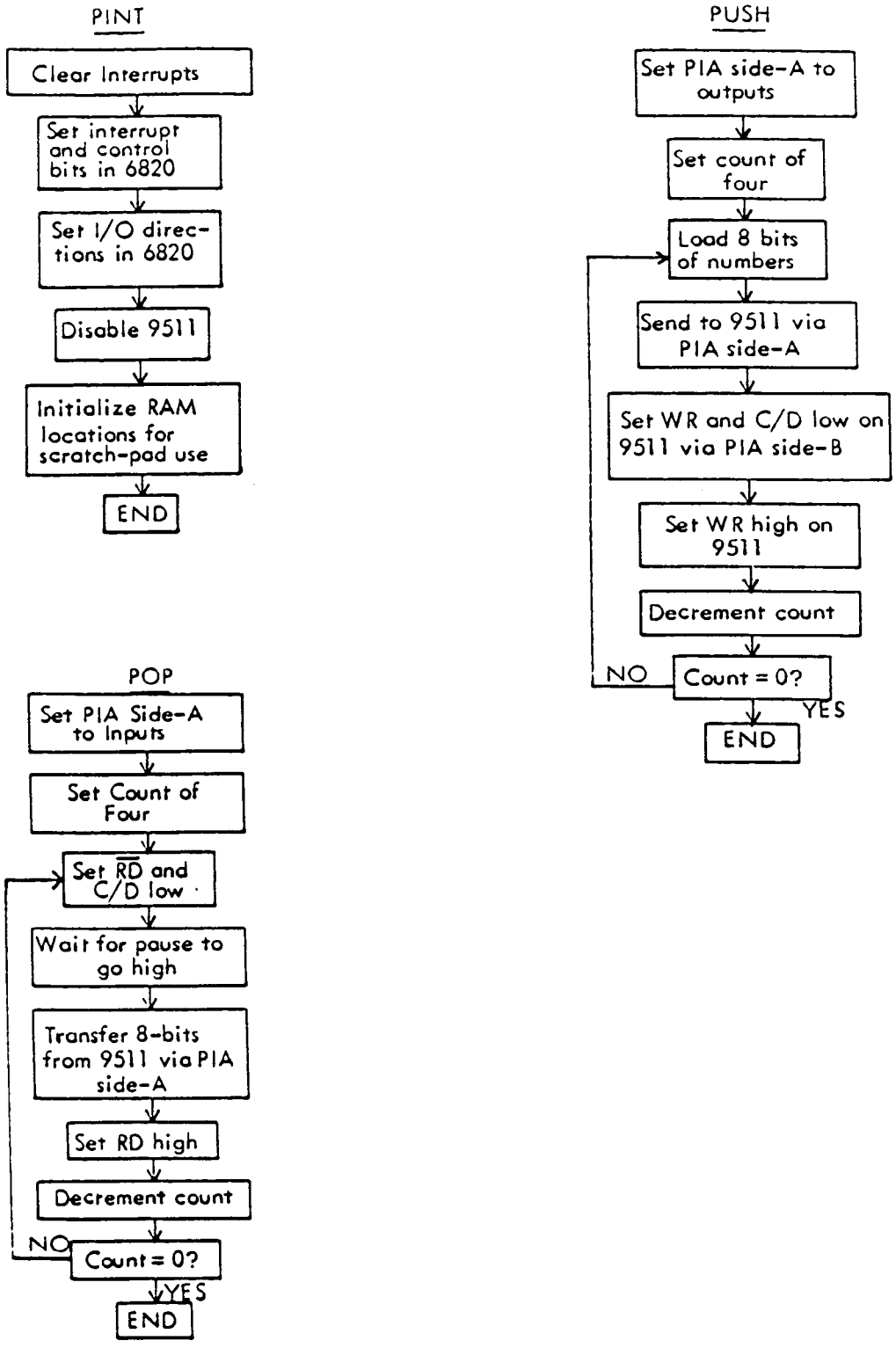

Figure 4. Logic flow diagrams illustrating steps control program executes to communicate with 9511.

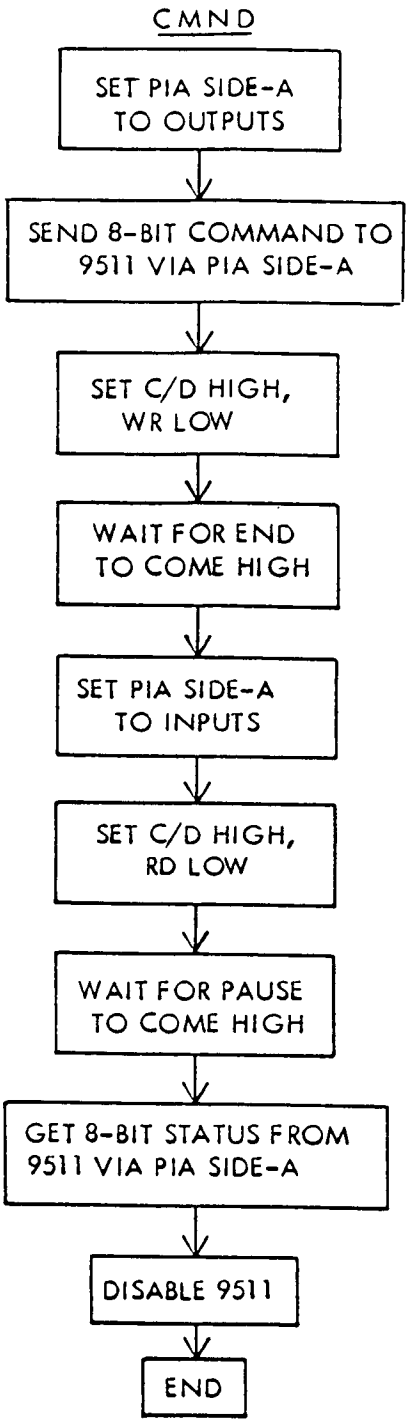

Figure 4. Concluded.

Appendix A. Co-efficients For the 5-band and Secular Change in COT48.

The coefficients (a_{ij}) for the magnetic variation in the conterminous United States (5 bands).

	Band 1	Band 2	Band 3	Band 4	Band 5
a_{00}	-0.12544E 02	-0.26754E 01	0.66671E 01	0.13031E 02	0.15997E 02
a_{10}	0.47404E 00	0.30498E 00	0.73577E-02	-0.24981E 00	-0.40370E 00
a_{11}	-0.79262E 00	-0.85269E 00	-0.62856E 00	-0.36471E 00	-0.20406E 00
a_{20}	-0.14935E-01	-0.11933E-01	-0.75537E-02	0.84073E-03	0.83811E-02
a_{21}	0.47508E-02	0.18570E-01	0.23621E-01	0.19160E-01	0.47466E-02
a_{22}	0.73049E-02	0.19648E-01	-0.99458E-02	-0.17215E-01	-0.65055E-02
a_{30}	0.28976E-03	0.64489E-03	0.57882E-03	0.14505E-03	0.36041E-03
a_{31}	0.46111E-03	-0.73539E-03	-0.29531E-03	-0.10708E-02	-0.16699E-05
a_{32}	-0.15079E-02	-0.16288E-02	0.70147E-03	0.35821E-03	0.17397E-03
a_{33}	0.12362E-02	-0.10931E-02	0.58517E-04	-0.12490E-02	0.22972E-02
a_{40}	0.25381E-04	0.31737E-04	0.54348E-04	0.13665E-04	-0.14418E-04
a_{41}	-0.29623E-04	0.46667E-04	0.10017E-04	-0.63934E-05	-0.40691E-04
a_{42}	-0.18112E-04	-0.51048E-04	0.77275E-04	0.10816E-03	0.88690E-04
a_{43}	0.55077E-04	-0.72203E-04	0.14306E-03	-0.50373E-04	0.18677E-04
a_{44}	0.62795E-04	-0.60910E-03	0.55063E-04	0.31817E-04	-0.51783E-04
a_{50}	0.23134E-06	-0.19467E-05	-0.40952E-05	-0.82114E-06	-0.32150E-05
a_{51}	-0.15270E-05	0.26542E-05	-0.25156E-05	0.60160E-05	0.21843E-05
a_{52}	0.14304E-05	-0.59918E-05	-0.88037E-05	-0.89843E-05	-0.16671E-06
a_{53}	-0.38852E-05	-0.58384E-05	-0.82214E-05	0.65151E-05	-0.13895E-04
a_{54}	0.55360E-05	0.38753E-04	-0.14001E-04	0.58428E-05	0.16509E-04
a_{55}	-0.76365E-05	0.44242E-04	-0.45236E-05	0.19349E-04	-0.37717E-04
a_{60}	-0.62672E-07	-0.76459E-07	-0.12253E-06	-0.20612E-07	0.25454E-07
a_{61}	0.79694E-07	-0.62486E-07	0.17499E-07	-0.41744E-09	0.13351E-06
a_{62}	0.15540E-06	0.17782E-06	0.39251E-07	-0.10090E-06	-0.44300E-06
a_{63}	0.97851E-07	-0.30012E-07	-0.27612E-07	0.57044E-07	0.11357E-05
a_{64}	0.11556E-06	0.24909E-06	-0.15699E-05	-0.84960E-06	-0.14101E-05
a_{65}	-0.76126E-06	0.74355E-06	-0.18538E-05	0.62532E-06	-0.66000E-06
a_{66}	0.23144E-07	0.48778E-05	-0.38992E-06	-0.45290E-07	0.10900E-05
a_{70}	-0.16860E-09	0.24723E-08	0.84712E-08	0.10184E-08	0.65007E-08
a_{71}	0.43030E-09	-0.38370E-08	0.44108E-08	-0.11497E-07	-0.76103E-08
a_{72}	-0.69117E-08	0.19785E-07	0.77909E-08	0.16786E-07	-0.13459E-07
a_{73}	0.33027E-08	-0.76731E-08	-0.37480E-09	0.64112E-09	0.84721E-07
a_{74}	0.93928E-08	-0.40025E-07	0.88535E-07	0.27692E-07	-0.69438E-07
a_{75}	0.91628E-08	0.52668E-07	0.12561E-06	-0.93332E-07	0.29615E-07
a_{76}	0.22806E-07	-0.21183E-06	0.14212E-06	0.52297E-08	-0.85699E-07
a_{77}	0.56746E-08	-0.29999E-06	-0.15083E-07	-0.54997E-07	0.19369E-06

The coefficients (a_{ij}) for the secular change in the cot48 region.

a_{00}	-0.95533E 01
a_{10}	0.11582E 00
a_{11}	-0.93474E-01
a_{20}	0.13750E-01
a_{21}	-0.22416E-01
a_{22}	0.12437E-01
a_{30}	0.27558E-05
a_{31}	0.53560E-03
a_{32}	-0.70816E-03
a_{33}	0.32333E-03
a_{40}	-0.49965E-04
a_{41}	0.18579E-04
a_{42}	0.38544E-05
a_{43}	0.11451E-04
a_{44}	-0.63005E-05
a_{50}	-0.23992E-06
a_{51}	0.35195E-06
a_{52}	-0.26724E-06
a_{53}	-0.53815E-06
a_{54}	0.44979E-06
a_{55}	-0.12145E-06
a_{60}	0.85465E-07
a_{61}	-0.70500E-07
a_{62}	0.26013E-07
a_{63}	0.30705E-09
a_{64}	-0.12121E-07
a_{65}	-0.15529E-08
a_{66}	0.23462E-08

Appendix B. FORTRAN Program Listing of "MAGVAR".

```
C
C     THIS PROGRAM COMPUTES THE MAGNETIC VARIATION AS A
C     FUNCTION OF LATITUDE AND LONGITUDE.  THE SECULAR
C     CHANGE IS ALSO CALCULATED.  IT IS BASED ON THE
C     USD 80 POLYNOMIAL MODEL DEVELOPED BY FABIANO AND
C     OTHERS AT THE UNITED STATES GEOLOGICAL SURVEY IN
C     DENVER CO. PLEASE CONSULT USGS CIRCULAR NO.810 FOR DETAILS.
C                                   RAJAN KAUL - 3/84
C
C     THE INPUT VARIABLES ARE ALAT,ALON AND YEAR
C     REPRESENTING LATITUDE, LONGITUDE AND YEAR.
C     VARIABLES A AND A1 ARE THE COEFFICIENTS TO BE READ
C
      DIMENSION A(8,8),A1(8,8)
      DATA EAST/'EAST'/,WEST/'WEST'/
C
C     READ LATITUDE AND LONGITUDE
C
      WRITE(6,9)
9     FORMAT(1X,'TYPE LAT. AND LONG. AS NNN.NN NNN.NN (F6.2,1X,F6.2)')
      READ(7,8) ALAT,ALON
8     FORMAT(F6.2,1X,F6.2)
C
C     DETERMINE WHICH BAND THE POINT IS IN TO LOAD CORRECT
C     SET OF COEFFICIENTS CORRESPONDING TO PARTICULAR BAND.
C
      IF(ALON.GE.66.0.AND.ALON.LT.78.0) K=11
      IF(ALON.GE.78.0.AND.ALON.LT.90.0) K=12
      IF(ALON.GE.90.0.AND.ALON.LT.102.0) K=13
      IF(ALON.GE.102.0.AND.ALON.LT.114.0) K=14
      IF(ALON.GE.114.0.AND.ALON.LT.126.0) K=15
C
C     READ NORMALIZED LONGITUDE FOR PARTICULAR BAND AND THE
C     COEFFICIENTS.
C
      READ(K,7) DLON
7     FORMAT(F6.2)
      DO 5 NN=1,8
      DO 6 II=1,NN
      READ(K,3,END=13) A(NN,II)
3     FORMAT(E12.5)
6     CONTINUE
5     CONTINUE
C
C     DEFINE COLATITUDE AND NORMALIZED EAST LONGITUDE
C
13    DLA=90.0-ALAT
      DLO=360.0-ALON
C
C     INITIALIZE MAGNETIC VARIATION AND PERFORM CALCULATION
C
      AK=0.0
      DO 1 N=1,8
      DO 2 I=1,N
      KK=IABS(N-I)
      JJ=IABS(I-1)
      DL=DLO-DLON
      IF(DL.EQ.0.0) DL=360.0
      AK=AK+(A(N,I)*((DLA-52.01)**KK)*((DL)**JJ))
2     CONTINUE
1     CONTINUE
C
C     READ COEFFICIENTS FOR SECULAR CHANGE CALCULATION
C
      DO 15 NN=1,7
      DO 16 II=1,NN
      READ(16,23,END=14) A1(NN,II)
23    FORMAT(E12.5)
16    CONTINUE
15    CONTINUE
C
```

```
C
C     DEFINE COLATITUDE AND NORMALIZED EAST LONGITUDE
C
14    DLA=90.0-ALAT
      DLO=360.0-ALON
C
C     INITIALIZE SECULAR CHANGE AND PERFORM CALCULATION
C
      SV=0.0
      DO 11 N=1,7
      DO 12 I=1,N
      KK=IABS(N-1)
      JJ=IABS(I-1)
      DL=DLO-DLON
      IF(DL.EQ.0.0) DL=360.0
      SV=SV+(A(N,I)*((DLA-52.01)**KK)*((DL)**JJ))
12    CONTINUE
11    CONTINUE
C
C     READ YEAR
C
      WRITE(6,17)
17    FORMAT(5X,'TYPE YEAR AS NN.N (F4.1) E.G. JUN 84 = 84.5')
      READ(7,18) YEAR
18    FORMAT(F4.1)
C
C     COMPUTE SECULAR VARIATION ANNUAL AND TO PRESENT DATE.
C     ALSO COMPUTE MAGNETIC VARIATION
C
      SECVAR=SV*(YEAR-85.0)/60.0
      SS=SV/60.0
      VAR=AK+SECVAR
      IF(VAR.LT.0.0) DIR=WEST
      IF(VAR.GT.0.0) DIR=EAST
      V=ABS(VAR)
      WRITE(6,4) ALAT,ALON,V,DIR,SS
4     FORMAT(5X,'LATITUDE = ',F6.2/,5X,'LONGITUDE = ',F6.2/,5X,'MAGNETIC
     & VARIATION = ',F6.2,1X,A4/,5X,'SECULAR CHANGE (ANNUAL) = ',F6.2)
      STOP
      END
```

Appendix C. Instruction Set for the AM9511*.

COMMAND SUMMARY

Command Code 7	6	5	4	3	2	1	0	Command Mnemonic	Command Description
FIXED-POINT 16-BIT									
w	1	1	0	1	1	0	0	SADD	Add TOS to NOS. Result to NOS. Pop Stack.
w	1	1	0	1	1	0	1	SSUB	Subtract TOS from NOS. Result to NOS. Pop Stack.
w	1	1	0	1	1	1	0	SMUL	Multiply NOS by TOS. Lower half of result to NOS. Pop Stack.
w	1	1	1	0	1	1	0	SMUU	Multiply NOS by TOS. Upper half of result to NOS. Pop Stack.
w	1	1	0	1	1	1	1	SDIV	Divide NOS by TOS. Result to NOS. Pop Stack.
FIXED-POINT 32-BIT									
w	0	1	0	1	1	0	0	DADD	Add TOS to NOS. Result to NOS. Pop Stack.
w	0	1	0	1	1	0	1	DSUB	Subtract TOS from NOS. Result to NOS. Pop Stack.
w	0	1	0	1	1	1	0	DMUL	Multiply NOS by TOS. Lower half of result to NOS. Pop Stack.
w	0	1	1	0	1	1	0	DMUU	Multiply NOS by TOS. Upper half of result to NOS. Pop Stack.
w	0	1	0	1	1	1	1	DDIV	Divide NOS by TOS. Result to NOS. Pop Stack.
FLOATING-POINT 32-BIT									
w	0	0	1	0	0	0	0	FADD	Add TOS to NOS. Result to NOS. Pop Stack.
w	0	0	1	0	0	0	1	FSUB	Subtract TOS from NOS. Result to NOS. Pop Stack.
w	0	0	1	0	0	1	0	FMUL	Multiply NOS by TOS. Result to NOS. Pop Stack.
w	0	0	1	0	0	1	1	FDIV	Divide NOS by TOS. Result to NOS. Pop Stack.
DERIVED FLOATING-POINT FUNCTIONS									
w	0	0	0	0	0	0	1	SQRT	Square Root of TOS. Result in TOS.
w	0	0	0	0	0	1	0	SIN	Sine of TOS. Result in TOS.
w	0	0	0	0	0	1	1	COS	Cosine of TOS. Result in TOS.
w	0	0	0	0	1	0	0	TAN	Tangent of TOS. Result in TOS.
w	0	0	0	0	1	0	1	ASIN	Inverse Sine of TOS. Result in TOS.
w	0	0	0	0	1	1	0	ACOS	Inverse Cosine of TOS. Result in TOS.
w	0	0	0	0	1	1	1	ATAN	Inverse Tangent of TOS. Result in TOS.
w	0	0	0	1	0	0	0	LOG	Common Logarithm (base 10) of TOS. Result in TOS.
w	0	0	0	1	0	0	1	LN	Natural Logarithm (base e) of TOS. Result in TOS.
w	0	0	0	1	0	1	0	EXP	Exponential (e^x) of TOS. Result in TOS.
w	0	0	0	1	0	1	1	PWR	NOS raised to the power in TOS. Result in NOS. Pop Stack.
DATA MANIPULATION COMMANDS									
w	0	0	0	0	0	0	0	NOP	No Operation.
w	0	0	1	1	1	1	1	FIXS	Convert TOS from floating point to 16-bit fixed point format.
w	0	0	1	1	1	1	0	FIXD	Convert TOS from floating point to 32 bit fixed point format.
w	0	0	1	1	1	0	1	FLTS	Convert TOS from 16-bit fixed point to floating point format.
w	0	0	1	1	1	0	0	FLTD	Convert TOS from 32-bit fixed point to floating point format.
w	1	1	1	0	1	0	0	CHSS	Change sign of 16-bit fixed point operand on TOS.
w	0	1	1	0	1	0	0	CHSD	Change sign of 32-bit fixed point operand on TOS.
w	0	0	1	0	1	0	1	CHSF	Change sign of floating point operand on TOS.
w	1	1	1	0	1	1	1	PTOS	Push 16-bit fixed point operand on TOS to NOS (Copy).
w	0	1	1	0	1	1	1	PTOD	Push 32 bit fixed point operand on TOS to NOS (Copy).
w	0	0	1	0	1	1	1	PTOF	Push floating point operand on TOS to NOS (Copy).
w	1	1	1	1	0	0	0	POPS	Pop 16-bit fixed point operand from TOS. NOS becomes TOS.
w	0	1	1	1	0	0	0	POPD	Pop 32-bit fixed point operand from TOS. NOS becomes TOS.
w	0	0	1	1	0	0	0	POPF	Pop floating point operand from TOS. NOS becomes TOS.
w	1	1	1	1	0	0	1	XCHS	Exchange 16-bit fixed point operands TOS and NOS.
w	0	1	1	1	0	0	1	XCHD	Exchange 32-bit fixed point operands TOS and NOS.
w	0	0	1	1	0	0	1	XCHF	Exchange floating point operands TOS and NOS.
w	0	0	1	1	0	1	0	PUPI	Push floating point constant "π" onto TOS. Previous TOS becomes NOS.

NOTES:

1. TOS means Top of Stack. NOS means Next on Stack.
2. AMD Application Brief "Algorithm Details for the Am9511A APU" provides detailed descriptions of each command function, including data ranges, accuracies, stack configurations, etc.
3. Many commands destroy one stack location (bottom of stack) during development of the result. The derived functions may destroy several stack locations. See Application Brief for details.
4. The trigonometric functions handle angles in radians, not degrees.
5. No remainder is available for the fixed point divide functions.
6. Results will be undefined for any combination of command coding bits not specified in this table.

*Original not available at time of publication.

Appendix D. 6502 Assembly Language Program Listing of the Magnetic Variation Implementation on the Ohio University Loran-C Receiver.

```
        ORG $A8
BASE    BSS 2           BASE ADDRESS OF SCRATCHPAD RAM
        ORG $55
CTRN    BSS 1           COUNTER FOR OUTER LOOP IN LEAST SQUARES ALGOTITH
CTRI    BSS 1           COUTNER FOR INNER LOOP IN LEAST SQUARES ALGORITH
COFCTR BSS 1            COUNTER TO POINT AT THE RIGHT COEFFICIENT TO BE
*                       USED IN LEAST SQUARES ALGORITHM
COFTAB BSS 2            ADDRESS OF COEFFICIENT TABLE
MTEMP  BSS 1            TEMPORARY LOCATION USED BY MAGVAR CALCULATION.
MTEMP1 BSS 1            USED BY MAGVAR
*
*   EQUATES TO SUBROUTINE CALLS
*
PUSH    EQU $28AC       SUBROUTINE TO PUSH NUMBER ON TO 9511 STACK
POP     EQU $28DC       SUBROUTINE TO POP NUMBER FROM 9511 STACK
CMND    EQU $290C       SUBROUTINE TO ISSUE COMMAND TO 9511 TO PERFORM
*                      OPERATION
*
*   EQUATES TO VARIABLE ADDRESSES USED IN RNAV
*
PHGS    EQU $E0         LATITUDE OF RECEIVER
THGS    EQU $DC         LONGITUDE OF RECEIVER
P18     EQU $2C         180.0/PI
PAI2    EQU $30         2*PI
F90     EQU $24         PI/2
*         AM9511A COMMANDS.
*
PWR     EQU $0B
FADD    EQU $10
FSUB    EQU $11
FMUL    EQU $12
FDIV    EQU $13
SQRT    EQU 1
CHSF    EQU $15
*         CONSTANTS AND VARIABLES
BAND    EQU $0          ADDR FOR NORMALIZED LONGITUDE FOR PARTICULAR BAN
*           FOLLOWED BY 36 CO-EFFICIENTS FOR EACH BAND AT LOCATION
*           $C800 TO $CCFF - ONE PAGE FOR EACH OF 5 BANDS.
*
*
*   CONSTANTS FOR DIVISION IN LEAST SQUARES ALGORITHM FOR MAGVAR.
*
MZERO   EQU $0          -0.0
MONE    EQU MZERO+4     - 1.0
MTWO    EQU MONE+4      -2.0
MTHREE EQU MTWO+4       -3.0
MFOUR   EQU MTHREE+4    -4.0
MFIVE   EQU MFOUR+4     -5.0
MSIX    EQU MFIVE+4     -6.0
MSEVEN EQU MSIX+4       -7.0
*
*   CONSTANTS THAT DEFINE LIMITS IN BANDS OF COT48 TO DETERMINE
*   WHICH SET OF CO-EFFICIENTS NEED TO BE USED IN THE ALGORITHM
*   TO DETERMINE MAGNETIC VARIATION.
*
A78     EQU MSEVEN+4
A90     EQU A78+4
A102    EQU A90+4
A114    EQU A102+4
A5201   EQU A114+4       NORMALIZED LATITUDE = 52.01*PI/180 RADIANS
F180    EQU A5201+4     PI/180
ATEMP   EQU F180+4      TEMPORARY LOCATION USED WHILE DETERMINING THE PA
NDL     EQU ATEMP+4     MDLO-NORMALIZED LONGITUDE FOR PARTICULAR BAND.
MDLA    EQU NDL+4       PI/2-PHGS (DEGREES)
MDLO    EQU MDLA+4      2*PI-THGS (DEGREES)
MDLA52 EQU MDLO+4       MDLA-A5201
MAGVAR EQU MDLA52+4     CUMULATIVE MAGNETIC VARIATION
RLTEMP EQU MAGVAR+4     TEMPERORY LOCATION
MAGVD   EQU RLTEMP+4    MAGNETIC VARIATION
*
*
*
        ORG $C000
```

```
*
*   MOVE CONSTANT NUMBER TABLE IN SCRATCH SPACE
*
        LDA =1
        STA BASE+1      BASE = $0100
        LDA =0
        LDY =0
MO      LDA TABLE1,Y
        STA (BASE),Y
        INY
        CPY =56
        BNE MO
*
*
*   MAGNETIC VARIATION CALCULATION
*
        LDA =0
        STA CTRN
        STA CTRI        INITIALIZE COUNTERS
*
*   CALCULATE MDLA
*
        INC BASE+1
        INC BASE+1      BASE = $0300
        LDY =F90
        JSR PUSH
        DEC BASE+1      BASE = $0200
        LDY =PHGS
        JSR PUSH
        LDA =FSUB
        JSR CMND
        INC BASE+1      BASE = $0300
        LDY =P18
        JSR PUSH
        LDA =FMUL
        JSR CMND
        DEC BASE+1
        DEC BASE+1      BASE = $0100
        LDY =MDLA       MDLA = 90-PHGS
        JSR POP
*
*   CALCULATE MDLO
*
        INC BASE+1
        INC BASE+1      BASE = $0300
        LDY =PA12
        JSR PUSH
        DEC BASE+1      BASE = $0200
        LDY =THGS
        JSR PUSH
        LDA =FSUB
        JSR CMND
        INC BASE+1      BASE = $0300
        LDY =P18
        JSR PUSH
        LDA =FMUL
        JSR CMND
        DEC BASE+1
        DEC BASE+1      BASE = $0100
        LDY =MDLO
        JSR POP         MDLO = 360-THGS
*
*   CALCULATE MDLA52
*
        LDY =MDLA
        JSR PUSH
        LDY =A5201
        JSR PUSH
        LDA =FSUB
        JSR CMND
        JSR CMND
        LDY =MDLA52
        JSR POP         MDLA52 = MDLA-52
```

```
*
        INC BASE+1      BASE = $0200
        LDY =THGS
        JSR PUSH
        DEC BASE+1      BASE = $0100
        LDY =RLTEMP
        JSR POP         PUT THGS IN RLTEMP FOR COMPARISION PURPOSES IN T
*                    HE NEXT SEGMENT TO DETERMINE WHICH BAND TO USE
*               TO CALCULATE MAGVAR.
*
*   DETERMINE WHICH BAND IT IS TO CALCULATE MAGVAR.
*
        LDY =A78
        JSR PUSH
        LDY =RLTEMP
        JSR PUSH
        LDA =FSUB
        JSR CMND
        LDY =ATEMP
        JSR POP         ATEMP = 78*PI/180 - THGS
        LDY =ATEMP
        LDA (BASE),Y
        BPL M1          IF ATEMP IS +VE -- BAND 1, IF NOT TRY FOR BAND 2
*
        LDY =A90
        JSR PUSH
        LDY =RLTEMP
        JSR PUSH
        LDA =FSUB
        JSR CMND
        LDY =ATEMP
        JSR POP         ATEMP = 90*PI/180 - THGS
        LDY =ATEMP
        LDA (BASE),Y
        BPL M2          IF ATEMP IS +VE - BAND 2, IF NOT TRY FOR BAND 3
*
        LDY =A102
        JSR PUSH
        LDY =RLTEMP
        JSR PUSH
        LDA =FSUB
        JSR CMND
        LDY =ATEMP
        JSR POP         ATEMP = 102*PI/180 - THGS
        LDY =ATEMP
        LDA (BASE),Y
        BPL M3          IF ATEMP IS +VE - BAND 3, IF NOT TRY BAND 4
*
        LDY =A114
        JSR PUSH
        LDY =RLTEMP
        JSR PUSH
        LDA =FSUB
        JSR CMND
        LDY =ATEMP
        JSR POP         ATEMP = 114*PI/180 - THGS
        LDY =ATEMP
        LDA (BASE),Y
        BPL M4          IF ATEMP IS +VE - BAND 4
        JMP M5          MUST BE BAND 5
*
*   SET CO-EFFICIENT TABLE ADDRESS TO CORRESPOND WITH PARTICULAR BAND
*
M1      LDY =MDLO
        JSR PUSH
        LDA =$C8
        STA BASE+1
        STA COFTAB+1    BAND 1
        JMP M6
*
M2      LDY =MDLO
        JSR PUSH
        LDA =$C9
```

```
        STA BASE+1
        STA COFTAB+1    BAND 2
        JMP M6
*
M3      LDY =MDLO
        JSR PUSH
        LDA =$CA
        STA BASE+1
        STA COFTAB+1    BAND 3
        JMP M6
*
M4      LDY =MDLO
        JSR PUSH
        LDA =$CB
        STA BASE+1
        STA COFTAB+1    BAND 4
        JMP M6
*
M5      LDY =MDLO
        JSR PUSH
        LDA =$CC
        STA BASE+1
        STA COFTAB+1    BAND 5
*
M6      LDA =0
        STA COFTAB
        LDY =BAND
        JSR PUSH
        LDA =FSUB
        JSR CMND
        LDA =1
        STA BASE+1      BASE = $0100
        LDY =NDL
        JSR POP         NDL=MDLO-NORMALIZED LONGITUDE FOR PARTICULAR BAN
        LDA =4
        STA COFCTR      SET CO-EFFICIENT COUNTER TO POINT TO CO-EFFICIEN
C2      CLC
        LDA CTRN        LOAD OUTER LOOP COUNTER
        ROL A
        ROL A           POINT TO LOCATION FOR EXPONENTS FOR LEAST SQUARE
        STA MTEMP
        LDY MTEMP
        JSR PUSH
        LDA CTRI        LOAD INNER LOOP COUNTER
        ROL A
        ROL A           POINT TO LOCATION FOR EXPONENTS
        STA MTEMP
        LDY MTEMP
        JSR PUSH
        LDA =FSUB
        JSR CMND        N-1
        LDY =RLTEMP
        JSR POP         (N-1)
        LDY =MDLA52
        JSR PUSH
        LDY =MDLA52
        LDA (BASE),Y
        BPL C6
        LDA =1          SET FLAG IF NEGATIVE AND CHANGE SIGN
        STA MTEMP1
        LDA =CHSF
        JSR CMND
        JMP C9
C6      LDA =0
        STA MTEMP1
C9      LDY =RLTEMP
        JSR PUSH
        LDA =PWR
        JSR CMND        MDLA52**(N-1)
        CLC
        LDA CTRN
        SBC CTRI
        AND =1          EXPONENT EVEN ?
```

```
        BNE C4          YES, LOOP OUT
        LDA MTEMP1      NO, IS NEGATIVE FLAG SET ?
        BEQ C4          NO, FLAG NOT SET -- LOOP OUT
        LDA =CHSF       EXPONENT WAS ODD AND NEGATIVE FLAG
        JSR CMND        WAS SET --- THEREFORE CHANGE SIGN AGAIN
C4      LDY =ATEMP
        JSR POP         MDLA52**(N-1)
        CLC
        LDA CTRI        LOAD INNER LOOP COUNTER FOR LEAST SQUARES PROCED
        ROL A
        ROL A           POINT TO LOCATION FOR EXPONENTS
        STA MTEMP
        LDY MTEMP
        JSR PUSH
        LDY =RLTEMP
        JSR POP
        LDY =NDL
        JSR PUSH
        LDY =NDL
        LDA (BASE),Y
        BPL C7
        LDA =0
        STA MTEMP1
        LDA =CHSF
        JSR CMND
        JMP C8
C7      LDA =1
        STA MTEMP1
C8      LDY =RLTEMP
        JSR PUSH
        LDA =PWR
        JSR CMND        NDL**I
*
* IN THIS NEXT SEGMENT A TEST IS DONE TO MAKE SURE THE CORRECT SIGN
* IS ATTACHED WITH THE RESULT AFTER THE EXPONENT CALCULATION.
*
        LDA CTRI
        AND =1
        BEQ C5
        LDA MTEMP1
        BNE C5
        LDA =CHSF
        JSR CMND
C5      LDY =ATEMP
        JSR PUSH
        LDA =FMUL
        JSR CMND        MDLA52**(N-1)*NDL**I
        LDA COFTAB+1
        STA BASE+1      PUT CO-EFFICIENT TABLE ADDRESS IN BASE
        LDY COFCTR      POINT TO CO-EFFICIENT COUNTER
        JSR PUSH
        LDA =FMUL
        JSR CMND        A(NI)*NDL**(I)*MDLA52**(N-1)
        LDA =1
        STA BASE+1      BASE = $0100
        LDY =MAGVAR
        JSR PUSH
        LDA =FADD
        JSR CMND        ADD TO ACCUMULATE THE VALUE OF MAGVAR
        LDY =MAGVAR
        JSR POP         MAGVAR=MAGVAR+A(N,I)*NDL**I*MDLA52**(N-1)
        INC COFCTR
        INC COFCTR
        INC COFCTR
        INC COFCTR      POINT TO NEXT SET OF CO-EFFICIENTS
        LDA CTRN
        CMP CTRI
        BEQ C1          IF THEY ARE EQUAL INNER LOOP DONE, CHECK IF OUTE
        INC CTRI
        JMP C2          IF NOT, GO BACK AND COMPLETE OUTER LOOP
C1      LDA CTRN        CHECK TO SEE IF OUTER LOOP COMPLETE
        CMP =7
        BEQ C3          OUTER LOOP ALSO DONE, BRANCH OUT
```

```
        INC CTRN        INCREMENT OUTER LOOP COUNTER
        LDA =0
        STA CTRI        INITIALIZE INNER LOOP COUNTER
        JMP C2          START OVER
C3      RTS             RETURN FROM MAGVAR TO MAIN PROGRAM
*
*   TABLE OF CONSTANTS USED BY MAGNETIC VARIATION STORED
*   STARTING AT $0100 IN SCRATCHPAD RAM LOCATION.
*
TABLE1 HEX 00,00,00,00 - 0.0 (MZERO)
       HEX 01,80,00,00 - 1.0 (MONE)
       HEX 02,80,00,00 - 2.0 (MTWO)
       HEX 02,C0,00,00 - 3.0 (MTHREE)
       HEX 03,80,00,00 - 4.0 (MFOUR)
       HEX 03,A0,00,00 - 5.0 (MFIVE)
       HEX 03,C0,00,00 - 6.0 (MSIX)
       HEX 03,E0,00,00 - 7.0 (MSEVEN)
       HEX 01,AE,40,F1 - 78*PI/180 (A78)
       HEX 01,C9,0F,DA - 90*PI/180 (A90)
       HEX 01,E3,DE,C4 - 102*PI/180 (A102)
       HEX 01,FE,AD,AE - 114*PI/180 (A114)
       HEX 06,D0,0A,3D - 52.01*PI/180 (A5201)
       HEX 7B,8E,FA,35 - PI/180.0 (F180)
*
*   CO-EFFICIENTS FOR THE FIVE BANDS OF THE COT48
*   THE DATA LABELED BAND(N) IS THE NORMALIZED
*   LONGITUDE FOR EACH BAND. THE CO-EFFICIENTS
*   ARE STORED IN ONE PAGE CHUNKS STARTING AT
*   $3800 TO $3CFF.
*
       ORG $C800
BAND1  HEX 09,90,81,48 - 289.01
       HEX 84,C8,B2,96
       HEX 7F,F2,B6,07
       HEX 80,CA,E9,68
       HEX FA,F4,B3,9C
       HEX 79,9B,AC,C4
       HEX 79,EF,5E,07
       HEX 75,97,EB,10
       HEX 75,F1,C0,9A
       HEX F7,C5,A5,66
       HEX 77,A2,06,A6
       HEX 71,D4,E9,7F
       HEX F1,F8,7E,E8
       HEX F1,97,F0,15
       HEX 72,E7,02,28
       HEX 73,83,B0,EB
       HEX 6A,F8,66,41
       HEX ED,CC,F2,4A
       HEX 6D,BF,FC,83
       HEX EF,82,5D,9D
       HEX 6F,B9,C1,F7
       HEX F0,80,1E,7A
       HEX E9,86,96,3E
       HEX 69,AB,24,13
       HEX 6A,A6,DD,20
       HEX 69,D2,22,6E
       HEX 69,F8,29,C8
       HEX EC,CC,59,1D
       HEX 67,C6,CD,89
       HEX E0,B9,62,17
       HEX 61,EC,8F,0F
       HEX E5,ED,7C,38
       HEX 64,E2,F5,2F
       HEX 66,A1,5E,31
       HEX 66,9D,6A,60
       HEX 67,C3,E7,CE
       HEX 65,C2,FA,4F
       ORG $C900
BAND2  HEX 09,8A,81,48 - 277.01
       HEX 82,AB,39,97
       HEX 7F,9C,26,DD
       HEX 80,DA,4A,06
```

```
        HEX FA,C3,82,A1
        HEX 7B,98,1F,46
        HEX 7B,A0,F5,0D
        HEX 76,A9,0D,F8
        HEX F6,C0,C6,EB
        HEX F7,D5,7C,74
        HEX F7,8F,48,07
        HEX 72,85,1D,21
        HEX 72,C3,BC,D9
        HEX F2,D6,1C,5F
        HEX F3,97,6B,BF
        HEX F6,9F,AC,25
        HEX EE,82,A3,89
        HEX 6E,B2,1F,27
        HEX EF,C9,0D,58
        HEX EF,C3,E7,79
        HEX 72,A2,8A,81
        HEX 72,B9,90,7C
        HEX E9,A4,31,BA
        HEX E9,86,30,51
        HEX 6A,BE,EF,E4
        HEX E8,80,E6,8B
        HEX 6B,85,BA,65
        HEX 6C,C7,98,81
        HEX 6F,A3,AC,54
        HEX 64,A9,E4,CF
        HEX E5,83,D6,58
        HEX 67,A9,F4,1D
        HEX E6,83,D2,DF
        HEX E8,AB,E8,48
        HEX 68,E2,35,A1
        HEX EA,E3,72,90
        HEX EB,A1,0D,C3
        ORG $CA00
BAND3   HEX 09,84,81,48 - 265.01
        HEX 03,D5,58,CD
        HEX 79,F1,19,1D
        HEX 80,A0,E9,70
        HEX F9,F7,84,B1
        HEX 7B,C1,81,09
        HEX FA,A2,F3,EB
        HEX 76,97,BB,AF
        HEX F5,9A,D3,6F
        HEX 76,B7,E2,A7
        HEX 72,F5,70,94
        HEX 72,E3,F3,4B
        HEX 70,A8,0F,1E
        HEX 73,A2,0E,7C
        HEX 74,96,03,2F
        HEX 72,E6,F3,C5
        HEX EF,89,69,28
        HEX EE,A8,D1,DA
        HEX F0,93,B3,7A
        HEX F0,89,EE,A5
        HEX F0,EA,E5,68
        HEX EF,97,C9,C6
        HEX EA,83,91,11
        HEX 67,96,50,EE
        HEX 68,A8,95,5F
        HEX E7,ED,2E,8D
        HEX ED,D2,B5,5A
        HEX ED,F8,D0,15
        HEX EB,D1,56,79
        HEX 66,91,88,D2
        HEX 65,97,8D,FC
        HEX 66,85,D8,91
        HEX E1,CE,0C,45
        HEX 69,BE,20,A2
        HEX 6A,86,DF,B0
        HEX 6A,98,99,19
        HEX E7,81,8F,35
        ORG $CB00
```

```
BAND4   HEX 08,FD,02,8F - 253.01
        HEX 04,D0,80,9D
        HEX FE,FF,CE,74
        HEX FF,BA,BB,CB
        HEX 76,DC,64,B4
        HEX 7B,9C,F5,DA
        HEX FB,8D,07,85
        HEX 74,98,19,1A
        HEX F7,8C,5B,C3
        HEX 75,BB,CE,22
        HEX F7,A3,B4,25
        HEX 70,E5,42,BA
        HEX EF,D6,86,8B
        HEX 73,E2,D2,E2
        HEX F2,D3,47,EB
        HEX 72,85,73,91
        HEX EC,DC,6C,A8
        HEX 6F,C9,DD,4E
        HEX F0,96,BB,67
        HEX 6F,DA,9C,74
        HEX 6F,C4,0D,19
        HEX 71,A2,4F,72
        HEX E7,B1,0E,7D
        HEX E1,E5,7D,2D
        HEX E9,D8,AD,43
        HEX 68,F5,00,52
        HEX EC,E4,10,69
        HEX 6C,A7,DC,02
        HEX E8,C2,84,C6
        HEX 63,8B,F8,78
        HEX E6,C5,86,8A
        HEX 67,90,31,E7
        HEX 62,B0,3B,29
        HEX 67,ED,DE,B1
        HEX E9,C8,6D,A5
        HEX 65,B3,B1,5E
        HEX E8,EC,36,48
        ORG $CC00
BAND5   HEX 08,F1,02,8F - 241.01
        HEX 04,FF,F4,F1
        HEX FF,CE,B2,29
        HEX FE,D0,F4,95
        HEX 7A,89,50,CC
        HEX 79,9B,89,C9
        HEX F9,D5,2C,6D
        HEX 75,BC,F5,25
        HEX ED,E0,20,A4
        HEX 74,B6,6B,73
        HEX 78,96,8C,74
        HEX F0,F1,E6,21
        HEX F2,AA,AC,0F
        HEX 73,B9,FF,23
        HEX 71,9C,AD,69
        HEX F2,D9,31,E5
        HEX EE,D7,C0,F0
        HEX 6E,92,95,4D
        HEX EA,B3,02,45
        HEX F0,E9,1C,DA
        HEX 71,8A,7C,2A
        HEX F2,9E,31,E4
        HEX ED,D2,B5,5A
        HEX ED,F8,D0,15
        HEX EB,D1,56,79
        HEX 66,91,88,D2
        HEX 65,97,8D,FC
        HEX 66,85,D8,91
        HEX E1,CE,0C,45
        HEX 69,BE,20,A2
        HEX 6A,86,DF,B0
        HEX 6A,98,99,19
        HEX E7,81,8F,35
        ORG $CB00
```

```
BAND4   HEX 08,FD,02,8F - 253.01
        HEX 04,D0,80,9D
        HEX FE,FF,CE,74
        HEX FF,BA,BB,CB
        HEX 76,DC,64,B4
        HEX 7B,9C,F5,DA
        HEX FB,8D,07,85
        HEX 74,98,19,1A
        HEX F7,8C,5B,C3
        HEX 75,BB,CE,22
        HEX F7,A3,B4,25
        HEX 70,E5,42,BA
        HEX EF,D6,86,8B
        HEX 73,E2,D2,E2
        HEX F2,D3,47,EB
        HEX 72,85,73,91
        HEX EC,DC,6C,A8
        HEX 6F,C9,DD,4E
        HEX F0,96,BB,67
        HEX 6F,DA,9C,74
        HEX 6F,C4,0D,19
        HEX 71,A2,4F,72
        HEX E7,B1,0E,7D
        HEX E1,E5,7D,2D
        HEX E9,D8,AD,43
        HEX 68,F5,00,52
        HEX EC,E4,10,69
        HEX 6C,A7,DC,02
        HEX E8,C2,84,C6
        HEX 63,8B,F8,78
        HEX E6,C5,86,8A
        HEX 67,90,31,E7
        HEX 62,B0,3B,29
        HEX 67,ED,DE,B1
        HEX E9,C8,6D,A5
        HEX 65,B3,B1,5E
        HEX E8,EC,36,48
        ORG $CC00
BAND5   HEX 08,F1,02,8F - 241.01
        HEX 04,FF,F4,F1
        HEX FF,CE,B2,29
        HEX FE,D0,F4,95
        HEX 7A,89,50,CC
        HEX 79,9B,89,C9
        HEX F9,D5,2C,6D
        HEX 75,BC,F5,25
        HEX ED,E0,20,A4
        HEX 74,B6,6B,73
        HEX 78,96,8C,74
        HEX F0,F1,E6,21
        HEX F2,AA,AC,0F
        HEX 73,B9,FF,23
        HEX 71,9C,AD,69
        HEX F2,D9,31,E5
        HEX EE,D7,C0,F0
        HEX 6E,92,95,4D
        HEX EA,B3,02,45
        HEX F0,E9,1C,DA
        HEX 71,8A,7C,2A
        HEX F2,9E,31,E4
        HEX 67,DA,A5,80
        HEX 6A,8F,5A,F3
        HEX EB,ED,D6,25
        HEX 6D,98,6D,AB
        HEX ED,BD,43,5B
        HEX EC,B1,2A,FE
        HEX 6D,92,4C,1D
        HEX 65,DF,5D,34
        HEX E6,82,BE,74
        HEX E6,E7,39,BF
        HEX 69,B5,F0,07
        HEX E9,95,1D,C7
        HEX 67,FE,63,A2
        HEX E9,B8,09,B0
        HEX 6A,CF,F8,D4
        END
```

A PROGRAM DOWNLOADER AND OTHER UTILITY SOFTWARE FOR THE DATAC BUS MONITOR UNIT*

Stanley M. Novacki, III
Avionics Engineering Center
Department of Electrical and Computer Engineering
Ohio University
Athens, Ohio

*Published as Ohio University Technical Memorandum 92, July 1984.

A set of programs designed to facilitate software testing on the DATAC Bus Monitor is described.

I. INTRODUCTION

The DATAC Bus Monitor Unit (BusMon) is a Z8000-based microcomputer system designed to receive, interpret, and display selected data items appearing on a DATAC Digital Data Bus. Software for the Bus Monitor Unit is developed on a Tektronix 8550 Microprocessor Development System (MDS). Once a program is written and compiled to object code, it may be tested using the in-circuit emulation and memory-partitioning capabilities of the 8550. The in-circuit emulator allows the MDS to imitate the Z8000 processor, giving the operator extensive control of the test system, while memory partitioning allows the prototype system to utilize memory in the 8550 as though it were part of the target system's memory. This is a great help in lab-testing of the prototype system because of the simplicity of loading and running the test software.

Because of the size of the Tektronix hardware, it is somewhat cumbersome to transport the entire MDS and the prototype system to a field installation simply to test programs in situ. To make on-site testing easier, a series of programs was developed to allow the Z8000 system, running in a standalone mode, to receive program code via its RS232C ports and ports on the host system, which stores the test program in a disk file. Once the program design is finalized, another utility program allows the Z8000 system to send the test software in ASCII form to a ProLog PROM programmer, eliminating the need for an integral PROM programmer on the MDS. These software tools are intended to simplify the development and testing of the data acquisition, reduction, and display routines planned for the DATAC Bus Monitor Unit.

II. IMPLEMENTATION

On the Tektronix 8550 MDS:

Once a program for the Z8000 system has been written and reduced to machine code, it can be transferred to a DOS/50 disk file. DOS/50 is the operating system currently in use on the MDS. The file format consists of lines of ASCII characters in a format called Standard TEKHEX (figs. 1, 2). There are two types of records in a TEKHEX file: data records and the "null" or terminator record. The format for a data record begins with the slash character "/" which denotes the start of a valid record. The slash is followed by 4 hex digits which specify the absolute loading address for the data contained in this record. Next are two hex digits which specify the number of bytes of data contained in the record. The following two digits form a nybble checksum of the load address and the datum count; that is, each digit of the load address and byte count are added together. This number, modulo 256, provides the first checksum. Following the checksum comes the data bytes representing the actual machine code of the program. After the data is the data nybble checksum. As with the first checksum, this is the sum of the individual hex digits of the data, modulo 256. Each record is terminated by an ASCII CR (0D hex). The last record in a TEKHEX file is the "null" record, that is, one with a datum count of zero. An address/byte-count checksum is still generated, usually with a zero value.

A file in this format can be sent to a slave system via RS232C communications ports on the slave and the MDS. The host system will read a record from the TEKHEX file, send it to the prototype system, and wait for a single ASCII token to indicate a good (ACK) or bad (NAK) reception. The 8550 uses the digits "0" as the ACK token and "7" as the NAK symbol. If the prototype system replies with an ACK, the MDS will send the next record, wait for the prompt for that record and so on until the entire file is sent. If the prototype system fails to reconstitute the same checksums sent in the TEKHEX record, it will reply with the NAK token. The 8550 will recognize this as a failed transmission and re-send the same record. The 8550 will continue to send the flagged record until the slave system elects to abort the load operation with an abort message, which appears on the 8550 console and halts the load operation, or the number of retries exceeds a limit set by the host system operator. After all data records are sent, followed by the null record, the 8550 exits from the load routines and and resumes terminal emulation. From this point, the MDS may simply be used as a console device to the prototype and the program is run on the prototype.

On The Bus Monitor Unit:

The loader program for the Z8000-based system (fig. 3; listing 1) is designed to accept serial ASCII data TEKHEX format, convert it to machine code, and store it in the prototype system memory. The processor monitor software for the Bus Monitor Unit provides serial I/O routines which allow it to transmit and receive blocks of ASCII data via serial port A, the default console port, by using the Z8000 System Call instruction, SC #0. The Z8000 loader program begins by sending the ACK token to the host system to indicate that it is ready to receive characters. The input operation of SC #0 returns a string in memory terminated by a carriage return. Once a string has been read, the loader routine scans the input buffer to find the "/" character to define the beginning of the record. If the slash does not occur in the first 80 bytes, it is assumed that part of the record was lost; TEKHEX records do not usually exceed 73 characters including the terminating carriage return. The loader routine sends a NAK token to request a re-send and waits for the next transmission.

Once a record has been received and the slash found, the load address and byte count are converted from ASCII representations to their actual hexadecimal values. This is done by shifting the seven-bit-code for the most-significant-digit of a data byte (i.e, a single ASCII character) to the left by 4 bits, producing a datum of the form "x0" from "zx" in hex. The next character ("zy"), the least-significant digit of the datum being reconstituted, is logically ANDed with 0F hex to zero the high order bits, leaving a "0y" pattern in hex. The loader then ORs the two patterns together, giving a byte of the form "xy". If the character being converted is a numeric, the binary-coded decimal (BCD) representation of the number and the least significant nybble match exactly and the conversion process may proceed. If the hex character is an alphabetic, A-F, some adjustment is needed because the 4 low-order bits of the ASCII characters A through F do not correspond to the hexadecimal values A through F (10 to 15 decimal). In fact, the low-order nybble of ASCII characters A-F has the values 1-6

in BCD. Because of the sequential value, we may correct these characters' codes to correspond to their actual value by adding 09 hex to the character code before the masking process. This addition bumps the low-order bits to a pattern corresponding to the binary representation of their namesakes. With this correction, the characters A-F can then be processed like the numerics 0-9. The alphabetic character adjustment is handled by subroutine TSTNUM and the ASCII-to-hexadecimal conversion is performed by ASCHEX.

Once the load address and byte count are reconstituted, the first checksum is generated. If the computed and transmitted checksums do not agree, a NAK token is sent and the Bus Monitor waits for a new transmission. Otherwise, the program reconstitutes the data stream using ASCHEX, stores it using the load address it generated earlier, and maintains a running checksum. After all data have been stored in the prototype's RAM, the data checksum is reconstituted from the string buffer and compared with the calculated value. If a mismatch occurs, a NAK token is sent and the Bus Monitor waits for the the same record to be retransmitted from the host. Otherwise, it issues an ACK, waits for the next record, and continues the load-and-store process until the entire file has been sent. In the event 5 successive checksum errors occur, the Bus Monitor will abort the load operation by sending an "Abort Load" record, whose message is displayed on the system console (line 198 of listing 1). When the null record is received, the Z8000 returns to the resident monitor via SC #3. No integrity check is performed on the checksum, since a transmission error at this point doesn't affect any data that has been stored.

On the CP/M-based Bus Monitor Console System:

In field experiments, a DEC VT-180 will be used as the host for the program down-loading in addition to being a data display/command input device. The file down-loader (listing 2) is written in the "C" language for the CP/M environment by Manx Software Systems. This loader contains two deviations from the 8550 down-load procedure: one is that the VT-180 itself counts errors and exits on 5 successive errors; the other is that on completion of file transmission, the loader is exited and the VT-180 returns to the CP/M command processor rather than to terminal mode.

Prolog PROM Programmer Support:

This utility can be thought of as a complement to the downloader program for the Z8000. The program (listing 3) sends machine code from the Bus Monitor Unit to a Prolog PROM Programmer equipped with an RS-232C serial port. Two factors complicate this seemingly simple task: one is that the serial port drivers for the PROM programmer expect to see only ASCII data. The other is that the memory for a Z8000 system is organized as 16-bit words. As yet, there are no 16-bit-wide memory devices being manufactured. The designers of these microcomputer systems routinely solve the latter problem by using 2 byte-wide RAMs or ROMs in parallel, one device located at an even byte address, the other at the subsequent odd address. The first "trick" is that we must read alternating memory locations (all even or all odd) addresses when sending data to the programmer.

We will solve the former problem by a procedure which complements the ASCHEX subroutine described earlier. The program produces two ASCII characters from one hexadecimal byte by splitting the byte into high and low-order nybbles and then shifting the high order nybble to the right 4 bit places. For example, byte "xy" becomes two bytes "0x" and "0y". For the hexadecimal digits 0-9, we simply add 30 hex to each byte and we have the ASCII character corresponding to the BCD digit. The hex digits A-F again pose another problem: the ASCII collating sequence has specified that the low-order nybbles of of the codes for the characters A-F are 1-6 decimal, not A-F hex. Further, the high order nybble of those letter digits is a hex 4, not a 3, as is the case for the numeric characters. To handle this case, the program tests the nybble being converted to see if it lies in the range of A-F. If so, an adjuster of 07 hex is added to the nybble first. This corrects the least significant digit to the proper value and puts a 1 in the most significant digit. For example, to turn 0C hex to 43 hex (the ASCII code for the letter "C") the following happens: add 07 to 0C giving 13 hex, then add 30 hex giving 43 hex, giving the desired character code.

The PROLOG utility is usually used with the 8550 running in processor emulation mode in the Bus Monitor system. A data rate of 2400 baud between the test system and the PROM programmer is assumed. The programmer support routine normally resides at address 4000 hex. If this conflicts with the intended load address of the program being sent to the PROM programmer, the support routine can be moved to another memory location. This is possible because the utility program uses only relative addresses, excepting the I/O port addresses which present no relocatability problems. Once the utility program and the application program have been loaded into Bus Monitor memory, the PROM programmer is set to receive the first block (even or odd) of data. Using the 8550 emulator or the Resident Monitor, the following CPU registers are initialized: R10 contains the address of the first byte if the program being sent to the programmer, R11 contains the address of the last byte to be programmed, and R12 contains a 0 if even-numbered bytes are being ROMmed, and a 1 if odd-numbered bytes are being sent to the programmer. Execution begins at the label GO; the "B" serial port on the serial I/O card is used to send data to the PROM programmer, R9 points to the machine code being processed. A pass is complete when R9 is greater than R11, the stop address. For convenience, a breakpoint can be set at GO + 4C hex, so that R12 can be toggled to send the second block of data bytes without having to reset R10 and R11. With R12 readied for the next series of data and the programmer fitted with a new chip, execution may be resumed with a "GO" command, completing the programming process.

III. SUMMARY

The software described in this paper will facilitate the design and testing of software for the DATAC Bus Monitor Unit. By providing a means to simplify program loading, firmware generation, and subsequent testing of programs, we can reduce the overhead involved in software evaluation and use that time more productively in performance, analysis and improvement of current software.

IV. ACKNOWLEDGMENTS

I would like to thank Mr. Kim Constantikes of Carnegie-Mellon University, Mr. John Simmons of Tektronix, Inc., and Mr. Jim Ramsay and Mr. Bill Lynn, both of Kentron International, for their support and patience during the development of these programs.

V. BIBLIOGRAPHY

[1] Kernighan, Brian W. and Ritchie, Dennis M., "The C Programming Language", Prentice-Hall, Inc.; 1978.

[2] Hancock, Les and Krieger, Morris, "The C Primer", McGraw-Hill Book Company, New York; 1982.

[3] "8550 Series B Z8001/Z8002 Assembler Specifics", Tektronix, Inc., Beaverton, OR.

[4] "ProLog Series 90 PROM Programmer Operating Manual", ProLog Corp., Monterey, CA.

[5] "Aztec C II Users' Guide," Manx Software Systems, Shrewsbury, NJ; 1981.

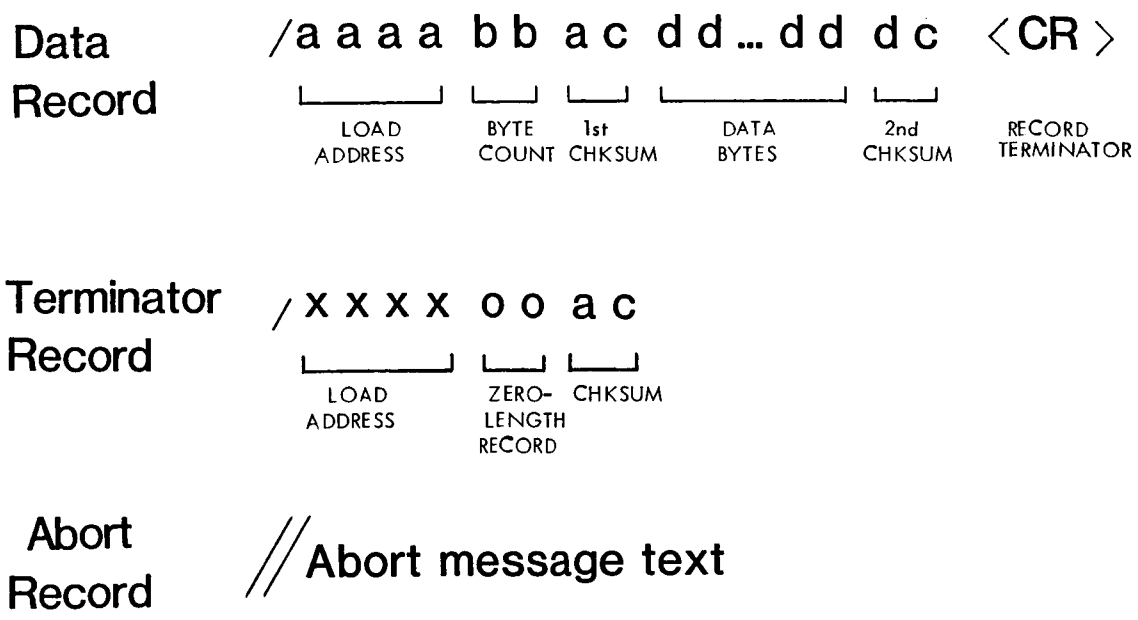

Figure 1. TEKHEX-format records used by BusMon loader program.

```
/1010080A21E462ABBC6E2F3270

/1018030D103FB220

/101B000D
```

Figure 2. Sample TEKHEX file.

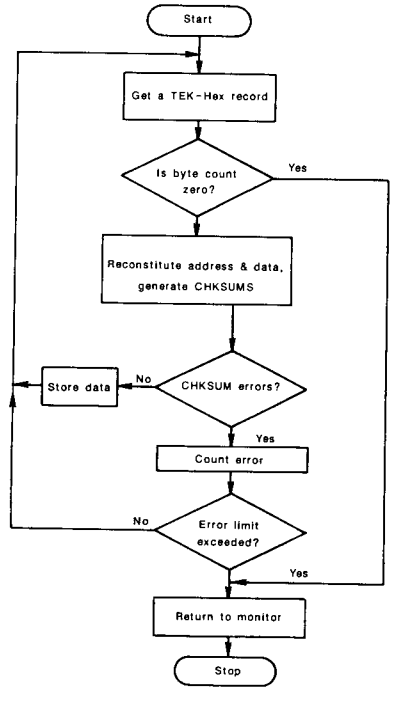

Figure 3. Z8000 loader outline.

APPENDIX A

LISTING 1

```
ASM     Z8001/Z8002
V01.01-01  (8550)                                   01-DEC-83/08:48:48

 1                          ;       DATAC BUS MONITOR:
 2                          ;       LOADER FOR Z8000 PROCESSOR INTERFACE TO DATAC SYSTEM
 3                          ;       AUTHOR:  S.M. NOVACKI     2 SEPT 83
 4                          ;       REV 22 NOV 83: INCLUDES ERROR HANDLER- EXITS TO MONITOR
 5                          ;
 6                          ; MACRO DEFINITIONS HERE:
 7                                  MACRO   NYBSUM
 8                                  LDB     RL2,RH2         ;TRANSPOSE HEX DIGITS
 9                                  SRAB    RL2,#04         ;MAKE HOD THE LOD
10                                  AND     R2,#0F0FH       ;MASK OFF HO BITS
11                                  ADDB    RH2,RL2         ;ADD NYBBLES W/O CARRY
12                         ;RH2 HOLDS NYBBLE CHECKSUM, TRANSFERRED TO RH7
13                                  ENDM
14                         ;THIS MACRO PERFORMS A TEST FOR CHECKSUM ERRORS, IF >5 THE LOAD IS ABORTED
15                                  MACRO   ERRMSG
16                                  INC     R13             ;COUNT NEW ERROR OCCURRENCE
17                                  CP      R13,#5          ;REACH MAX# OF ERRORS?
18                                  JR      UGT,ABRTLD      ;TOO MANY ERRORS- RETURN TO MONITOR
19                                  SET     R12,#01         ;SET 'OLD STRING, REPEAT' FLAG
20                                  LDB     ACKBUF,#NAK     ;READY BAD TX MSG
21                                  JR      NEWSTR          ;REQUEST REPEAT OF MSG AND CLEAR INBUF
22                                  ENDM
23                         ;
24              FE00 R              ORG     0FE00H
25                         ;I/O STRING BUFFER DEFINITIONS, MUST BE ORG'D IN RAM
26  0000FE00      4        ACKBUF BLOCK   4       ;THREE BYTE BUFFER TO HANDSHAKE WITH 8550 DURING FILE TX
27  0000FE04     50        INBUF  BLOCK   80      ;80 BYTE BUFFER FOR RECEIVING TEKHEX FILES
28  0000FE54      8        TKHXIN BLOCK   8
29  0000FE5C      8        TKINAK BLOCK   8       ;I/O FC BLOX (WORKSPACE)
30                         ;
31              80E R               ORG     080EH
32                         ;CONSTANT DEFINITIONS:
33                3E       PROMPT EQU     3EH     ;8550 HANDSHAKE PROMPT CHAR
34                30       ACK    EQU     30H     ;MSG RECEIVED TOKEN
35                37       NAK    EQU     37H     ;MSG NOT RECEIVED TOKEN
36                0D       RECEND EQU     0DH     ;CR USED TO TERMINATE PROMPT STRING
37                2F       RECMRK EQU     2FH     ;'SLASH' CHAR USED TO DELIMIT TEKHEX RECORDS
38                         ;
39
40
42                         ;
43                         ; BEGINNING OF LOADER ROUTINE;
44                         ; CONSULT ZMON.DASSY AND .DUMP TO DETERMINE ACTUAL ADDRESSES
45                         ; BEGINNING OF ROMABLE ROUTINES, ALL JUMPS RELATIVE, ONLY
46                         ; RAM REFERENCES ARE ABSOLUTE FOR DURATION OF LOADER OPERATION
47                         ;
48  0000080E 53544420      TMMSG  ASCII    'STD TEKHEX LOADER '    ; NOTE# OF BYTES IN STRING MUST BE EVEN
            54454B48
            4558204C
            4F414445
            5220
49                         ;
50  00000820 4D08FE00 R    INTCOM  CLR     ACKBUF          ;ONLY 3 OF 4 BYTES USED
51  00000824 4D08FE02 R            CLR     ACKBUF+2        ;IN HANDSHAKE SEQUENCE
52  00000828 4C05FE01 R            LDB     ACKBUF+1,#RECEND        ;READY STRING FOR
            0D0D
53  0000082E 4C05FE02 R            LDB     ACKBUF+2,#PROMPT        ;TEK HANDSHAKE
            3E3E
54  00000834 8DC8                  CLR     R12             ;FLAG: 0=NEW STRING, 1=REP'T OF LAST STRING
55  00000836 DF56                  CALR    SETIO           ;SET UP FCB FOR INPUT OPERATIONS
56                                                         ;SET UP FCB FOR OUTPUT OPERATIONS
57  00000838 8CA8          NEWSTR  CLRB    RL2             ;(R2)=0 FOR ZAPPING
58  0000083A 210A0050              LD      R10,#80         ;NUMBER OF BYTES TO BE ZAPPED
59  0000083E 2109FE04 R            LD      R9,#INBUF
60  00000842 729A0A00      ZAPWRD  LDB     R9(R10),RL2     ;ZERO OUT INBUF (I HOPE..)
61  00000846 ABA0                  DEC     R10
62  00000848 EEFC                  JR      NZ,ZAPWRD;
63  0000084A 2101FE5C R    OUTMSG  LD      R1,#TKINAK      ;SELECT SIGNAL MODE FOR TEK
64  0000084E 7F00                  SC      #0              ;OUTPUT PROMPT VIA MONITOR ROUTINE
```

```
65                                      ;
66                                      ;HOPEFULLY WITH A SERIAL LINE DEDICATED TO THE Z8K-TEK INTERFACE
67                                      ;THERE WON'T BE ANY JUNK BEFORE THE PROMPT AND THE FIRST HEX RECORD.
68                                      ;UNTIL THAT SERIAL LINE IS ESTABLISHED, WE'LL SHARE THE ONE WITH
69                                      ;Z8K CONSOLE DEVICE AND PROVIDE FOR GETTING RID OF ANY BAD DATA
70                                      ;WE MAY HAPPEN TO READ.  ONCE A SEPARATE SERIAL LINE IS AVAILABLE, WE CAN
71                                      ;DISCARD THE 'FIND START-OF-RECORD' ROUTINE
72                                      ;
73                                      ;IDLE 8550 BEGINS TO TX AFTER THE PROMPT SENT BY OUTMSG
74                                      ;
75  00000850 2101FE54 R                 GETSTR LD       R1,#TKHXIN      ;SELECT HEX RECORD READ-MODE
76  00000854 7F00                               SC      #0              ;GET HEX RECORD AND SAVE IT AT INBUF
77  00000856 7608FE04 R                         LDA     R8,INBUF        ;SET BASE ADDRESS OF HEX STRING
78                                      ;AT THIS POINT, WE SHOULD HAVE ONE COMPLETE TEKHEX RECORD FOR PROCESSING
79                                      ;REGISTER ASSIGNMENTS FOR REDUCING THE ASCII STRING
80                                      ;       R1:     TRANSIENT AREA FOR CONSOLE I/O
81                                      ;       R2:     WORK AREAS FOR CHECKSUM COMPUTATION
82                                      ;       R3,R4: WORK AREAS FOR ASCII HEX CONVERSION
83                                      ;       R5:     WORKSPACE FOR FINDING INCOMING ASCII STRING
84                                      ;       R6:     CONTAINS THE LOAD ADDRESS OF THE DATA
85                                      ;       RH7:    CONTAINS THE NYBBLE CHECKSUMS
86                                      ;       RL7:    CONTAINS THE# OF DATA BYTES IN THE RECORD
87                                      ;       R8:     POINTER INTO ASCII STRING FOR HEX GENERATION

88                                      ;       R13:    CONTAINS CHECKSUM ERROR COUNT
89                                      ;
90                                      ;FIRST WE'LL SCAN FOR JUNK THAT THE Z8K MAY HAVE READ BEFORE
91                                      ;THE 8550 STARTED TX OF THE HEX FILE; THIS SECTION CAN BE
92                                      ;DELETED IF WE DEDICATE A SERIAL PORT FOR 8550/Z8K COMMUNICATION
93                                      ; 'SLASH' CHR DELIMITS START OF DATA
94  0000085A 0B08FE54 R                 SEEK    CP      R8,#INBUF+80    ;AT THE END OF THE INPUT BUFFER?
95  0000085E E605                               JR      EQ,STREQ        ;IF SO, THE WHOLE RECORD WAS JUNK,GET ANOTHER
96  00000860 0C812F2F                           CPB     @R8,#RECMRK     ;SCAN INBUF FOR THE 'SLASH' CHARACTER
97  00000864 E606                               JR      EQ,TSTSTR       ;FOUNDIT!
98  00000866 A980                               INC     R8              ;ON TO THE NEXT CHAR
99  00000868 EEF8                               JR      NE,SEEK         ;HEADER NOT FOUND,TRY AGAIN
100 0000086A 4D05FE00 R             STREQ   LD      ACKBUF,#NAK     ;BAD TX,ASK FOR REPEAT OF STRING
                0037
101 00000870 E8E3                           JR      NEWSTR          ;DO THE ASKIN'
102                                     ;END OF SOH-SCANNER ROUTINE
103                                     ;
104                                     ;WE'LL ASSUME THAT A VALID RECORD HAS BEEN READ
105                                     ;
106 00000872 8DC4                       TSTSTR TEST     R12             ;IS THIS NEW OR OLD DATA?
107 00000874 EE01                           JR      NZ,OLDSTR       ;DON'T RESET ERROR ACCUM IF THIS IS A REPEAT
108 00000876 8DD8                           CLR     R13             ;ZERO OUT CKSUM ERROR ACCUMULATOR
109 00000878 DF84                       OLDSTR CALR     CHKTRM          ;SEE IF THE RECORD IS  THE ZERO-LENGTH TERMINATOR
110                                     ;IF TERM RECORD IS FOUND, RETURN TO MONITOR
111 0000087A A980                           INC     R8              ;MOVE POINTER PAST HEADER TO FIRST ASCII CHARACTER
112                                     ;(R8)=ADDRESS OF FIRST CHAR IN HEX STRING
113 0000087C DF97                           CALR    ASCHEX          ;GET 1ST BYTE OF ADDRESS
114 0000087E A042                           LDB     RH2,RH4         ;1ST BYTE TO CKSUM ACCUMULATOR
115                             M           NYBSUM
116 00000880 A02A               M           LDB     RL2,RH2         ;TRANSPOSE HEX DIGITS
117 00000882 B2A9FCFC           M           SRAB    RL2,#04         ;MAKE HOD THE LOD
118 00000886 07020F0F           M           AND     R2,#0F0FH       ;MASK OFF HO BITS
119 0000088A 80A2               M           ADDB    RH2,RL2         ;ADD NYBBLES W/O CARRY
122 0000088C A027                           LDB     RH7,RH2         ;TO CHECKSUM ACCUMULATOR
123 0000088E A046                           LDB     RH6,RH4         ;HOBYTE OF ADDRESS TO R6
124 00000890 A980                           INC     R8              ;NEXT DIGIT
125 00000892 DFA2                           CALR    ASCHEX          ;GET SECOND BYTE OF LOAD ADDRESS
126 00000894 A042                           LDB     RH2,RH4         ;2ND BYTE TO CKSUM ACCUMULATOR
127                             M           NYBSUM
128 00000896 A02A               M           LDB     RL2,RH2         ;TRANSPOSE HEX DIGITS
129 00000898 B2A9FCFC           M           SRAB    RL2,#04         ;MAKE HOD THE LOD
130 0000089C 07020F0F           M           AND     R2,#0F0FH       ;MASK OFF HO BITS
131 000008A0 80A2               M           ADDB    RH2,RL2         ;ADD NYBBLES W/O CARRY
134 000008A2 8027                           ADDB    RH7,RH2         ;ADD IT TO ACCUM
135 000008A4 A04E                           LDB     RL6,RH4         ;LOBYTE TO R6; LOAD ADDRESS IS NOW COMPLETE
```

```
136                                     ;
137  000008A6 A980                      INC     R8              ;ON TO THE BYTE COUNT
138  000008A8 DFAD                      CALR    ASCHEX          ;GET# OF BYTES IN MSG
139  000008AA A042                      LDB     RH2,RH4         ;ADD IT TO CHKSUM
140                              M      NYBSUM
141  000008AC A02A               M      LDB     RL2,RH2         ;TRANSPOSE HEX DIGITS
142  000008AE B2A9FCFC           M      SRAB    RL2,#04         ;MAKE HOD THE LOD
143  000008B2 07020F0F           M      AND     R2,#0F0FH       ;MASK OFF HO BITS
144  000008B6 80A2               M      ADDB    RH2,RL2         ;ADD NYBBLES W/O CARRY
147  000008B8 8027                      ADDB    RH7,RH2         ;ADD RUNNING NYBBLE CHECKSUM
148  000008BA A04F                      LDB     RL7,RH4         ;SAVE# OF DATA BYTES IN HEX FOR RAM LOAD
149  000008BC A980                      INC     R8              ;GET CHAR CNT FROM STRING
150  000008BE DFAA                      CALR    CHKSUM          ;TEST 1ST BYTE-CHECKSUM
151  000008C0 E609                      JR      EQ,SUMOK        ;NO PROBS,GO ON
152                              M      ERRMSG
153  000008C2 A900               M      INC     R13             ;COUNT NEW ERROR OCCURRENCE
154  000008C4 0B0D0005           M      CP      R13,#5          ;REACH MAX# OF ERRORS?
155  000008C8 EB25               M      JR      UGT,ABRTLD      ;TOO MANY ERRORS- RETURN TO MONITOR
156  000008CA A5C1               M      SET     R12,#01         ;SET 'OLD STRING, REPEAT' FLAG
157  000008CC 4C05FE00           MR     LDB     ACKBUF,#NAK     ;READY BAD TX MSG
                 3737           M
158  000008D2 E8B2               M      JR      NEWSTR          ;REQUEST REPEAT OF MSG AND CLEAR INBUF
160  000008D4 8C78               SUMOK  CLRB    RH7             ;RESET ACCUMULATOR FOR FOR SECOND CHECKSUM
161  000008D6 A980               HXLOAD INC     R8              ;NXT CHR
162  000008D8 DFC5                      CALR    ASCHEX          ;FORM DATA BYTE
163  000008DA A042                      LDB     RH2,RH4         ;SENT TO CKSUM ACCUM
164                              M      NYBSUM
165  000008DC A02A               M      LDB     RL2,RH2         ;TRANSPOSE HEX DIGITS
166  000008DE B2A9FCFC           M      SRAB    RL2,#04         ;MAKE HOD THE LOD
167  000008E2 07020F0F           M      AND     R2,#0F0FH       ;MASK OFF HO BITS
168  000008E6 80A2               M      ADDB    RH2,RL2         ;ADD NYBBLES W/O CARRY
171  000008E8 8027                      ADDB    RH7,RH2         ;ANOTHER DIGIT TO BE SUMMED
172  000008EA 2E64                      LDB     @R6,RH4         ;STORE MACHINE CODE
173  000008EC A960                      INC     R6              ;NEXT RAM LOCATION...
174  000008EE AAF0                      DECB    RL7             ;ONE LESS BYTE TO STORE
175  000008F0 EEF2                      JR      NE,HXLOAD       ;UNTIL (RL7)=0, STORE THEM BYTES!
176                                 ;RECORD LOAD COMPLETE
177  000008F2 A980                      INC     R8
178  000008F4 DFC5                      CALR    CHKSUM          ;PRODUCE AND COMPARE SECOND BYTE-CHECKSUM
179  000008F6 E609                      JR      EQ,GOODRX       ;NO ERRORS
180                              M      ERRMSG
181  000008F8 A9D0               M      INC     R13             ;COUNT NEW ERROR OCCURRENCE
182  000008FA 0B0D0005           M      CP      R13,#5          ;REACH MAX# OF ERRORS?
183  000008FE EB0A               M      JR      UGT,ABRTLD      ;TOO MANY ERRORS- RETURN TO MONITOR
184  00000900 A5C1               M      SET     R12,#01         ;SET 'OLD STRING, REPEAT' FLAG
185  00000902 4C05FE00           MR     LDB     ACKBUF,#NAK     ;READY BAD TX MSG
                 3737           M
186  00000908 E897               M      JR      NEWSTR          ;REQUEST REPEAT OF MSG AND CLEAR INBUF
188  0000090A 4C05FE00           R      GOODRX LDB     ACKBUF,#ACK     ;SET ACKNOWLEGE TOKEN
                 3030
189  00000910 8DC8                      CLR     R12             ;CLEAR FLAG FOR A NEW STRING
190  00000912 E892                      JR      NEWSTR          ;SEND IT TO THE 8550
191  00000914 2101091C           R      ABRTLD LD      R1,#MSGBLK      ;READY ERROR MSG FOR TX TO TEK CONSOLE
192  00000918 7F00                      SC      #0              ;SEND IT OUT
193  0000091A 7F03                      SC      #3              ;RETURN TO Z8000 MONITOR
194  0000091C 0200               MSGBLK WORD    0200H           ;TX MODE FOR SC#0
195  0000091E 0000                      WORD    0000H           ;NOT USED
196  00000920 0924               R      WORD    ENDMSG          ;ADDRESS OF ERROR MSG
197  00000922 002B                      WORD    LSTCHR-ENDMSG   ;# OF CHARS IN STRING TO BE TX'D
198  00000924 2F2F2020           ENDMSG ASCII   '//  ERROR LIMIT EXCEEDED, LOAD IS ABORTED'    ;SELF-EXPLANATORY
                 4552524F
                 52204C49
                 4D495420
                 45584345
                 45444544
                 2C204C4F
                 41442049
                 53204142
                 4F525445
                 44
199  0000094D 0D0A               CRLF   BYTE    0DH,0AH
200  0000094F 00                 LSTCHR BYTE    0
```

```
                        ;END OF MAIN ROUTINE; HERE ARE THE SUBROUTINES...
                        ;
                        ;ASCHEX: THE ASCII CHARACTERS WHOSE ADDRESSES ARE (R8) AND (R8)+1 ARE
                        ;CONSOLIDATED TO FORM ONE HEXADECIMAL BYTE. R3 AND R4 ARE THE WORK SPACE WITH
                        ;THE FORMED HEX BYTE LEFT IN RH4.
                        ;
00000950 208C           ASCHEX LDB     RL4,@R8          ;GET 1ST ASCII CHARACTER
00000952 DFD3                  CALR    TSTNUM           ;ADJUST ASCII IF CHR IS A-F
00000954 060C0F0F              ANDB    RL4,#0FH         ;MASK OFF ZONE BITS
00000958 B2C90404              SLAB    RL4,#04          ;LSBITS BECOME MSBITS
0000095C A0C4                  LDB     RH4,RL4          ;READY FOR NXT DIGIT
0000095E A980                  INC     R8               ;NEXT DIGIT
00000960 208C                  LDB     RL4,@R8          ;GET IT
00000962 DFDB                  CALR    TSTNUM           ;ADJUST ASCII IF CHR IS A-F
00000964 060C0F0F              ANDB    RL4,#0FH         ;PROCESS IT
00000968 84C4                  ORB     RH4,RL4          ;FORM COMPLETE BYTE OF DATA
0000096A 9E08                  RET                      ;GO HOME
                        ;
                        ;CHKSUM: COMPARE THE COMPUTED CHECKSUM WITH THE VALUE CONTAINED IN THE
                        ;STRING TRANSMITTED FORM THE 8550. RUNNING CHECKSUM IS MAINTAINED IN
                        ;RH7. THIS ROUTINE CALLS ASCHEX TO READ THE ASCII STRING AND GEN THE
                        ;TX CHECKSUM.
                        ;
0000096C D00F           CHKSUM CALR    ASCHEX           ;GET 1ST BYTE-CHECKSUM
0000096E 8A47                  CPB     RH7,RH4          ;COMPARE CALCULATED AND GIVEN CHECKSUMS
00000970 9E08           EXIT   RET                      ;REQUEST ANOTHER TX OF THE STRING IF NEEDED
                        ;
                        ;CHKTRM: SCANS THE INPUT BUFFER FOR A BYTE COUNT OF ZERO. USES ASCHEX
                        ;TRANSLATE THE TWO ASCII CHARACTERS OF THE DATA COUNT TO HEX. IF THE
                        ;BYTE COUNT IS ZERO,THE LOAD IS CONCLUDED WITHOUT A CHECKSUM SCAN AND CONTROL
                        ;IS RETURNED TO THE MONITOR
                        ;ENTER WITH (R8)= LOCATION OF 1ST CHAR IN LOAD ADDRESS
                        ;
00000972 A18A           CHKTRM LD      R10,R8           ;SAVE CURRENT POSITION IN STRING
00000974 A984                  INC     R8,#5            ;AIM AT 1ST CHR OF BYTE COUNT
00000976 D014                  CALR    ASCHEX           ;FORM BYTE COUNT
00000978 A1A8                  LD      R8,R10           ;RECOVER ORIGINAL POINTER
0000097A 8C44                  TESTB   RH4              ;IS DATA STRING LENGTH ZERO?
0000097C 9E0E                  RET     NE               ;NO, GO BACK AND FINISH PROCESSING
                        ;AT THIS POINT, WHO CARES ABOUT A BIT-ERROR?
0000097E 4D05FE00 R             LD      ACKBUF,#ACK      ;SIGNAL THE END
              0030
00000984 2101FE5C R             LD      R1,#TKINAK       ;READY THE MSG
00000988 7F00                   SC      #0               ;SIGNAL TRANSFER END TO HOST COMPUTER
0000098A 7F03                   SC      #3               ;LOAD COMPLETED, RETURN TO MONITOR
                        ;SETIO: USED TO RESET FCB FOR SC#0
0000098C 210AFE54 R     SETIO  LD      R10,#TKHXIN      ;DEST FOR MOVE
00000990 210B099E R             LD      R11,#IOBLK       ;SOURCE FOR MOVE
00000994 21090008               LD      R9,#08H          ; # OF WORDS TO MOVE
00000998 BBB109A0       WMOVE  LDIR    @R10,@R11,R9     ;DO IT!
0000099C 9E08                   RET                      ;GO HOME..
0000099E 0100           IOBLK  WORD    0100H    ;BLOCK RECEIVE MODE  OF MONITOR CONSOLE HANDLER
000009A0 0000                  WORD    0000H    ;NOT USED
000009A2 FE04      R           WORD    INBUF    ;INBUF BUFFER LOCATION
000009A4 0050                  WORD    0050H    ;STRING LENGTH IS 80 DECIMAL BYTES TO ALLOW FOR JUNK
                        ;
000009A6 0200                  WORD    0200H    ;BLOCK TRANSMIT MODE FOR SYSTEM CALL #0
000009A8 0000                  WORD    0000H    ;NOT USED
000009AA FE00      R           WORD    ACKBUF   ;START ADDRESS OF PROMPT-ACKNOWLEGE BUFFER
000009AC 0003                  WORD    0003H    ;ONE BYTE FOR PROMPT,ONE FOR ACK-NAK TOKEN,ONE FOR EOL TOKEN
                        ; TSTNUM: CORRECTS ASCII CHARACTERS FROM A TO F TO ALLOW FOR SIMPLE
                        ; MANIPULATION TO HEX FORM
000009AE 0A0C3939       TSTNUM CPB     RL4,#39H
000009B2 E202                  JR      LE,ISNUM ;IF 0-9, NO CORRECTION NEEDED
000009B4 000C0909              ADDB    RL4,#9   ;ELSE ADD OFFSET OF 9 TO PRODUCE USEABLE LO NYBBLE
000009B8 9E08           ISNUM  RET              ;BACK TO ASCHEX
                        ;end of loader and subroutines
          00000820              END     INTCOM; PROGRAM START ADDRESS FOR ASSEMBLER
```

```
ASM     Z8001/Z8002 SYMBOL TABLE
V01.01-01  (8550)                                   01-DEC-83/08:48:48

Scalars
ACK----------00000030     NAK----------00000037     PROMPT----------0000003E     RECEND----------0000000D
RECMRK----------0000002F

Strings & Macros

ERRMSG---------- M   NYBSUM---------- M

Section = $BMLLOAD, Inpage Relocatable, Size = 0000FE64

ABRTLD----------00000914     ACKBUF----------0000FE00     ASCHEX----------00000950     CHKSUM----------0000096C
CHKTRM----------00000972     CRLF----------0000094D     ENDMSG----------00000924     EXIT----------00000970
GETSTR----------00000850     GOODRX----------0000090A     HXLOAD----------000008D6     INBUF----------0000FE04
INTCOM----------00000820     IOBLK----------0000099E     ISNUM----------000009B8     LSTCHR----------0000094F
MSGBLK----------0000091C     NEWSTR----------00000838     OLDSTR----------00000878     OUTMSG----------0000084A
SEEK----------0000085A     SETIO----------0000098C     STREQ----------0000086A     SUMOK----------000008D4
TKHXIN----------0000FE54     TKINAK----------0000FE5C     TMMSG----------0000080E     TSTNUM----------000009AE
TSTSTR----------00000872     WMOVE----------00000998     ZAPWRD----------00000842


230 Lines Read
268 Lines Processed
0 Errors
```

APPENDIX B

LISTING 2

```
 1: /*
 2: -
 3: - BUSLODR.C:     8550 DOWNLOAD EMULATOR FOR DEC VT-180
 4: -                WRITTEN IN AZTEC C FOR THE CP/M ENVIRONMENT
 5: -
 6: - AUTHOR: S. NOVACKI
 7: - CREATED: JULY, 1984
 8: -
 9: */
10:
11: #include "b:stdio.h"       /* standard I/O used for file handling  */
12: #define ACK '0'            /* definitions of: the ACK token        */
13: #define NAK '7'            /*                 the NAK token        */
14: #define CR 13              /*                 end-of-line flag     */
15: #define TX_RDY 0x01        /* UART transmitter ready flag bit      */
16: #define RX_RDY 0x02        /* receiver ready bit                   */
17: #define COMM_DATA 0x58     /* UART data register port number       */
18: #define COMM_STAT 0x59     /* status register port number          */
19:
20: /*
21: infile:
22:        pointer for source file (from disk)
23: numchar:
24:        subscript for reading characters from disk file into buffer vector
25: outptr:
26:        subscript for sending buffer characters to UART
27: argc:
28:        command line argument count, used by "C" console processor
29: errcount:
30:        number of consecutive reception errors
31: iolinebuffer:
32:        array used in moving characters from disk file using standard
33:        I/O to UART using system-specific hardware
34: reply:
35:        token read from BusMon system to indicate quality of message
36: tx_stat, rx_stat:
37:        UART register statuses used during character-send procedure
38:
39: */
40:
41: FILE *infile,*fopen();
42: int numchar,outptr,argc,errcount = 0;
43: char iolinebuffer[80],reply,tx_stat,rx_stat;
44:
45: /*************************************************************************/
46:
47: main(argc,argv)
48: char *argv[];
49:
50: {
51:
52: /*
```

```
53:    open disk file to be sent to the BUSMON system
54:    if a NULL is returned, OPEN has failed, exit to CP/M
55: */
56: if ((infile = fopen(*++argv, "r")) == NULL) {
57:        printf("open failure on file %s\n", *argv); exit(99);
58:        }
59:
60:        while ()    {       /* a DO-ALWAYS loop, a la BASIC                    */
61: get_reply();      /* get first ACK to commence file transmission             */
62: get_line();       /* read a line from the TEKHEX disk file                   */
63:
64: #ASM
65:                   /* after reading a line from the disk file, kill IRQs for */
66:     DI            /* polled serial I/O for both the record output            */
67:                   /* and the REPLY input                                     */
68: #ENDASM
69:
70: tx_line();        /* send record to waiting BusMon unit                      */
71: get_reply();
72: errcount == 0;    /* zero error count for each record being sent             */
73: while (reply != ACK)  {  /* if NAK is received:                             */
74:       retrans_record();
75:       get_reply();
76:       }
77: }
78:
79: #ASM
80:
81:     EI              /* bring back IRQs for BDOS/BIOS disk I/O routines */
82:
83: #ENDASM
84:
85: }
86:
87: /*************************************************************************/
88:
89: get_line()
90: /* function to read <=80 character from the TEKHEX disk file              */
91: {
92: for (numchar =1; numchar <= 80; ++numchar) {    /* for numchar = 1 to 80  */
93:     iolinebuffer[numchar] = getc(infile);       /* read from infile to
94:                                                    the line buffer        */
95:     if (iolinebuffer[numchar] == EOF) {         /*have we reached the end? */
96:        fclose(infile);                  /* if so, close the disk file     */
97:        exit(0);                         /* and back to CP/M...            */
98:        }
99:     if (iolinebuffer[numchar] == CR) break;    /* if a CR, exit from the read
100:    }                                           routine and move on       */
101: }
102:
103: /*************************************************************************/
104:
```

```
105: tx_line()
106: /* function to send a character at a time to the 8251A UART                */
107: {
108: /* send all the chars in the line buffer to the 8251A                       */
109: for (outptr =1; outptr <= numchar; ++outptr) {
110: /* idle until UART transmitter is ready */
111:    while (((tx_stat = in(COMM_STAT)) && TX_RDY) != TX_RDY) {}
112:    out(COMM_DATA,iolinebuffer[outptr]);        /* send out the character   */
113:    }
114: }
115:
116: /*************************************************************************/
117:
118: get_reply()
119: /* receives reply token from the BusMon unit after tx_line is performed    */
120: {
121: while (((rx_stat = in(COMM_STAT)) && RX_RDY) != RX_RDY) {}
122: /* idle until UART receiver is ready */
123: reply = in(COMM_DATA);                /* get ACK/NAK token */
124: if (reply != ACK) {
125:    if (++errcount > 5) load_error(); /* if too many errors, exit */
126:    }
127: }
128:
129: /*************************************************************************/
130:
131: retrans_record()
132: /* tx_line by another name, done for improved legibility
133: /* since numchar is not destroyed by tx_line, this offers a very convenient
134: /* way to retransmit the same line of characters                           */
135: {
136: tx_line();
137: }
138:
139: /*************************************************************************/
140:
141: load_error()
142: /* only if five successive load errors are reported by the BusMon          */
143: {
144:
145: /* EI          /* restore IRQs for standard I/O functions */
146:
147: printf("error limit exceeded, load operation aborted\n");
148: fclose(infile); /* close the disk file                                     */
149: exit(88);       /* return to CP/M with error code 88                       */
150: }
151:
```

APPENDIX C

LISTING 3

```
ASM     Z8001/Z8002                                          Page    1
V01.01-01  (8550)                                    30-NOV-83/12:00:49

     1              4000 R              ORG     4000H
     2  00004000 21007A3A       GO      LD      R0,#7A3AH       ;SET UP UART FOR 2400 BAUD,
     3  00004004 3A060006               OUTB    0006H,RH0       ;EVEN PARITY, 1 STOP BIT
     4  00004008 3A860006               OUTB    0006H,RL0       ;7 DATA BITS ON 6SIO
     5  0000400C C827                   LDB     RL0,#27H        ;'B' SERIAL PORT TO DUMP
     6  0000400E 3A860007               OUTB    0007H,RL0       ;BYTES TO THE PROLOG
     7                          ;
     8                          ; R10:  START ADDRESS (BYTE BOUNDARY) OF PROGRAM TO BE SENT TO PROLOG
     9                          ; R11:  END ADDRESS (BYTE BOUNDARY) OF PROGRAM
    10                          ; R12:  0=FOR EVEN NUMBERED BYTES, 1 FOR ODD NUMBERED BYTES
    11                          ;
    12                          ; NOTE: PLEASE RECALL THAT THE EVEN BYTES ARE LOW ORDER ADDRESSES BUT
    13                          ;       ARE ACTUALLY THE HIGH ORDER DATA BYTE. PLEASE REMEMBER THIS WHEN
    14                          ;       YOU USE THE NOTATION 'HIGH ORDER BYTE' WHEN DETERMINING WHICH
    15                          ;       PROM YOU ARE PROGRAMMING
    16                          ;
    17  00004012 A1A9           INIT    LD      R9,R10          ;USE R9 AS WORKSPACE, SAVE R10 FOR NXT LOAD
    18  00004014 81C9                   ADD     R9,R12          ;SET EVEN/ODD ADDRESSES TO BE DUMPED
    19  00004016 209B           MOVE    LDB     RL3,@R9         ;GET DATUM
    20  00004018 A0B3                   LDB     RH3,RL3         ;COPY DATUM TO WORK ON EACH NYBBLE
    21  0000401A 0703F00F               AND     R3,#0F00FH      ;ISOLATE EACH NYBBLE
    22  0000401E B231FCFC               SRLB    RH3,#4          ;REDUCE HO DIGIT TO HEX DIGIT
    23  00004022 0A030909               CPB     RH3,#9          ;IS DIGIT DECIMAL OR HEX??
    24  00004026 E302                   JR      ULE,NOTHX       ;IF DECIMAL, NO OFFSET NEEDED
    25  00004028 00030707               ADDB    RH3,#7          ;IF HEX, ADD 7 TO PUSH ASCII CODE TO ALPHA
    26  0000402C 00033030       NOTHX   ADDB    RH3,#30H        ;IN ANY EVENT, ADD ZONE BITS TO MAKE ASCII CHAR
    27  00004030 A03C                   LDB     RL4,RH3         ;MOVE FOR OUTPUT TO PROLOG
    28  00004032 DFF3                   CALR    PUTCHR          ;SEND IT OUT
    29  00004034 0A0B0909               CPB     RL3,#9          ;SAME AS ABOVE
    30  00004038 E302                   JR      ULE,NOTHX2      ;THIS TIME FOR LO NYBBLE
    31  0000403A 000B0707               ADDB    RL3,#7          ;SAME OFFSET
    32  0000403E 000B3030       NOTHX2  ADDB    RL3,#30H        ;SAME ZONE BITS
    33  00004042 A0BC                   LDB     RL4,RL3         ;PUT LETTER IN THE MAILBOX
    34  00004044 DFFC                   CALR    PUTCHR          ;HERE COMES THE POSTMAN
    35  00004046 A991                   INC     R9,#2           ;MOVE TO NEXT BYTE OF THE PROGRAM
    36  00004048 8BB9                   CP      R9,R11          ;AT THE END OF THE PROGRAM?
    37  0000404A E3E5                   JR      ULE,MOVE        ;IF NOT, GET ANOTHER BYTE!!
    38  0000404C E8E2                   JR      INIT            ;BREAKPOINT SET TO STALL HERE, THEN
    39                                                          ; GO TO INIT FOR NEXT PROM
    40  0000404E 3AE40005       PUTCHR  INB     RL6,0005H       ;GET STATUS BITS
    41  00004052 A760                   BIT     R6,#0           ;IS UART STILL BUSY?
    42  00004054 E6FC                   JR      Z,PUTCHR        ;IF SO, WAIT UNTIL CHAR IS SENT...
    43  00004056 3AC60004               OUTB    0004H,RL4       ;SEND DATUM TO THE B-PORT
    44  0000405A 9E08                   RET                     ;BACK TO MAIN PROG
    45              4000                END     GO              ;THAT'S ALL FOLKS!!!


ASM     Z8001/Z8002 SYMBOL TABLE
V01.01-01  (8550)                                    30-NOV-83/12:00:49

Section = $PROLOADLOAD, Inpage Relocatable, Size = 0000405C

GO----------------00004000   INIT------------00004012   MOVE------------00004016     NOTHX-----------0000402C
NOTHX2----------0000403E   PUTCHR----------0000404E

   45 Lines Read
   45 Lines Processed
    0 Errors
```

INVESTIGATION OF AIR TRANSPORTATION TECHNOLOGY AT PRINCETON UNIVERSITY, 1984

Robert F. Stengel
Department of Mechanical and Aerospace Engineering
Princeton University
Princeton, New Jersey

SUMMARY OF RESEARCH

The Air Transportation Technology Program at Princeton University, a program emphasizing graduate and undergraduate student research, proceeded along four avenues during 1984:

- Guidance and Control Strategies for Penetration of Microbursts and Wind Shear
- Application of Artificial Intelligence in Flight Control Systems
- Effects of Control Saturation on Closed-Loop Stability and Response of Open-Loop-Unstable Aircraft

Areas of investigation relate to guidance and control of commercial transports as well as general aviation aircraft. Interaction between the flight crew and automatic systems is a subject of principal concern.

Recently, it has become apparent that severe downdrafts and resulting high velocity outflows present a significant hazard to aircraft on takeoff and final approach. This condition is called a microburst, and while it often is associated with thunderstorm activity, it also can occur in the vicinity of dissipating convective clouds that produce no rainfall at ground level. Microburst encounter is a rare but extremely dangerous phenomenon that accounts for one or two air carrier accidents and numerous general aviation accidents each year (on average). Conditions are such that an aircraft's performance envelope may be inadequate for safe penetration unless optimal control strategies are known and applied. While a number of simulation studies have been directed at the problem, there are varied opinions in the flying community regarding the best piloting procedures, and optimal control strategies remain to be defined.

Graduate student Mark Psiaki has undertaken a study of guidance and control strategies for penetration of microbursts when encounter is unavoidable. In work completed in 1984 [1], it was shown that simple control laws could greatly reduce an aircraft's response to wind shear. Although the response mechanism is the same, jet transport and general aviation aircraft behave somewhat differently in microbursts; the larger, heavier aircraft are more adversely affected by variations in the horizontal wind, while the smaller, lighter aircraft have greater difficulty with the downdraft.

The work in 1984 focused on the determination of optimal control strategies for the microburst encounter. The study began with the computation of optimal control histories using steepest-descent and second-order gradient algorithms. Once an envelope of safe flight has been determined for a typical jet transport, attention will be directed at a general aviation type, and optimal closed-loop control laws will be investigated. During 1984, a survey paper on the subject was presented at the NASA Workshop on Wind Shear/Turbulence Inputs to Flight Simulation and Systems Certification[2].

Undetected system failures and/or inadequately defined recovery procedures have contributed to numerous air carrier incidents and accidents. The infamous DC-10 accident at Chicago's O'Hare Airport, in which loss of an engine pod, subsequent loss of subsystems, and asymmetric wing stall led to disaster, provides a prototype for the kind of tragedy that could be averted by intelligent flight control systems. (An intelligent control system is one that uses artificial intelligence concepts, e.g., an expert systems program, to improve performance and fault tolerance.) Although

many methods of modern control theory are applicable, the scope of the problem is such that none of the existing theories provides a complete and practical solution to the problem. At the same time, heuristic logic may be applicable, but it has yet to be stated in satisfactory format.

Graduate student David Handelman has begun to develop a knowledge-based reconfigurable flight control system that will be implemented with the Pascal programming language using parallel microprocessors. This expert system could be considered a prototype for a fault-tolerant control system that could be constructed using existing hardware. In a parallel effort, graduate student Chien Huang used the LISP programming language to investigate the utility of a string-oriented, recursive logical system in the same role. A principal distinction between this and the previous approach is that flight control code will be modified in response to control system failures.

One of the virtues of highly reliable electronic flight control systems is that an aircraft's stability and response, i.e., its closed-loop flying qualities, can be tailored to the pilot's needs. For reasons of performance and maneuverability, it may be desirable to design the aircraft so that its natural (unaugmented) modes of motion are unstable, with the understanding that the flight control system will provide the necessary stability by deflecting control surfaces to counter potentially divergent motions. Because control surfaces have limitations on their displacements and rates of travel, stability can be restored only within a bounded region about the trim point. If the aircraft's motions exceed the boundaries, the available control forces and moments will not be sufficient to prevent divergence.

Graduate student Prakash Shrivastava has been developing methodologies for determining the stability boundaries and control response for systems containing control saturation[3,4]. Analysis has been carried out using phase-plane plots, in which saturation and stability boundaries are represented by straight lines, stable trajectories approach equlibrium points, and unstable trajectories diverge to infinity. The analysis pertains to systems containing unequal saturation boundaries, as well as those with multiple saturating controls.

Future control-system engineers will benefit from design procedures that are computer-intensive, and it is important to create computer programs that allow designers to describe and analyze complex systems interactively. Russell Nelson has been developing a control-system design program based on the LISP language mentioned above *. Design algorithms will be based on classical concepts of transfer-function analysis, and LISP will allow multiloop systems to be assembled and tested within the computer.

The NASA grant supporting student research in air transportation technology has inestimable value in helping educate a new generation of engineers for the aerospace industry, and it is producing research results that are relevant to the continued excellence of aeronautical development in this country.

* Nelson, R. F., "Computer Aided Control System Design - Progress Report", Princeton University Independent Work Report, Jan. 1985. The goal of this independent project is to create a program, using LISP, that will serve as a tool in the design of control systems. The program will be menu driven and graphic with menu prompting. The frequency response of control systems will be examined through Bode analysis techniques. The program will enable the user to make rapid, interactive changes to a control system and then reevaluate the system's performance in order to optimize the design. The project also will give indication of LISP's usefulness in the field of control system design.

1. Psiaki, M. L., and Stengel, R. F., "Analysis of Aircraft Control Strategies for Microburst Encounter", AIAA Paper No. 84-238, Aerospace Sciences Meeting, Reno, Jan. 1984.

Penetration of a microburst during takeoff or approach is an extreme hazard to aviation, but analysis has indicated that risks could be reduced by improved control strategies. Attenuation of flight path response to microburst inputs by elevator and throttle control was studied for a jet transport and a general aviation aircraft using longitudinal equations of motion, root locus analysis, Bode plots of altitude response to wind inputs, and nonlinear numerical simulation. Energy management relative to the air mass, a pitch-up response to decreasing airspeed, increased phugoid-mode damping, and decreased phugoid natural frequency were shown to improve microburst penetration characteristics. Aircraft stall and throttle saturation were found to be limiting factors in an aircraft's ability to maintain flight path during a microburst encounter.

2. Stengel, R. F., "Unresolved Issues in Wind-Shear Encounter", presented at the NASA Workshop on Wind Shear/Turbulence Inputs to flight Simulation and Systems Certification, Hampton, May, 1984.

Much remains to be learned about the hazards of low-altitude wind shear to aviation. New research should be conducted on the nature of the atmospheric environment, on aircraft performance, and on guidance-and-control aids. In conducting this research, it is important to distinguish between near-term and far-term objectives, between basic and applied research, and between uses of results for aircraft design or for real-time implementation. Advances in on-board electronics can be applied to assuring that aircraft of all classes have near-optimal protection against wind shear hazards.

3. Shrivastava, P. C., and Stengel, R. F., "Stability Boundaries for Systems with Control Constraints", Proceedings of the 18th Conference on Information Science and Systems, Princeton, Mar. 1984.

Although unstable systems can be stabilized using feedback control, constraints on the rates and magnitudes of control variables limit the region of stability. Stability boundaries must be evaluated during control system design to assure satisfactory system performance. This analysis becomes more relevant where compromises between the degree of plant instability and upper limits on the rates and magnitudes of control variables have to be made. This paper presents stability boundaries for linear feedback control laws. The method of normal-mode decomposition using the phase-plane approach appears to be well-suited to the evaluation. It is concluded that although the saturation boundaries are dependent on feedback gain magnitudes, the stability boundaries principally depend on the open-loop system dynamics and the allowable control deflection.

4. Shrivastava, P. C., and Stengel, R. F., "Stability Boundaries for Closed-Loop Systems with Control Constraints", Proceedings of the 23rd Conference on Decision & Control, Las Vegas, Dec. 1984, pp. 1326-1329.

Constraints on the magnitudes of control variable limit the region where unstable systems can be stabilized using feedback control. Stability boundaries must be evaluated to assure satisfactory system performance. A method is presented to determine the stability boundaries for linear second-order plants with

saturating control and several classes of open-loop instability. In the saddle-point case, the modal axis of the stable mode centered on the equilibrium points and the saturation boundaries establish the regions of stability. For unstable nodes and foci, the stability boundaries are represented by unstable limit cycles enclosing the stable origin. The stability regions vary with changes in feedback gain. These results have fundamental significance for determining the degree to which unstable plants can be controlled in practical application.

SAFE MICROBURST PENETRATION TECHNIQUES: A DETERMINISTIC, NONLINEAR, OPTIMAL CONTROL APPROACH

Mark L. Psiaki
Mechanical and Aerospace Engineering Department
Princeton University
Princeton, NJ

WORK DONE SINCE DECEMBER 1983

Efforts in the first area involve the design of compensators for microburst disturbance rejection. Preliminary results indicate improvements when the microburst is modeled as a colored noise process. The second task is to model the unsteady aerodynamic effects upon an aircraft's longitudinal dynamics as related to the wind shear encounter problem. The third effort concentrates on the determination of optimal trajectories through microbursts. Standard techniques of deterministic nonlinear optimal control have been used. This is the main subject of this presentation.

- STOCHASTIC LINEAR OPTIMAL CONTROL WITH COLORED NOISE ASSUMPTIONS

- UNSTEADY AERODYNAMIC EFFECTS UPON LONGITUDINAL DYNAMICS

- DETERMINISTIC, NONLINEAR, OPTIMAL CONTROL THROUGH GIVEN MICROBURSTS

DETERMINISTIC, NONLINEAR, OPTIMAL CONTROL PROBLEM

To calculate an optimal trajectory, one must have some criterion by which a determination can be made of what is optimal. For the unconstrained, fixed-time, free-end-point problem, the criterion is that the scalar, positive definite cost function, J, be minimized. In this formulation x is the state vector, u is the control vector, and $\dot{x} = f(x,u,t)$ defines the plant dynamics including disturbance inputs. J is minimized by an appropriate choice of the control vector time history. Because the aircraft plant dynamics are represented by differential equations, the continuous-time formulation of this problem seems natural. Numerical solution techniques, on the other hand, are more appropriate to the discrete-time problem. Therefore, a zero-order-hold assumption is made for the control time history, and the continuous-time problem is transformed into a discrete-time problem. Now the optimal control problem is in the general form of a static, finite-dimensional, constrained optimization problem. Standard techniques may be applied. Two such techniques are the Steepest-Descent and Newton's Second Gradient methods. The Steepest-Descent method uses an initial guess for the control time history, then differentiates the cost with respect to it to determine an optimization step that will yield the largest decrease in the cost. Newton's method is merely a generalization of the Newton-Raphson method for determination of a root of a scalar equation. In this case it is applied to the set of simultaneous equations which comprise the necessary condition for optimality: $dJ/duk = 0.0$ for $k = 1...N-1$. A FORTRAN package was developed for the implementation of these solution techniques. It uses 4th order Runga-Kutta integration to transform the continuous time problem into the discrete time problem. The Steepest-Descent method is used for the initial improvements to the control time history because it is cheaper per optimization step and yields large changes in cost, J, per step when not in the neighborhood of the optimum. Newton's method is used to get to the final solution because it converges rapidly in the neighborhood of the solution.

CONTINUOUS TIME

GIVEN $\underline{x}(T_0) = \underline{x}_0$, $\dot{\underline{x}} = F(\underline{x},\underline{u},T)$

FIND $\underline{u}(T)$ FOR $T_0 < T < T_F$

TO MINIMIZE $J = \int_{T_0}^{T_F} L(\underline{x},\underline{u},T)DT + V(x(T_F))$

DISCRETE TIME

GIVEN $\underline{x}1$, $\underline{x}_{K+1} = \underline{F}(\underline{x}_K,\underline{u}_K,K)$

FIND $\underline{u}_K$ FOR $K = 1...N-1$

TO MINIMIZE $J = \sum_{K=1}^{N-1} L(\underline{x}_K,\underline{u}_K,K) + V(\underline{x}_N)$

SOLUTION TECHNIQUES

- STEEPEST DESCENT
- SECOND GRADIENT (NEWTON'S METHOD)

COST FUNCTION HISTORY FOR A STEEPEST-DESCENT/SECOND GRADIENT OPTIMIZATION

An optimal trajectory was calculated for the Boeing-727 model and the range dependent, sinusoidal microburst used in previous studies. After each optimization step the cost function was evaluated. This figure contains a plot of the cost as a function of the number of optimization steps. It took 51 steps to reach the optimum to within reasonable accuracy. Thirty-four steps were Steepest-Descent steps, and seventeen were taken using Newton's method. Note that the Steepest-Descent portion of the optimization required only about a third as much CPU time as the Newton's method portion, despite the fact that there were twice as many Steepest-Descent steps. This optimization probably could have been done more efficiently by waiting longer to make the switch from Steepest Descent to Newton's method. The erratic pattern of the cost function decreases, though typical of numerical optimization techniques, makes automation of the switching process difficult.

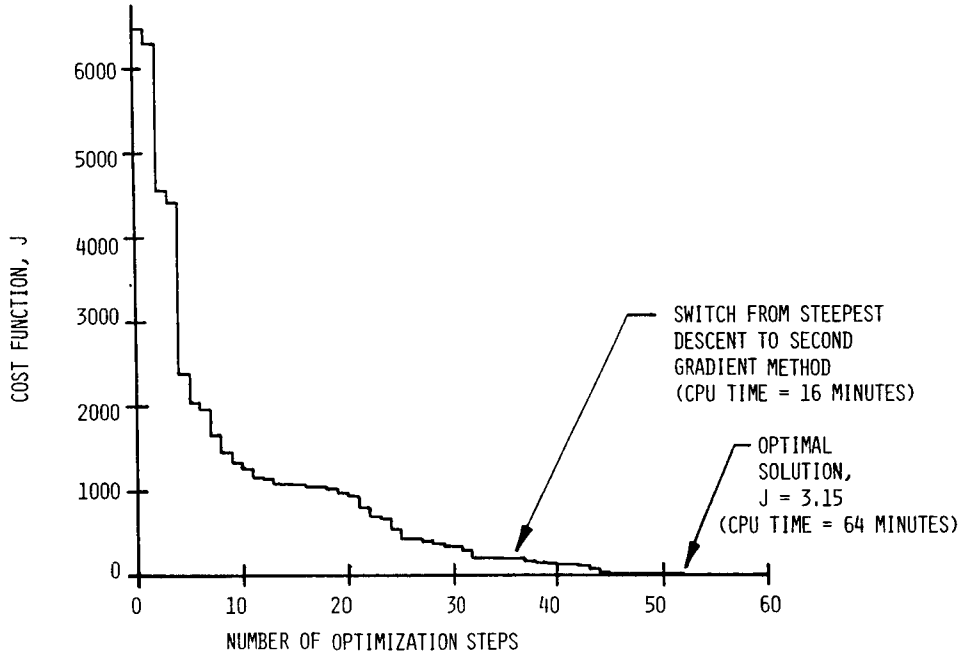

THREE TRAJECTORIES THROUGH A MICROBURST

The results of this trajectory optimization are compared with the results of two previous flights by the same model through the same microburst: an open-loop flight and a closed-loop flight. The control law used in the closed-loop flight was the best so far designed by the author using classical design techniques. On this plot the optimal trajectory is indistinguishable from the nominal trajectory, a -3 deg. glide slope. In fact, it deviated no more than 1.5 ft. from the nominal. The previously best trajectory (the closed-loop run) yielded a 180 ft. perturbation, while the open-loop perturbation was about 1000 ft.

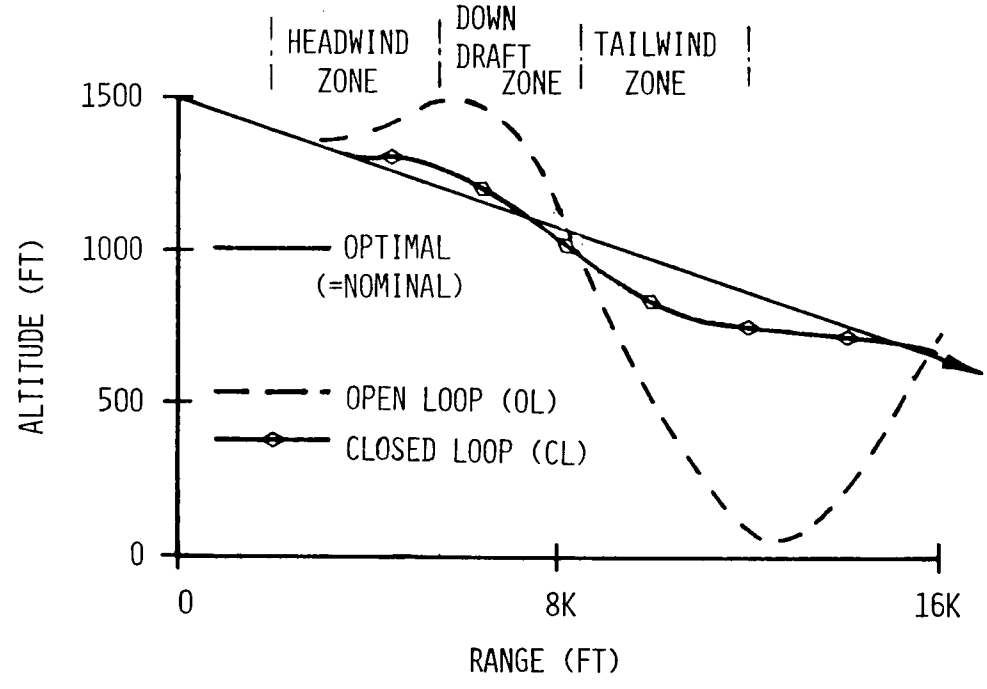

THREE AIRSPEED AND THREE THROTTLE SETTING TIME HISTORIES

For the optimal case, it is interesting that the airspeed variation is approximatly that of the microburst itself. The optimum solution expends little effort in trying to maintain airspeed. The airspeed for this case never comes near the 1-g stall speed, so no problem is encountered. The throttle activity is much lower for the optimum case than for the poorer performing closed-loop case. Its phase lead may partially explain this. Both the airspeed and the throttle time histories for the optimum case are perturbed from the nominal prior to the initial encounter of the microburst. This is due to the nature of the deterministic optimization; the algorithm "knows" ahead of time what is about to happen and acts accordingly. This behavior is also visible on the next figure. This fact precludes the implementation of this algorithm as a control law unless sensors can be developed which sense the wind ahead of the aircraft (a possibility which will be pursued at a later date). Also note that the headwind, downdraft and tailwind zones marked are approximate. The times of their encounters vary slightly from case to case.

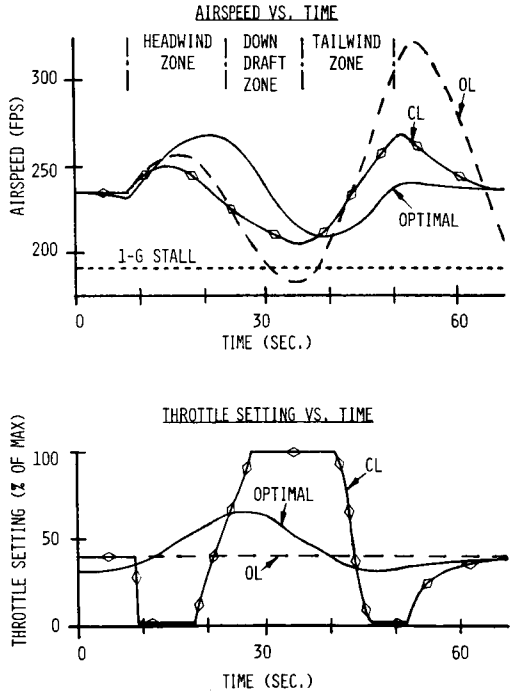

THREE ANGLE-OF-ATTACK AND THREE PITCH-ANGLE TIME HISTORIES

The open-loop and closed-loop angle-of-attack time histories are very similar to each other. The optimal angle-of-attack time history is out of phase with the corresponding airspeed variation. This indicates that the optimal glide slope control is primarily by angle-of-attack variation to maintain lift in the presence of airspeed variations. The pitch-angle time history bears out this interpretation, taking into account the changes in the relationship between the two angles due to the wind variations. In the open-loop and closed-loop cases, the pitch-angle is not held low enough during the headwind zone, and it is not held high long enough during the tailwind zone.

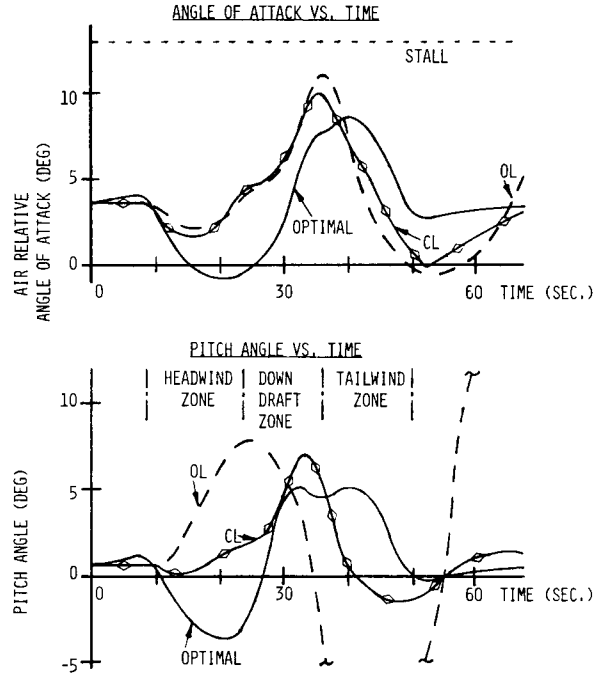

CONCLUSIONS

A relatively large amount of computer time (64 minutes of CPU activity on an IBM 3081 computer) was used for the calculation of this optimal trajectory, but it is subject to reduction with moderate effort. The Deterministic, Nonlinear, Optimal Control algorithm yielded excellent aircraft performance in trajectory tracking for the given microburst. It did so by varying the angle of attack to counteract the lift effects of microburst-induced airspeed variations. Throttle saturation and aerodynamic stall limits were not a problem for the case considered, proving that the aircraft's performance capabilities were not violated by the given wind field. All closed-loop control laws previously considered performed very poorly in comparison, and therefore do not come near to taking full advantage of aircraft performance.

- DETERMINISTIC, NONLINEAR, OPTIMAL CONTROL, AN EFFECTIVE THOUGH EXPENSIVE NOMINAL SOLUTION

- SUFFICIENT AIRCRAFT PERFORMANCE FOR SAFE ENCOUNTER OF GIVEN MICROBURST

- INSUFFICIENCY OF PRACTICAL CONTROL LAWS STUDIED TO DATE

PLANNED FUTURE WORK

Effort will be made to reduce the CPU time per trajectory optimization by improving the efficiency of the algorithm, but the basic approach will remain the same. The microbursts used thus far have been idealized. Microburst data from the JAWS project will be used to get realistic wind fields. These will be checked to see if and how any of these exceed aircraft performance limits by doing trajectory optimizations through them. Optimal trajectory solutions are also greatly affected by variations of the cost functions, L(x,u,t) and V[x(tf)]. These effects will be considered as will the optimum for a general aviation aircraft. Once the performance capabilities are well understood, the goal will be to design practical control laws which come as close to these limits as possible. The use of lead information about the wind shear will be considered during this phase to determine what information would be useful to a closed-loop control law. Unsteady aerodynamics effects remain to be studied to determine their impact on the validity of the aircraft models used here.

- DETERMINISTIC, NONLINEAR, OPTIMAL CONTROL (DNLOC) ALGORITHM IMPROVEMENTS
- FUTURE OPTIMIZATION RUNS
  - JAWS MICROBURSTS
  - VARYING COST FUNCTIONS, $L(\underline{x},\underline{u},\tau)$, $V(\underline{x}(\tau_F))$
  - GENERAL AVIATION AIRCRAFT
- PRACTICAL CONTROL STRATEGIES APPROACHING OPTIMUM PERFORMANCE
- UNSTEADY AERODYNAMIC EFFECTS

INTELLIGENT FAULT-TOLERANT CONTROLLERS

Chien Y. Huang
Princeton University
Princeton, NJ

OVERVIEW

- ROLE OF (ARTIFICIAL) INTELLIGENCE IN FAULT-TOLERANT CONTROLS
- DESCRIPTION OF THE SYSTEM BEING DESIGNED
- AN EXAMPLE OF NEW CONTROL RECONFIGURATION APPROACHES
- SUMMARY AND FUTURE WORK

A system with fault-tolerant controls is one that can detect, isolate, and estimate failures and perform necessary control reconfiguration based on this new information. Artificial intelligence (AI) is concerned with semantic processing, and it has evolved to include the topics of expert systems and machine learning. Our research represents an attempt to apply AI to fault-tolerant controls, hence, the name intelligent fault-tolerant control (IFTC).

We are seeking generic solutions to problems, providing a system based on logic in addition to analytical tools, and offering machine learning capabilities. The advantages, to name a few, are that redundant system-specific algorithms are no longer needed, that "reasonableness" is used to quickly choose the correct control strategy (among many available ones), and that the system can adapt to new situations by learning about its effects on system dynamics.

INTELLIGENT FAULT-TOLERANT CONTROLS

- FAULT-TOLERANT CONTROL
  - FAULT DETECTION AND ISOLATION
  - FAULT ESTIMATION
  - CONTROL RECONFIGURATION
- ARTIFICIAL INTELLIGENCE (AI)
  - SEMANTIC PROCESSING
  - EXPERT SYSTEM (PROBLEM SOLVERS)
  - MACHINE LEARNING
- INTELLIGENT FAULT-TOLERANT CONTROLS (IFTC)
  - HYBRID OF ANALYTICAL METHODOLOGY AND AI
  - DIFFERENCES TO CONVENTIONAL APPROACH
  - ADVANTAGES

The Intelligent Fault-Tolerant Control (IFTC) System, which is currently being designed at the Laboratory of Control and Automation in Princeton University, consists of three main sub-systems: front-end processor, which interfaces the system with the users; knowledge base, which houses the data base IFTC needs; and a heuristic and computational engine, which has both logic and numeric processing capabilities.

BLOCK DIAGRAM OF IFTC SYSTEM

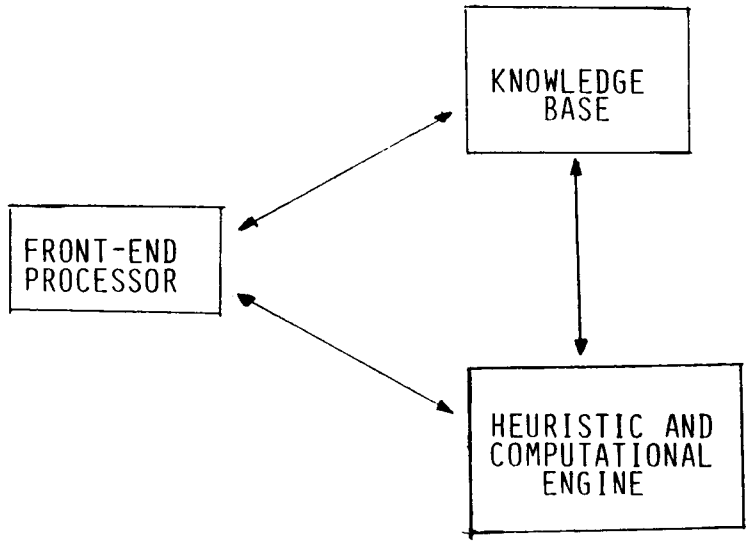

The front-end processor is responsible for providing a friendly interface between the system and aircraft crew and designers of control strategies and heuristic rules. Through it the knowledge base can be updated or augmented. It will also guide a designer (usually an expert in some aspect) through the process of creating new rules and control strategies.

FRONT-END PROCESSOR

- INTERFACES THE SYSTEM WITH AIRCRAFT CREW/DESIGNER
- UPDATES AND AUGMENTS THE KNOWLEDGE BASE
- GUIDES USER THROUGH THE PROCESS OF CREATING NEW RULES AND CONTROL STRATEGIES

The knowledge base stores the knowledge that the system has about itself and about the "WORLD" (i.e., the flight environment). It contains dynamic models of the aircraft in which the IFTC system is resident; control laws for different flight conditions (high, low Mach number, wind shear, etc.), the rules under which they apply, algorithms for failure detection, isolation and estimation, and an interconnection map (and status) of all devices present on the aircraft.

KNOWLEDGE BASE

STORAGE FOR

- DYNAMIC MODELS OF AIRCRAFT
- CONTROL LAWS FOR DIFFERENT FLIGHT CONDITIONS AS WELL AS RULES UNDER WHICH THEY APPLY
- FAULT DETECTION, ISOLATION, AND ESTIMATION ALGORITHMS
- INTERCONNECTION MAP FOR ONBOARD DEVICES

There are two distinct processors in the Heuristic and Computational Engine subsystem. The heuristic processor possesses the logic needed to prune branches in free-structure rule-space. It also has the power to make decisions when logic does not apply. The computational processor is endowed with sufficient numerical capability to find, for example, new gains for feedback and observer equations and to evaluate the effectiveness of a new control law by simulation.

HEURISTIC AND COMPUTATIONAL ENGINE

- HEURISTIC PROCESSOR
  - PRUNES BRANCHES IN TREE-STRUCTURE RULE-SPACE
  - PERFORMS HEURISTIC DECISIONS
- COMPUTATIONAL PROCESSOR
  - FINDS NEW CONTROL GAINS
  - EVALUATES EFFECTIVENESS OF THE CONTROL LAWS

The lateral dynamics of an F-8C aircraft provides an example. The objective is to control its lateral motions by model-following. Suppose that the system is warned about an aileron-failure after a maneuver (it became biased at 1°). The question is what to do now.

"INTELLIGENT" CONTROL RECONFIGURATION - AN EXAMPLE

- MODEL: F-8C LATERAL DYNAMICS

$$\dot{x} = Fx + Gu + w, \quad z = x, \quad u = -Cx + C_M x_M$$

$$x = (p\ r\ \beta\ \phi\ \omega\ \delta_A\ \delta_R\ \delta_{AC}\ \delta_{RC}),\ u = (\delta_{AC}\ \delta_{RC})$$

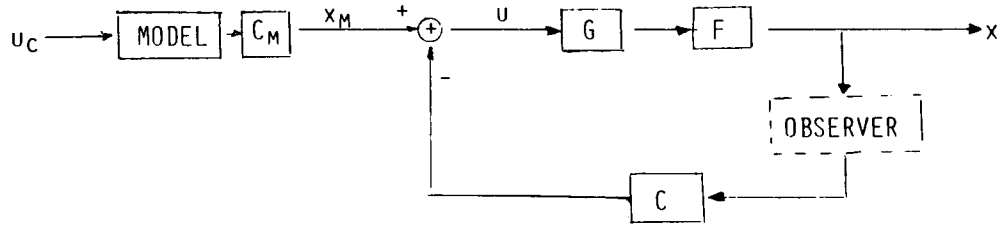

- FAILURE: AILERON BIASED AT 1° DEGREE
  (FAULT DETECTION AND ESTIMATION ASSUMED)

A possible solution in conventional approaches is to set aside a value slot in software to represent the bias and add it to aileron commands. This slot normally holds a zero until a bias is detected at which time the slot is set to the estimated bias magnitude. Disadvantages of this method are that extra computation is necessary even when no bias is present and one such slot must be provided for every control on the airplane.

Faced with the same problem, the IFTC will instead change the dynamic model to reflect the new knowledge it acquired. This solution differs from the previous one in that the codes which control the aileron are being changed in real time. Therefore there is no need for reserved slots and no extra computation is carried out when there is no failure. Futhermore, the command is generic so that it will handle all cases with biases. We call this approach incremental learning because the IFTC uses its own tools to modify its "world" knowledge without outside intervention. It must also be pointed out that this example actually illustrates a restructurable control (as opposed to reconfigurable control) in the sense that the structure of the system has been changed.

Other failures that will be addressed in the future are losses of actuator or sensor. We will also consider critical flight conditions like wind shear penetration, where we will provide IFTC with knowledge to carry out such a task. In all these cases, we see clearly the need for intelligent and generic controls.

CONTROL RECONFIGURATION

- CONVENTIONAL FIX: ADD BIAS TO COMMAND IN A RESERVED SLOT

- NEW APPROACH: CHANGE DYNAMIC MODEL (USING A GENERIC COMMAND) TO REFLECT THE NEW KNOWLEDGE (INCREMENTAL LEARNING)

- OTHER "FAILURE" SITUATION: LOSS OF ACTUATOR OR SENSOR, WIND SHEAR

  - NEED OF INTELLIGENT GENERIC CONTROLS

A simulation was run with an aileron failure; (A) shows the normal roll response to a doublet aileron command, and (B) shows the failed case where at the end of the doublet command, the aileron became biased at 1°. (C) shows the control restructured a half second after the failure occurred; thus bringing the roll back to a desired state (at 0 deg/sec). (D) shows the aileron command, failure, and restructuring.

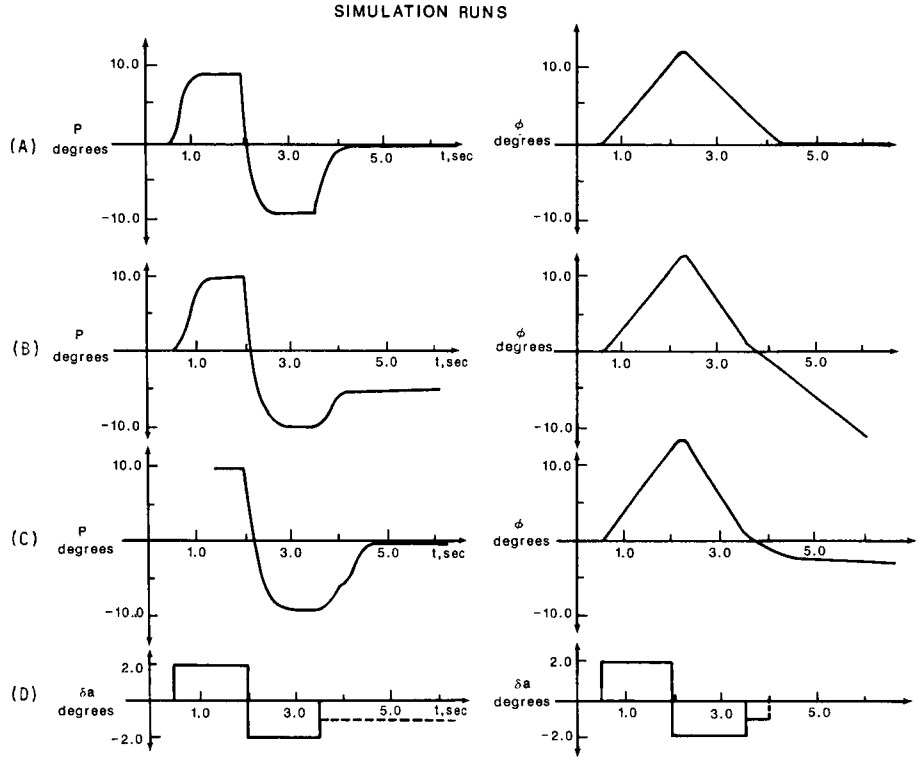

SUMMARY

WE HAVE

- OUTLINED AN INTELLIGENT FAULT-TOLERANT CONTROLLER
- ILLUSTRATED THE NEW APPROACH BY AN EXAMPLE

FUTURE WORK

- EXPAND ON THE SUBSYSTEMS
- EXPERIMENT WITH ANALYTIC FAULT DETECTION ALGORITHMS
- STUDY THE MACHINE LEARNING

STABILITY BOUNDARIES FOR COMMAND AUGMENTATION SYSTEMS

P. C. Shrivastava
Department of Mechanical and Aerospace Engineering
Princeton University
Princeton, NJ

INTRODUCTION

For statically unstable aircraft, there is an increased need to understand the effects of control saturation. The longitudinal mode of unstable aircraft usually has a single unstable pole, whereas the lateral-directional mode may have two real poles or a pair of complex-conjugate poles in the right half plane. Reduced-order models are often used to determine the stabiliy and performance of the aircraft approximately. This study examines the effects of control saturation using reduced-order models.

The stability boundaries for command augmentation systems are determined for three types of singularities: saddle-point, unstable nodes, and unstable foci. Control saturation imposes bounds on command vectors for which equilibrium can be attained. For the cases of saddle-point and unstable nodes, the region of stability reduces to zero for command vectors which demand a steady value of control exceeding the control saturation limits. In the case of unstable foci, the region of attraction does not gradually reduce in size, but at some point it breaks abruptly.

OVERVIEW

- INTRODUCTION
- PREVIOUS WORK
- COMMAND AUGMENTATION SYSTEMS
- CONCLUSIONS

STABILITY AUGMENTATION SYSTEM

A block diagram of the system under consideration is shown. It consists of a dynamic system to be controlled (the "plant"), a feedback controller, and a saturating element on one or more of the controls. Command inputs can be ignored in the stability analysis of this constant-coefficient system.

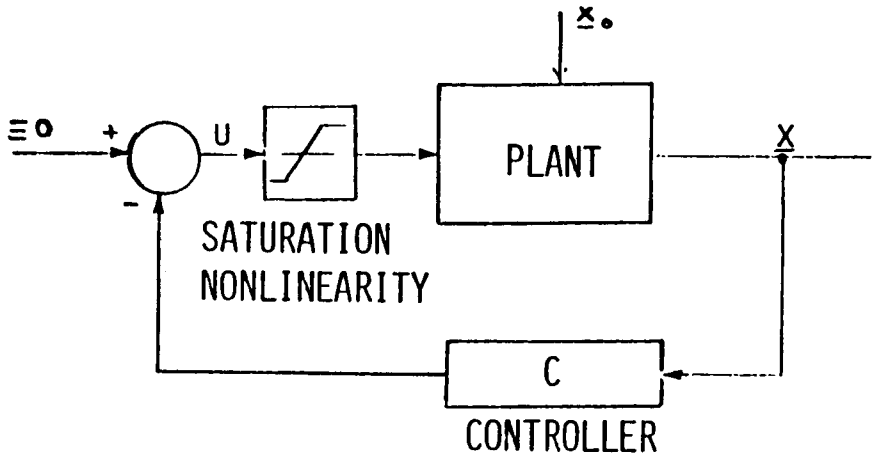

$$\dot{\underline{x}} = F\underline{x} + G\underline{u}$$

$$\underline{u} = -C\underline{x}$$

$$|\underline{u}| = < \underline{u}_M$$

COMMAND AUGMENTATION SYSTEM

Specific inputs and outputs must be considered in the command augmentation system. Defining y as an output vector that is a linear combination of state vector components, y* is the desired value of the output. The resulting closed-loop system is described by an ordinary differential equation, whose equilibrium state and control vectors, x* and u*, can be related to the desired output.

The steady-state value of control is independent of feedback gain, which can be obtained either from open- or closed-loop dynamics. For open-loop unstable systems, feedback is mandatory to achieve stability and command equilibrium. The linear feedback regulator provides satisfactory transient response to meet performance specifications otherwise not obtainable. The state equilibrium depends only on the open-loop dynamics and control magnitude. A steady-state control u* exists only for the "nonsingular" command vector.

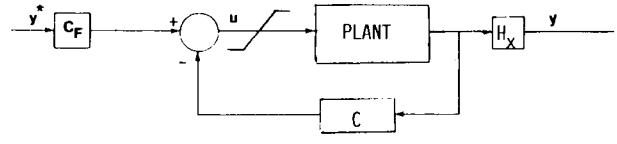

$$\dot{x} = Fx + Gu \qquad \text{OUTPUT:}$$

$$u = C_B x + C_F Y^* \qquad Y^* = Hx\, x^*$$

CLOSED-LOOP

$$\dot{x} = (F - G C_F)\, x + G C_F Y^*$$

EQUILIBRIUM

$$x^* = -(F - G C_F)^{-1} G C_F Y^*$$

$$u^* = - C_B (F - G C_F)^{-1} G C_F Y^* + C_F Y^*$$

WHERE

$$C_F = S_{22} + C S_{12}$$

$$S_{22} = - HxF^{-1} G$$

$$S_{12} = (-F^{-1}G) S_{22}$$

$$C_B = - C$$

OPEN LOOP EQUILIBRIUM:

$$x^* = - F^{-1} G u^*$$

$$Y^* = Hx\, x^* = - HxF^{-1} G u^*$$

$$u^* = (-HxF^{-1} G)^{-1} Y^*$$

$$= - (HxF^{-1} G)^{-1} Hx\, x^*$$

COMMAND AUGMENTATION SYSTEM (CONCLUDED)

IT CAN BE SHOWN THAT

$$\underline{u}^* = - C_B(F - G\,C_F)^{-1}\,G\,C_F\,\underline{Y}^* + C_F\,\underline{Y}^*$$

$$= (-H_X F^{-1}\,G)^{-1}\,\underline{Y}^*$$

- $\underline{U}^*$ INDEPENDENT OF GAIN C
- C DETERMINES RESPONSE
- $\underline{X}^*$ LOCATION DETERMINED BY STATE EQUATION
- $\underline{U}^*$ EXISTS FOR "NONSINGULAR COMMAND" EQUILIBRIUM

EFFECTS OF CONTROL SATURATION

The control saturation limits and open-loop dynamics determine the minimum and maximum values of state equilibrium. Saturation prevents the system from attaining the desired equilibrium and response, and it imposes bounds on achievable command vector y*. To avoid saturation, desired state equilibrium points must lie within the unsaturated region. However, this still does not guarantee that the trajectories would not enter a saturated-control region, for some initial conditions and/or commands. This is mainly determined by the eigenvectors in the unsaturated region. Thus, saturation enforces bounds on the command vectors for which equilibrium could actually be attained without saturation. Equilibrium cannot be attained for the command vectors for which the state equilibrium point is located in the saturated region.

Feedback gain C alters the response of the system, but it does not affect u*. The command vectors for which equilibrium can be attained are independent of feedback gain. H_x does not affect the state equilibrium or the feedback gain. It changes the prefilter gain which shapes input to achieve the desired equilibrium. u* changes with the command vector; hence, the saturation boundaries change with commands.

$$-\underline{U}_M < \underline{U}^* < +\underline{U}_M \quad : \quad \text{CONTROL SATURATION}$$

$$\underline{x}^* = -F^{-1} G \underline{u}^*$$

$$\underline{x} - \underline{U}_M < \underline{x}^* < \underline{x} + \underline{U}_M \quad : \quad \text{BOUNDS ON STATE EQUILIBRIUM}$$

$$\underline{Y}^* = Hx \underline{x}^* \quad :$$

BOUNDS ON ACHIEVABLE COMMANDS

$$\underline{Y} - \underline{U}_M < \underline{Y}^* < \underline{Y} + \underline{U}_M \quad :$$

- DEPENDENCE OF STATE EQUILIBRIUM ON $F^{-1} G$
- EFFECTS OF VARIATIONS OF C, H_x

STABILITY BOUNDARIES FOR THE SADDLE-POINT: MCE CASE

The stability boundaries for the minimum-control-energy (MCE) case are shown on the next three figures. Note the variations in saturation boundaries and location of x* with changes in the command vector. The region of stability remains unchanged. Equilibrium can be achieved only for those command vectors for which the equilibrium point lies within the saturated region. Invariance of stability boundaries with changes in command command vectors is a unique result for the saddle-point MCE case.

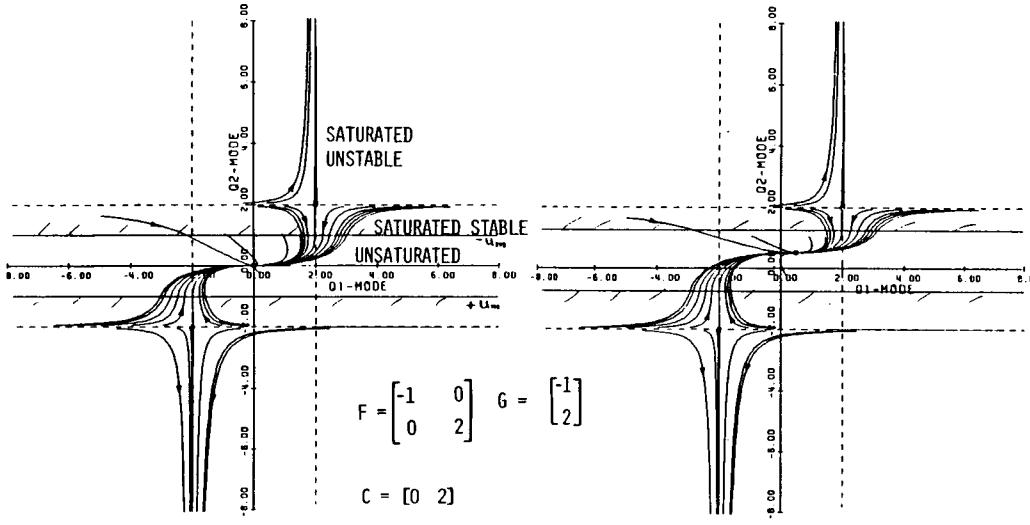

Y = 0.0 Y = 0.5

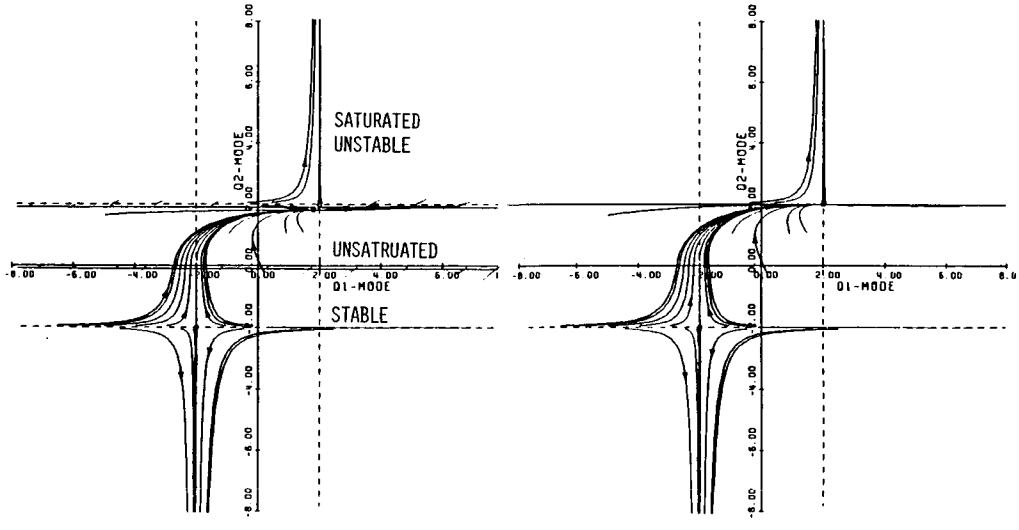

Y = 1.8 Y = 2.0

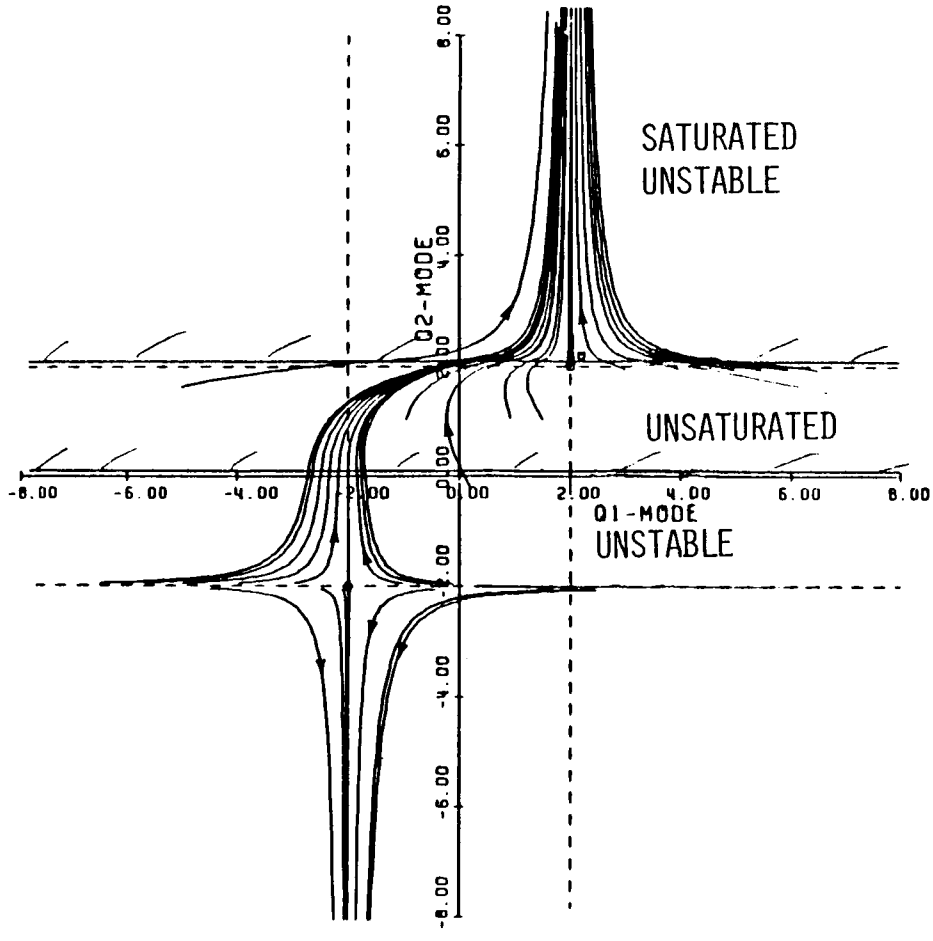
SATURATED
UNSTABLE
UNSATURATED
Q2-MODE
Q1-MODE
UNSTABLE
8.00
6.00
4.00
2.00
0.00
-2.00
-4.00
-6.00
-8.00
-8.00
-6.00
-4.00
-2.00
0.00
2.00
4.00
6.00
8.00

Y = 2.2

STABILITY BOUNDARIES FOR THE SADDLE-POINT: LOW GAIN CASE

The stability boundaries are shown on the next three figures, where unlike the minimum-control-energy (MCE) case, the stability boundaries change with commands. The locations of equilibrium points in the saturated region do not change with the command vectors. The region of stability is biggest for zero command, i.e., the maximum region of stability is achieved for the stability augmentation case. For non-zero command vectors, the stability region shrinks. It reduces to zero when the desired equilibrium control exceeds the saturation limits.

For each command vector, trajectories seek separate equilibrium points; hence, the trajectories starting from the same initial conditions follow entirely different paths in the phase plane. For this reason, markedly different time-histories for different command vectors are obtained, though the system eigenvalues/eigenvectors remain unchanged.

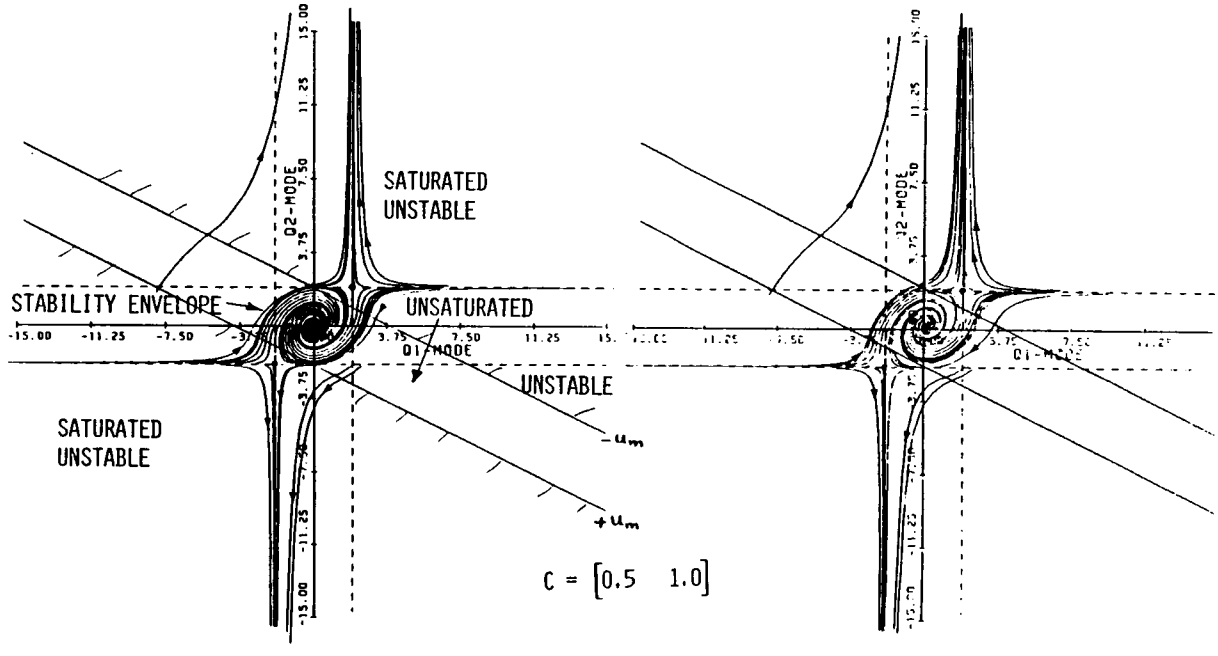

γ = 0.0 γ = 0.5

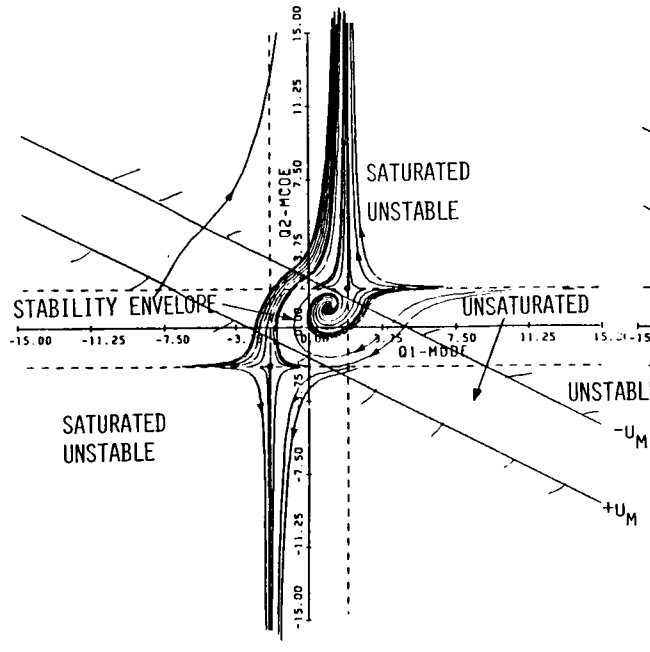

Y=1.5

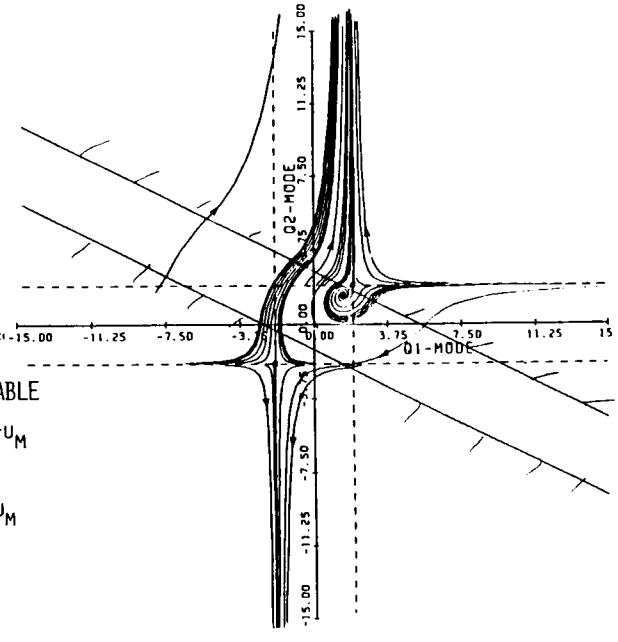

Y = 1.8

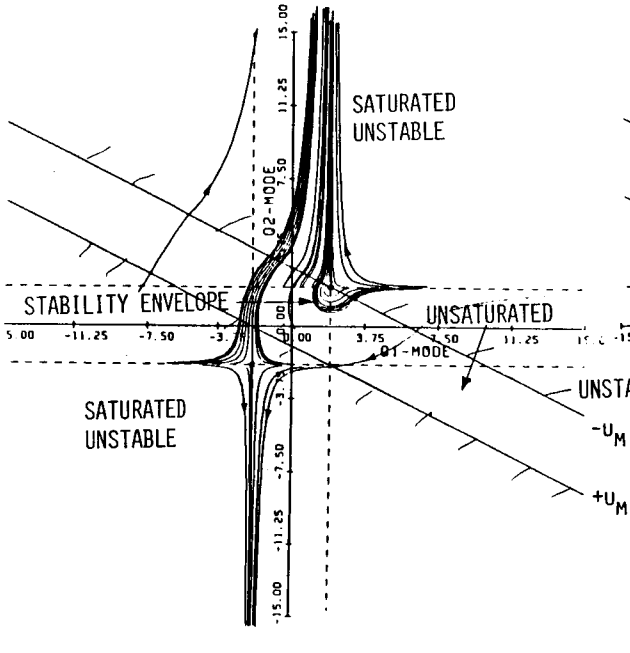

Y = 2.0

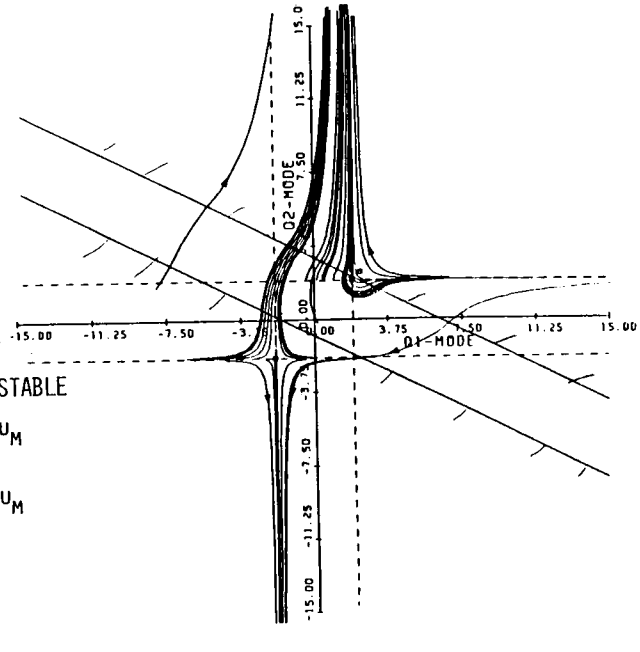

Y = 2.4

STABILITY BOUNDARIES FOR UNSTABLE NODES

The next three figures show the stability boundaries for the case of unstable nodes for various command vectors. As noticed before, the saturation boundaries here also change with changes in commands. The sizes of limit cycles, which represent the saturation boundaries, also change. The region of stability is biggest for the stability augmentation system (SAS) case. For increasing command magnitudes, the steady-state equilibrium point moves away from the origin. The region of stability shrinks, and eventually it reduces to zero for commands that require $u^* \geq |u_m|$.

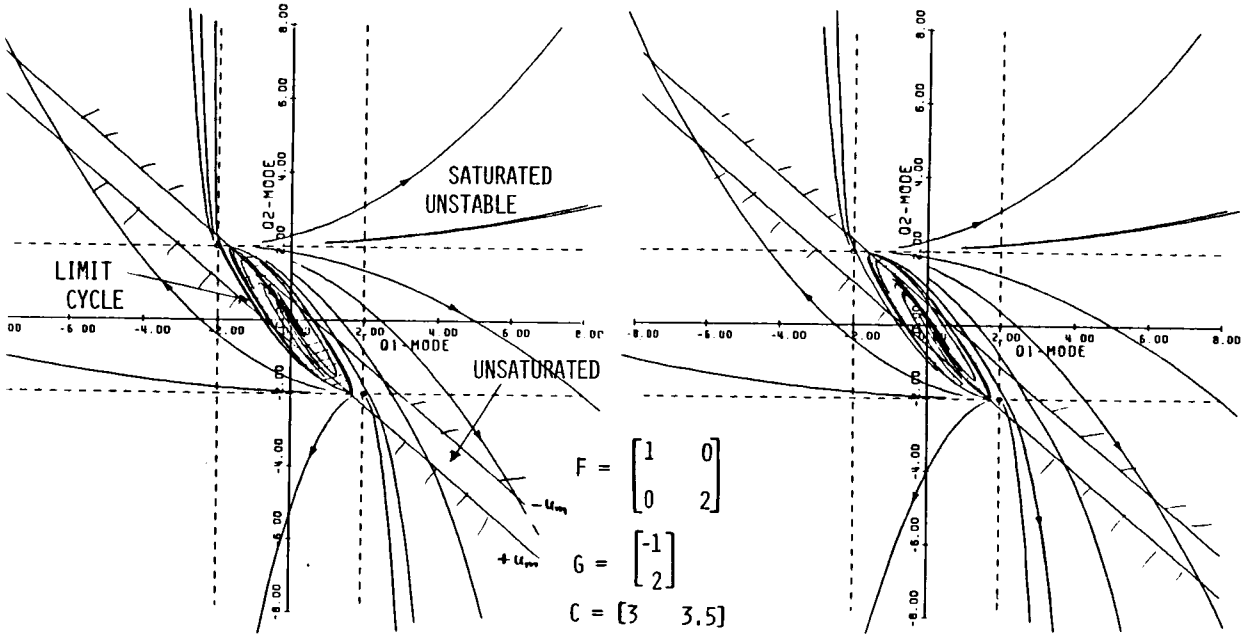

UNSTABLE MODES (CONCLUDED)

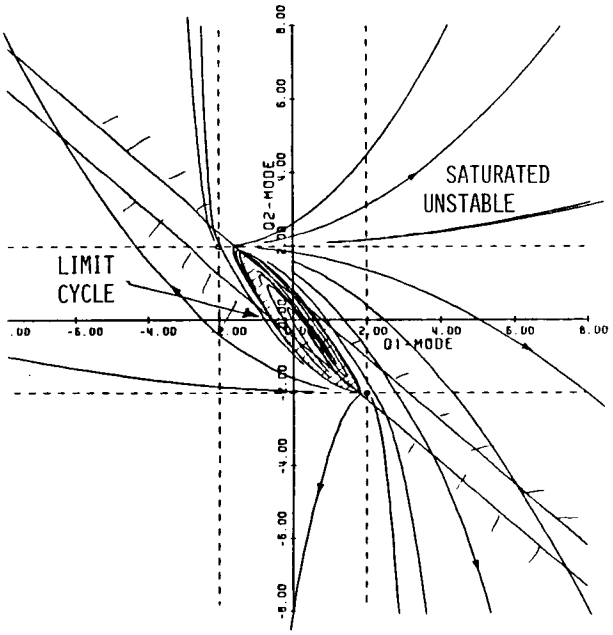

γ = 0.8

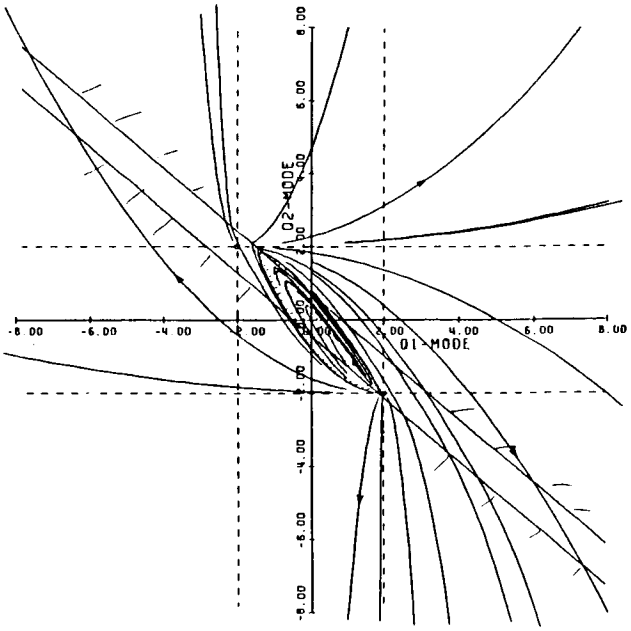

γ = 1.2

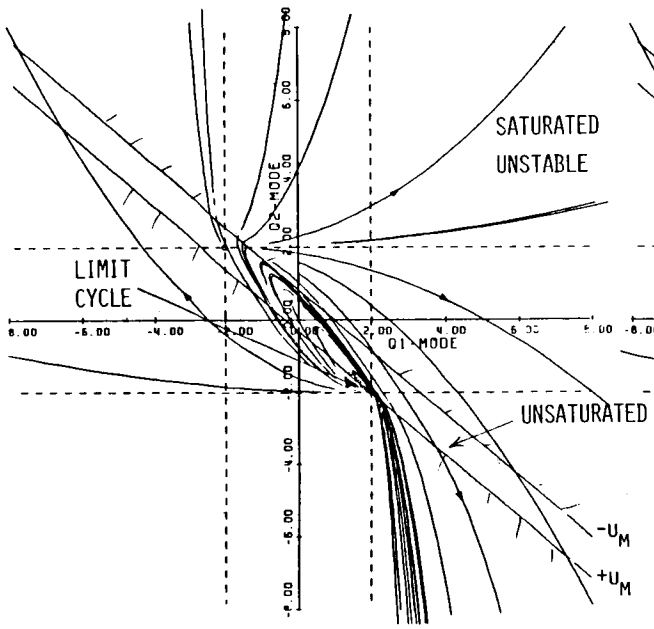

γ = 1.9

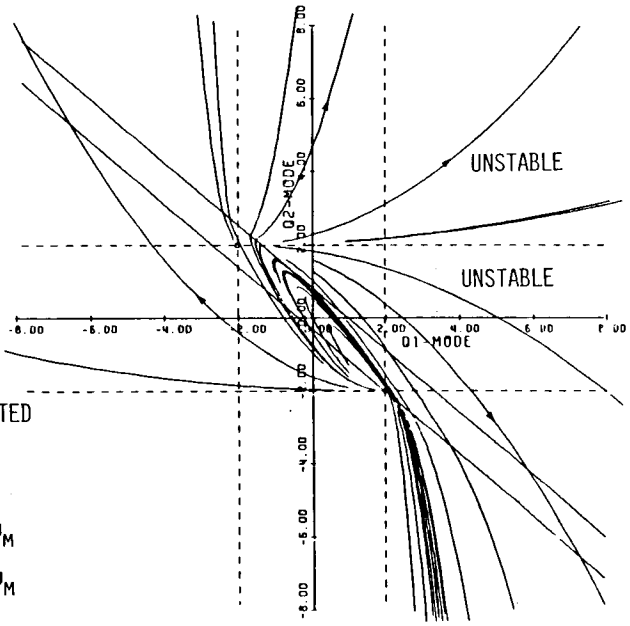

γ = 2.0

STABILITY BOUNDARIES OF UNSTABLE FOCI

The stability boundaries for the case of unstable foci are unstable limit cycles, as shown on the next six figures. Apparently, there is little variation in the size of stability region with commands. The stable equilibrium point moves to the right of the origin with increasing command values, and the saturation boundaries also shift. At control saturation limits, this equilibrium point lies on the saturation boundary, but the region of stablity does not shrink to zero, contrary to the cases of saddle-point and unstable nodes.

Further increase in commands moves the desired equilibrium point farther to the right, and another limit cycle emerges. The trajectories within it converge to this new limit cycle; those within the original limit cycle also converge to it. Thus, the new limit cycle is stable. This "inner" limit cycle grows with increase in commands, until it coincides with the "outer" limit cycle. Any further increase in command results in breaking of the closed stability region (or "bursting" of the limit cycle), making the entire region unstable. This peculiar result in the case of unstable foci is under further investigation.

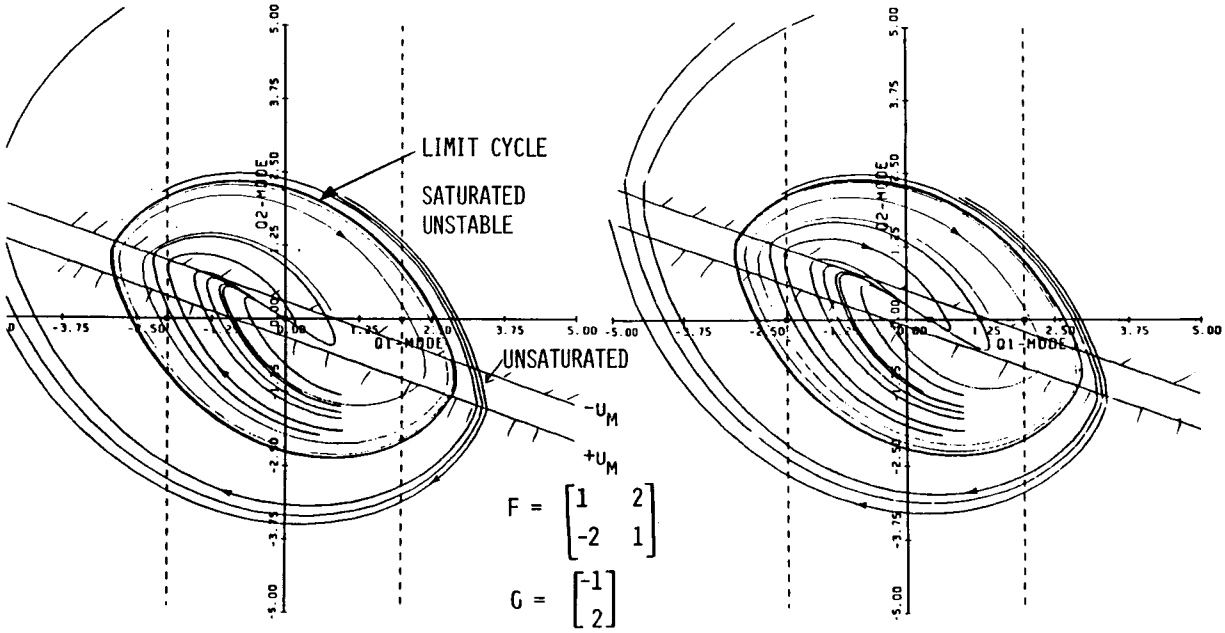

$$F = \begin{bmatrix} 1 & 2 \\ -2 & 1 \end{bmatrix} \qquad G = \begin{bmatrix} -1 \\ 2 \end{bmatrix}$$

$$C = [0.95 \quad 2.27]$$

$\gamma = 0.0$ $\qquad$ $\gamma = 0.4$

UNSTABLE FOCI (CONTINUED)

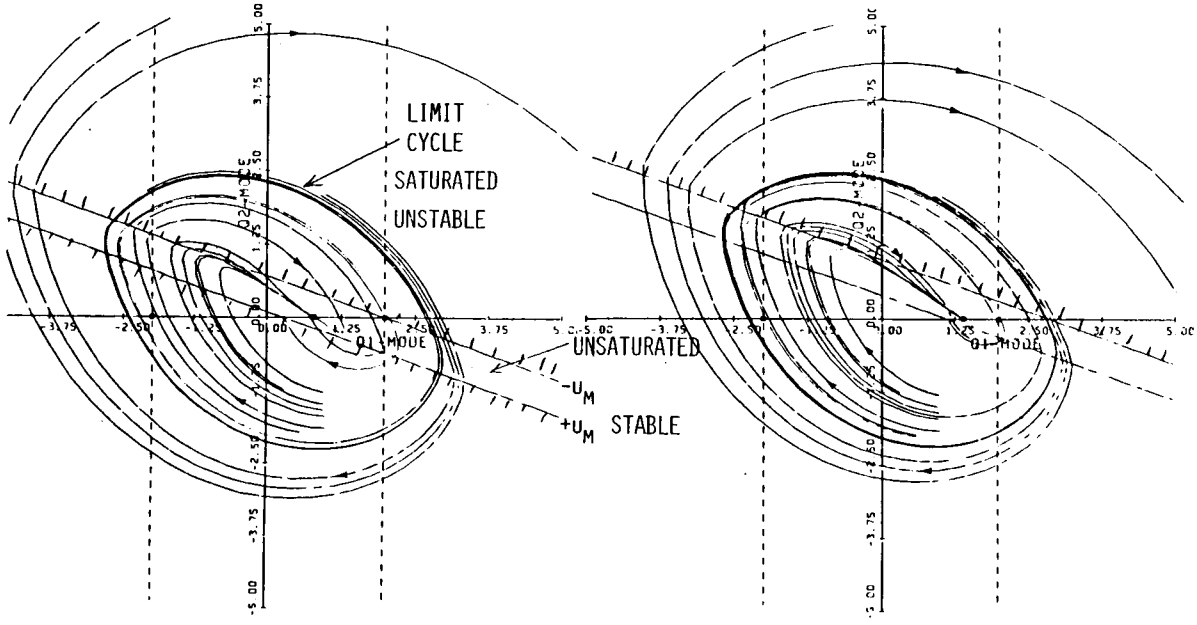

Y = 0.8

Y = 1.4

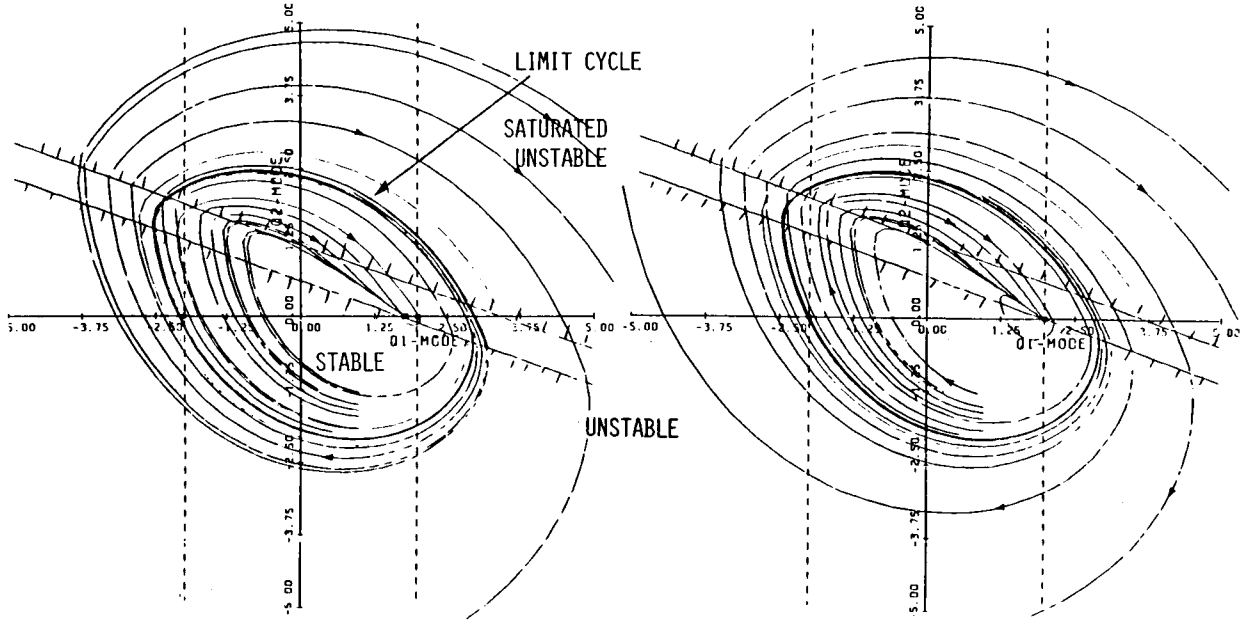

Y = 1.8

Y = 2.0

UNSTABLE FOCI (CONTINUED)

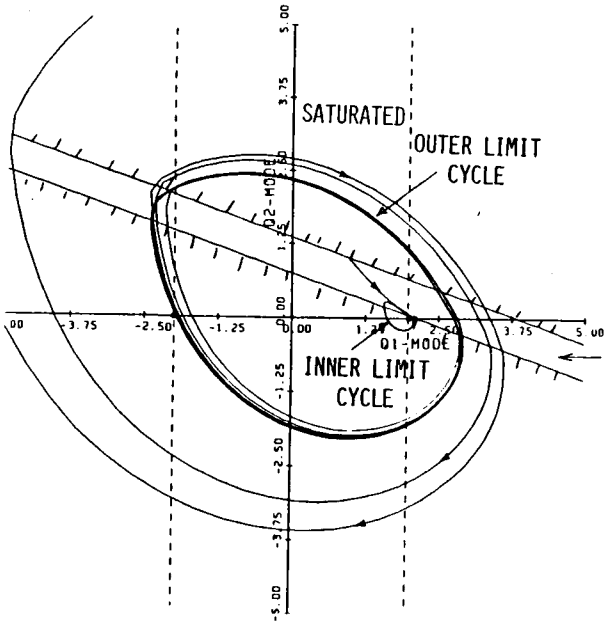

Y = 2.1

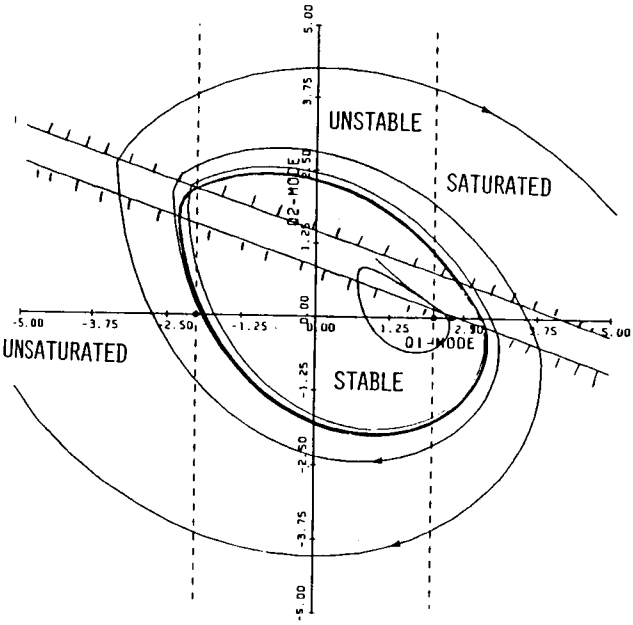

Y = 2.3

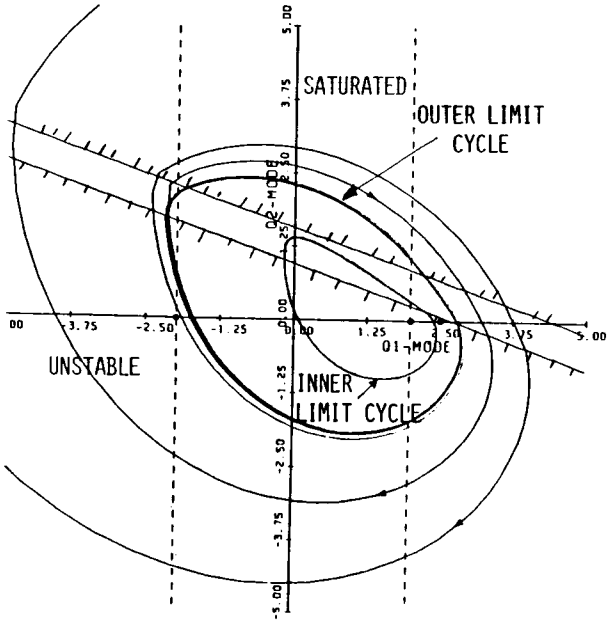

Y = 2.5

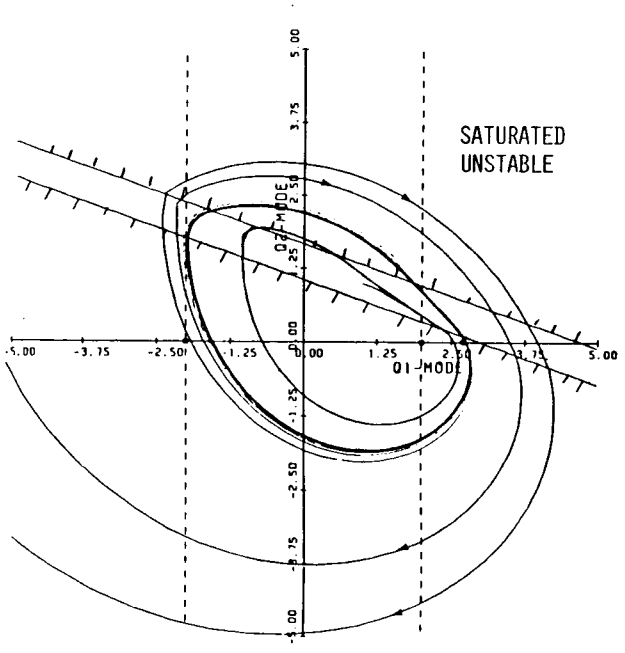

Y = 2.7

UNSTABLE FOCI (CONCLUDED)

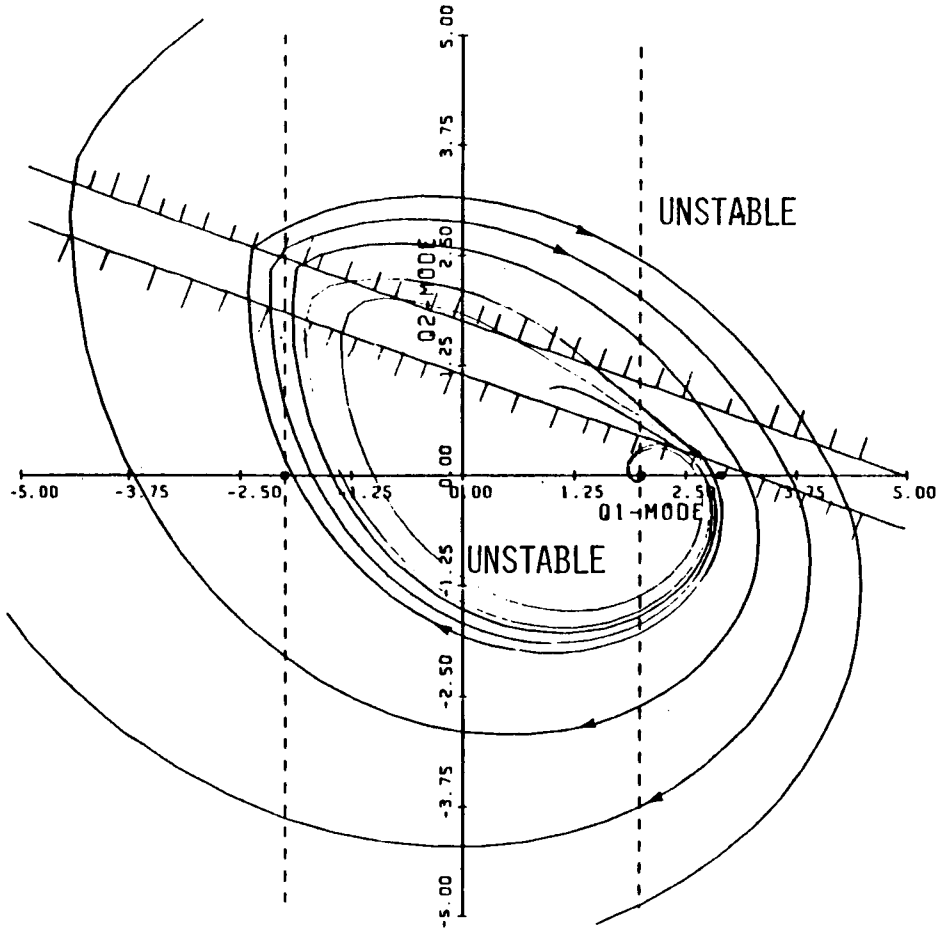

Y = 2.9

CONCLUSIONS AND FUTURE WORK

The Stability Augmentation System (SAS) is a special case of the Command Augmentation System (CAS). Control saturation imposes bounds on achievable commands. The state equilibrium depends only on the open-loop dynamics and control deflection. The control magnitude to achieve a desired command equilibrium is independent of the feedback gain. A feedback controller provides the desired response, maintains the system equilibrium under disturbances, but it does not affect the equilibrium values of states and control.

The saturation boundaries change with comands, but the locations of the equilibrium points in the saturated region remain unchanged. Nonzero command vectors yield saturation boundaries that are asymmetric with respect to the state equilibrium. Except for the saddle-point case with MCE control law, the stability boundaries change with commands. For the cases of saddle-point and unstable nodes, the region of stability decreases with increasing command magnitudes; it is reduced to zero for commands that require steady-state control $u^* \geq |u_m|$.

The regions of stability are biggest for the SAS. In the case of unstable foci, the region of stability does not vanish at $u^* = u_m$. An "inner" limit cycle is obtained, which grows with increase in commands until it coalesces with the "outer" limit cycle. Any further increase in command breaks this closed stability boundary. For a fixed degree of stability, different commands cause markedly different responses because they seek different equilibrium states.

- STABILITY AUGMENTATION SYSTEM: A SPECIAL CASE OF COMMAND AUGMENTATION SYSTEM
- CONTROL SATURATION LIMITS ACHIEVABLE COMMANDS
- DEPENDENCE OF STATE EQUILIBRIUM ON OPEN-LOOP DYNAMICS AND CONTROL
- STATE EQUILIBRIUM, STEADY-STATE CONTROL: INDPENDENT OF FEEDBACK GAIN
- FEEDBACK: TO ACHIEVE DESIRED RESPONSE: MAINTAIN EQUILIBRIUM IN PRESENCE OF DISTURBANCE

CONCLUSIONS

- SATURATION BOUNDARIES CHANGE WITH COMMAND VECTORS
- STABILITY BOUNDARIES CHANGE EXCEPT FOR MCE CASE
- BIGGEST REGION OF STABILITY FOR SAS
- REGION OF STABILITY REDUCES TO ZERO FOR $\gamma = \pm \gamma_{MAX}$ (EXCEPT IN THE CASE OF UNSTABLE FOCI)
- MARKEDLY DIFFERENT "LOOKING" RESPONSES FOR DIFFERENT COMMAND VECTORS

FUTURE WORK

- STABILITY BOUNDARIES FOR TWO-INPUT COMMAND AUGMENTATION SYSTEM
- DESIGN OF LATERAL-DIRECTIONAL COMMAND AUGMENTATION SYSTEM
- VARIATION OF STABILITY BOUNDARIES WITH FLIGHT CONDITIONS

Standard Bibliographic Page

1. Report No.	2. Government Accession No.	3. Recipient's Catalog No.
NASA CP-2452		

4. Title and Subtitle	5. Report Date
Joint University Program for Air Transportation Research - 1984	May 1987
	6. Performing Organization Code
7. Author(s)	8. Performing Organization Report No.
Frederick R. Morrell, Compiler	L-16255
9. Performing Organization Name and Address	10. Work Unit No.
NASA Langley Research Center Hampton, VA 23665-5225	505-66-01-07
	11. Contract or Grant No.
12. Sponsoring Agency Name and Address	13. Type of Report and Period Covered
National Aeronautics and Space Administration Washington, DC 20546-0001	Conference Publication
	14. Sponsoring Agency Code

15. Supplementary Notes

16. Abstract

This report summarizes the research conducted during 1984 under the NASA/FAA sponsored Joint University Program for Air Transportation Research. The material was presented at a meeting held at NASA Langley Research Center, Hampton, Virginia, January 18, 1985. The Joint University Program is a coordinated set of three grants sponsored by NASA Langley Research Center and the Federal Aviation Administration, one each with the Massachusetts Institute of Technology, Ohio University, and Princeton University. Completed works, status reports, and bibliographies are presented for research topics, which include navigation, guidance, control, and display concepts. An overview of the year's activities for each of the schools is also presented.

17. Key Words (Suggested by Authors(s))	18. Distribution Statement
Air transportation Avionics Low-frequency terrestrial navigation Aircraft guidance navigation and control control	Unclassified - Unlimited Subject Category 01

19. Security Classif.(of this report)	20. Security Classif.(of this page)	21. No. of Pages	22. Price
Unclassified	Unclassified	183	A09

For sale by the National Technical Information Service, Springfield, Virginia 22161

NASA-Langley, 1987